SOME FLOW PROBLEMS IN PERISTALSIS ON DISPERSION: EFFECTS OF WALL PROPERTIES

A thesis submitted to
Visvesvaraya Technological University,
Belagavi (Karnataka), India
for the award of the degree of

DOCTOR OF PHILOSOPHY
IN
MATHEMATICS

by

MALLINATH YASHWANT DHANGE
(2BL12PGN01)

Research Centre
Department of Mathematics
B.L.D.E.A's V.P. Dr. P. G. Halakatti College of Engineering and Technology,
Vijayapur - 586103

MARCH 2018

CERTIFICATE

This is to certify that **Mr. Mallinath Yashwant Dhange** has worked under my supervision for his doctoral thesis titled **"SOME FLOW PROBLEMS IN PERISTALSIS ON DISPERSION: EFFECTS OF WALL PROPERTIES"**. I also certify that the work is original and has not been submitted to any other University wholly or in part for any other degree.

Dr. Gurunath C. Sankad
Supervisor
Professor of Mathematics
Department of Mathematics
B.L.D.E.A's Vachana Pitamaha Dr. P. G. Halakatti College of Engineering and Technology, Vijayapur - 586103, Karnataka, India

Date: 18/03/2018
Place: Vijayapur

DECLARATION

I hereby declare that the entire work embodied in this doctoral thesis entitled **"SOME FLOW PROBLEMS IN PERISTALSIS ON DISPERSION: EFFECTS OF WALL PROPERTIES"**, is a bonafide work done by me under the supervision of **Prof. G. C. Sankad** and was not submitted elsewhere for the award of any diploma or degree of this or any other University.

I certify that this written submission represents my ideas in my own words and where other's ideas or words have been included, I adequately cited and referenced the original sources. I also declare that I have adhered to all principles of academic honesty and integrity and have not misrepresented or fabricated or falsified any idea / data / fact /source in my submission. I understand that any violation of the above will be a cause for disciplinary action by the Institute/University and can also evoke penal action from the sources which have thus not been properly cited or from whom proper permission has not been taken when needed.

Mallinath Yashwant Dhange
(USN No. 2BL12PGN01)
Research scholar

Date: 18-03-2018
Place: Vijayapur

Dedicated to

My Parents

and

Family Members

Acknowledgements

I thank the **Visvesvaraya Technological University (VTU), Belagavi** and **Vachana Pitamaha Dr. P. G. Halakatti College of Engineering and Technology, Vijayapur** particularly, the **Department of Mathematics**, for giving me an opportunity to do a Ph.D. and supporting me during my tenure at the Institute.

I would like to express my utmost gratitude to my beloved supervisor **Prof. G. C. Sankad**, who has always been a source of inspiration for me. I consider myself privileged to be one of his research students. Words are inadequate to express my appreciation for his parenthood support, guidance and encouragement during this work. His worthy comments, suggestions and valuable guidance enabled me in enhancing and improving my research ability. Without his generous help and support it was not possible for me to complete this work. I shall ever remain indebted to him. I also thank to **Sankad's family** for their hospitality and moral support during my research period.

It is my privilege to thank **Dr. P. K. Gonnagar**, Head, Department of Mathematics and Vice-Principal for his priceless support and inspiration and also for providing the essential facilities during the research period.

I extend my sincere thanks to senior faculties of the department **Dr. P. M. Hiremath** and **Dr. S. C. Desai** for devoting their precious time in providing valuable suggestions and encouragements on this work. I am also thankful to all faculty members and non-teaching staff of the department.

I am greatly indebted to **Sri M. B. Patil**, President, BLDEA's Vijayapur (Karnataka) for joyful encouragement in pursuing my research work. My profound and heartfelt thanks to our Principal **Dr. V. P. Huggi** for ceaseless support during my Ph.D. work.

I would also like to express my gratitude to friends **Dr. A. B. Patil, Dr. G. Ravikiran, Dr. N. Santhosh, Mrs. Pratima Nagathan** and **Mr. K. M. Chavan** for their friendship and companionship.

I owe special thanks to my **parents**, who have been my role models in striving for success through hard work. Words fail me to express my appreciation to my wife **Sow. Savitri**, who has always been an endless source of love and support to me. I cannot finish without expressing my heartiest feelings to our sweet kid **Chi. Shreyas**, whose love, I missed a lot during my Ph.D. studies.

Finally, I would like to thank everybody who was important to the successful realization of this thesis, as well as expressing my apology that I could not mention personally one by one.

- Mallinath Dhange

Visvesvaraya Technological University

Jnana Sangama, Belagavi – 590 018.

Prof.SatishAnnigeri Ph.D
Registrar (Evaluation)

Phone: (0831) 2498136
Fax: (0831) 2405461

Ref.No. VTU/BGM/Exam /2017-18/ 2710 Date: 12 MAR 2018

Acceptance Letter

Sir/Madam,

The soft copy of Ph.D./M.Sc. (Engineering by research) thesis of **Mr./Mrs. Mallinath Y Dhange.** bearing **USN 2BL12PGN01** has been submitted for Anti-plagiarism check at the office of the undersigned through "Turn-it-in" package. The scan has been carried out and the scanned output reveals a match percentage of **19% which is within the acceptable limit of 25%.**

To obtain the comprehensive report of the plagiarism test, research scholar can send a mail to apc@vtu.ac.inalong with the USN, Name, Name of the Guide/Co-guide, Research centre and title of the thesis.

Registrar (Evaluation)

To, **Mallinath Y Dhange**

Research Scholar

Mathematics

BLDES's College of Engineering & Technology, Bijapur.

Abstract

Bio-fluid mechanics is part of biomechanics which describes the kinematics and dynamics of body fluids in humans, animals and plants. It uses the general principles of fluid mechanics which involve some new applications to biological systems. Modern bio-fluid mechanics measures and analyzes the fluid flow in the blood vessels, the respiratory system, the lymphatic system, the gastrointestinal system, the urinary system and many other physiological situations. Studies in this area are important for clinical applications such as artificial organs, vascular vessel development, and design of medical tools and fabrication of materials membranes for orthopedics. The interaction of peristalsis with dispersion studies in this thesis since they are very important phenomena in biological, chemical, environmental and bio-medical processes. We briefly describe below the concepts of peristalsis and dispersion so that the problems studied in this thesis can be properly understood.

Peristalsis is a form of material transport induced by a progressive wave of area contraction or expansion travelling along the length of a distensible tube or channel containing the fluid. Physiologically, peristaltic action is an inherent property of smooth muscle contraction. Peristalsis is an automatic and vital process that drives the urine from the kidney to the bladder through the ureter, food through the digestive tract, bile from the gall bladder into the duodenum, the movement of spermatozoa in the ducts efferents of the male reproductive tract, movement of the ovum in the Fallopian tube, vasomotion in small blood vessels and many others. Peristaltic flows play an indispensable role in some biomedical instruments such as heart-lung machine. A major industrial application of this mechanism is in the design of the finger and roller pumps, which are used in pumping fluids without being contaminated due to the contact with the pumping machinery. This mechanism is also used for transport of

sensitive or corrosive fluids, sanitary fluids, slurries and noxious fluids in the nuclear industry. Although the peristaltic action is quite prevalent in biological systems, the first theoretical and experimental aspects of its fluid dynamics were discussed about four decades ago. Several theoretical and experimental studies have been made to understand the phenomenon of peristalsis using various geometries, fluids, wave shapes, etc. In view of its importance, a number of researchers have investigated peristaltic transport of Newtonian and non-Newtonian fluids under different circumstances.

Flow through porous medium has captivated significant attention in recent years due to its prospective applications in nearly all fields of engineering, biomechanics and Geo-fluid dynamics. Also, as most of the tissues in the body are deformable porous media. Peristaltic transportation of a bio-fluid through a conduit with permeable walls is of considerable importance in biology and medicine. Analysis of flow past a permeable medium is used immensely in biomedical problems to understand the transportation process in the lungs, gall bladder and kidneys, to investigate inter vertebral disc tissues, cartilage and bones etc. Some of the physiological systems such as blood vessel consists of porous layers. Peristalsis is also important in blood vessels; it will be interesting to know the effects of permeability on the peristaltic pumping. Flow through porous media has been of significant interest to understand the complexity of disease like bladder stones, intestinal cystitis, and bacterial infections of the kidneys. Porous medium models are applied to identify the various medical conditions and treatments. As the fluid displays a loss of adhesion at the wetted wall, the fluid is made to slide along the wall, resulting in slip flow, as seen in several applications like flow through pipes in wherein chemical reactions occur in the walls. Slippage is claimed to occur in Newtonian and non-Newtonian fluids, molten polymer and concentrated polymer solution.

Dispersion is the process by which matter is transported from one part of a system to another as a result of random molecular motions. Dispersion plays a chief role in applications like chromatographic separations in chemical engineering, pollutant transport in the environment, mixing and transport of drugs or toxins in physiological systems, and so on. Further, it is known to balance material in the bio artificial kidney and transporting of oxygen in the human body. The fluid mechanical aspects of hydrodynamic dispersion of a solute in a viscous fluid have received the attention of several investigators.

It is envisaged that peristalsis may enhance the dispersion of a solute in the fluid flow. This, in turn, may help in better absorption of nutrients and drugs in physiological systems. Further, the dynamical interaction between the fluid flow and movement of flexible boundaries may also be significant in peristaltic transport. Hence, the study of the interaction of peristalsis with dispersion under different conditions may lead to better understanding of the flow situation in physiological systems. This is the core reason why this thesis is aimed at these physiologically relevant phenomena.

In view of the above discussion, an attempt has been made in this thesis, to study dispersion of a solute in peristaltic motion of Newtonian and non-Newtonian fluids with wall properties by considering different characteristics such as porous media and magnetic field in a channel with elastic wall. The incompressible viscous fluid and couple stress fluid models are used since these are known to be better models for physiological fluids such as blood, bile, and chyme. The expression for the mean effective coefficient of dispersion is developed by using long wavelenght hypothesis and Taylor's limiting condition. Mathematica software is used to analyze the results graphically.

Contents

Chapter 1

Introduction

1.1 Preliminary

Fluid mechanics is concerned with understanding, expecting and governing the behavior of a fluid. Fluid dynamics is the branch of fluid mechanics dealing with the properties of fluids in motion. It has several sub disciplines. Fluid dynamics has a wide range of applications like computing forces on the aircraft, forecasting weather patterns, planning dams, irrigation canals and water supply systems, exploring the movement of biological liquids in human beings, determining the mass flow rate of petroleum through pipelines. Several of its principles are even used in traffic flow engineering, where traffic flow is treated as a continuous liquid.

The leading equations of fluid dynamics (Navier-Stokes equations) are extremely nonlinear. The exact results are attainable for some very special cases. In most of the circumstances, one can put faith on approximate solutions found by analytical and computational techniques. This is the approach of new investigative strategies for experiments, computational procedures and tools that has empowered researchers to test into the complexity of the subject. The strong point of this knowledge can serve the humankind, regarding forecasts of worldwide climate framework, manufacture of innovative aerodynamic vehicles, design of micro fluidic devices and etc. Because of the difficulty of the subject and an enormity of its applications, fluid dynamics is recognized to be a highly thrilling and challenging area of contemporary sciences. Fluid dynamics have raised the curiosity of many researchers in the recent years. In biological systems, fluid dynamics have several applications, which is broadly called bio-fluid dynamics. We describe below bio-fluid dynamics briefly.

1.2 Bio-fluid Dynamics

Mathematical modeling is the illustration of a system using scientific observation and linguistic. It is applied to study the complications in medical science. Bio-fluid dynamics is the branch of biomechanics which deals with the kinematics and dynamics of the fluids present in human beings, animals and plants. It spans from cells to organs, covering diverse aspects of functionality of systemic physiology, including cardiovascular, lymphatic, musculoskeletal, neurological, ocular, respiratory, reproductive, urinary, and auditory systems.

The latest study of bio-fluid mechanics measures and analysis the flow of physiological liquids, applicable for the clinical studies as in: cancer treatment, artificial organs and many more. It is well known fact that experimentation on physiological liquids is a difficult task to undertake and further the non-invasive experiments do not always give accurate results. Hence the understanding of bio-fluid dynamics in the flow of physiological fluids in a human body is rather a difficult task in comparison with the engineering applications. In addition, this necessitates the familiarity of both theoretical and computational bio-fluid dynamics to understand the bio-fluid dynamics in the human body.

The biological systems are very complex and have defied all attempts at satisfactory mathematical solutions. These complicated systems are studied theoretically by means of approximated models whose simplified nature becomes amenable to mathematical analysis and give meaningful mathematical solutions. Hence, the mathematical analysis and understanding of bio-fluid dynamics seem to be extremely important and useful for diagnosis and clinical purposes. They can lead to determination of significant physical parameters of human systems and development of sophisticated instruments.

In general, bio-fluid dynamics can be considered as the study of the human body and its components in the application of principles of mechanics, oriented with a sense to medical applications. The fundamental assumption here is that the world of the living and the world of non-living are governed by the same laws of physics. The role of a mathematician in biomechanical study is to build simplified mathematical models of the physical situation and analyze them.

We describe below the characteristics considered so that the problems studied in this thesis can be properly understood. Among these, the vital mechanism for fluid transport in bio-fluid dynamics is *peristalsis*. It is briefly described as follows.

1.3 Peristalsis

"Peristaltikos" is a Greek word which implies, clasping and compressing, from which arise the word 'Peristaltic'. Peristalsis is a coordinated response wherein a wave of contraction preceded by a wave of relaxation passes down a hollow viscus. Thus 'Peristalsis' is the rhythmic sequence of smooth muscle constrictions that progressively squeeze one small section of the tract and then the next, to push the content along the tract. As they are propelled along, would always enter a segment which had actively relaxed and enlarged to receive them. From the perspective of fluid dynamics, peristalsis is typified by the dynamical interface of the fluid flow and movement of the flexible boundaries of the conduit.

Peristalsis is an intrinsic properties of any smooth muscle like the bile duct, gastro intestinal tract, ureter, glandular duct, etc. The physiological applications of peristalsis is observed when the swallowed food moved into the esophagus, urine flow from kidney to the bladder, spermatozoa move in the male and female reproductive organs, lump move in the lymphatic vessels, bile juice flow in the bile duct, blood circulates in small blood vessels like arteries, venules and capillaries. Peristalsis has brought revolutionary developments in industrial appliances as well: transportation of sanitary liquid, caustic liquid, toxic liquid in the nuclear industry and also in the finger pump, roller pump and in biomedical instruments, for instance, blood and heart lung pump machinery. Peristalsis has found applications in Micro electro mechanical systems (MEMS) (Teymoori and Abbaspoursani [160]). Even the translocation of water in large trees is speculated to occur through peristalsis, through its porous matrix (Rathod and Kulkarni [118]). Bose (1923) was probably the first to ascertain that water was pumped upwards by alternate contractions and expansions of living cortical cells. Thane (1969) has proposed that phloem translocation is achieved by driving a sucrose solution by peristaltic contractions along tubules which traverse many sieve cells.

We describe below *esophagus*, *intestines*, *kidneys*, *bioengineering pumps*, *spermatozoa*, and *ovum* which works on the principle of peristalsis.

1.3.1 Esophagus

The usual stimulus of the esophagus is swallowing, which at any level results in the development of peristalsis. Thus, after reaching the esophagus, food is propelled into the stomach by peristalsis (Fig. 1.1). It consists of lumen obliterating contractions, 4-8 cms in length, which move down at a speed of 2 - 4 cm/sec. The strength of the peristaltic contractions is proportional to the size of the bolus entering the esophagus.

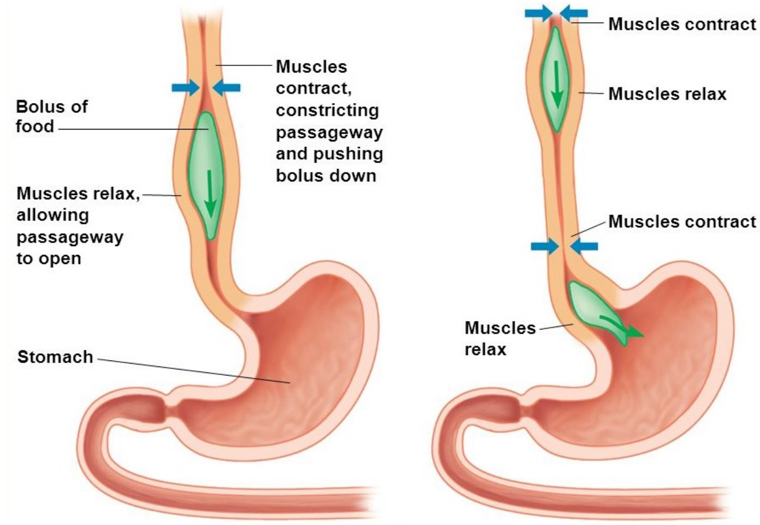

Figure 1.1

1.3.2 Intestines

Once the intestine wall is stretched or distended by chyme (food), a circular constriction form above the intestine because of contraction of the longitudinal muscle layer (Fig. 1.2). Therefore, the intestinal contents move towards the dilated part; then contraction of circular muscles spread to this part which in turn is constricted, while the segment below it is dilated by contraction of the longitudinal muscle layer. Several of these waves like contractions occur simultaneously along the length of the intestine. Each wave lasts for 1 - 2 seconds and propels the chyme a few centimeters.

1.3.3 Kidneys

Bergman [14] affirmed that urine flow from the kidney to the bladder within the ducts called ureters is due to peristalsis in the uteral wall (Fig. 1.3). The only function of the ureter is to drive the urine to the bladder from the kidneys, beginning right from the kidney and forwarding towards the bladder, through peristatic action. The ureter wall is made up of a number of layers (Krstic [61]). The luminal surface of the ureteral wall consists of a transitional epithelium and a lamina propia, comprising of a thick layer of finely vascularized and innervated connective tissue. The remaining portion of the wall is included of smooth muscle along with connective tissue called Tunica Muscularis (TMu). The TMu

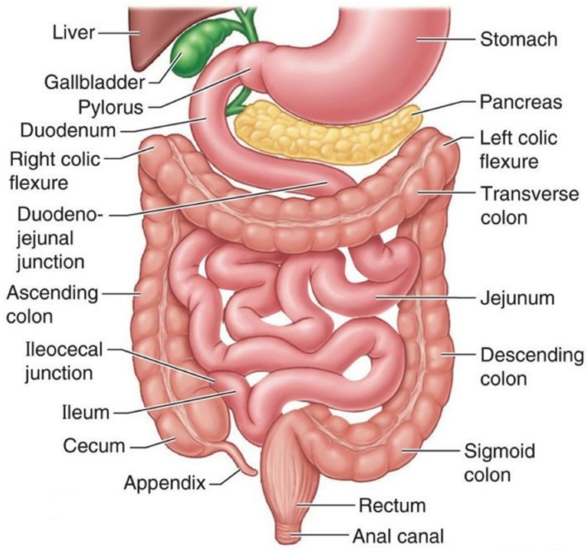

Figure 1.2

consists of smooth muscle bundles isolated by abundant loosely-fitted connective tissue ([100]). The peristaltic contractions are simplified by these muscle fibers.

1.3.4 Ovum and Spermatozoa

The ovum or the female reproductive cell is extruded onto the surface of the ovary near the ovarian end of the oviduct at the time of ovulation and is sucked into the oviduct because of the sweeping motion of the finger-like projections at this end of the oviduct, caused by the contraction and relaxation of the smooth muscles surrounding them. The epithelium of the oviduct is lined with cilia, i.e., hair-like projections on the walls. These cilia because of their beating motion send waves towards the interior of the duct and hence facilitate the motion of the ovum. Though the actual mechanism for the transport of the ovum in the oviduct towards the site of fertilization is not clearly known, it is speculated that peristalsis plays a very important role in the transport of the ovum in the oviduct (Fig1.4).

The spermatozoa are deposited, during the coitus, at the mouth of the cervix and are known to travel at an average speed of 1-3 mm/minute. The transport of the sperm to the site of fertilization (in the oviduct) is so rapid that the first sperm arrives within 45 minutes. This

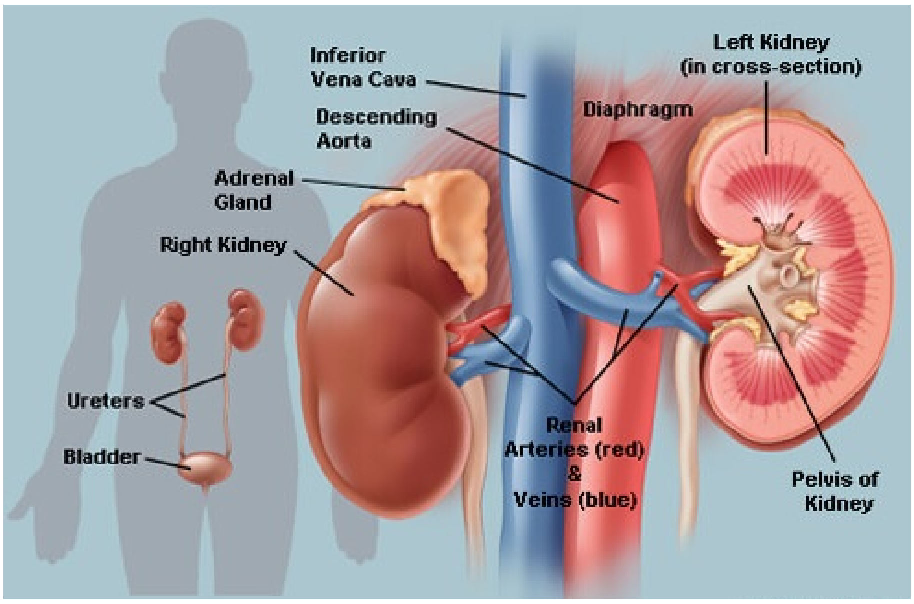

Figure 1.3

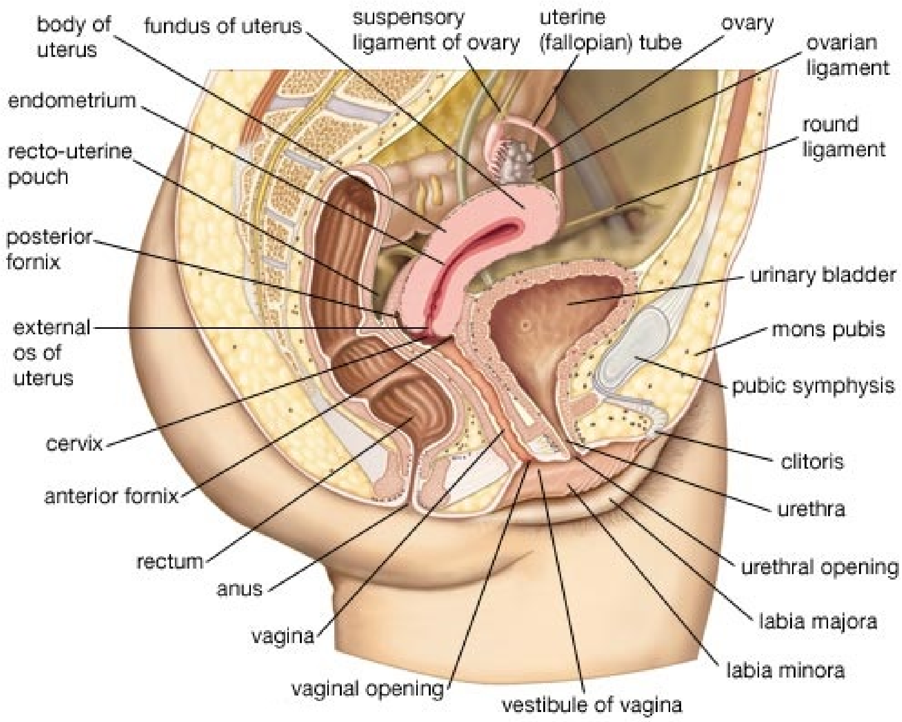

Figure 1.4

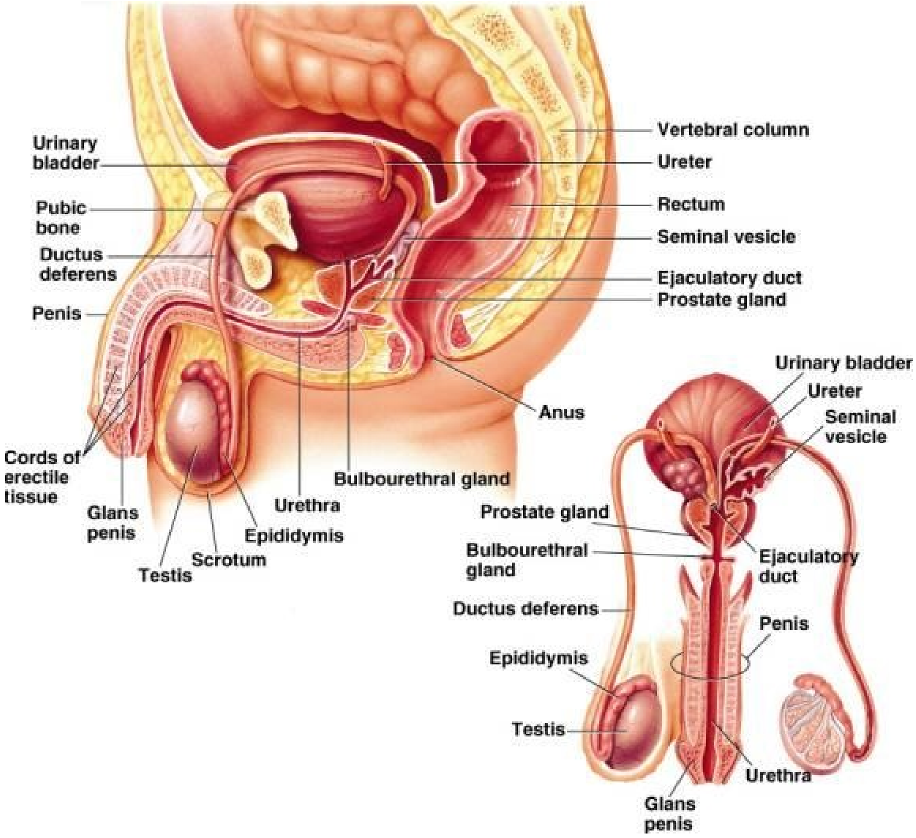

Figure 1.5

is far too rapid to be accounted for by the sperm's own motility. It is suggested that the movement produced by the wave motion along the sperm's tail is probably essential only in the final stages of the approach and penetration of the ovum. The act of coitus provides some impetus because of ejaculated fluid pressure and the pumping action of the penis (Fig. 1.5). Though the actual mechanism of spermatozoa moves in the female genital tract is not very well understood, it is speculated that peristalsis plays a very major role in this motion.

1.3.5 Bioengineering Pumps

The basic principle of a Bioengineering pump is a mechanical application of peristalsis. It can be broadly divided into two categories, one that are seen in the biological systems, i.e. naturally occurring pumps and other ones are the artificial ones made by human beings

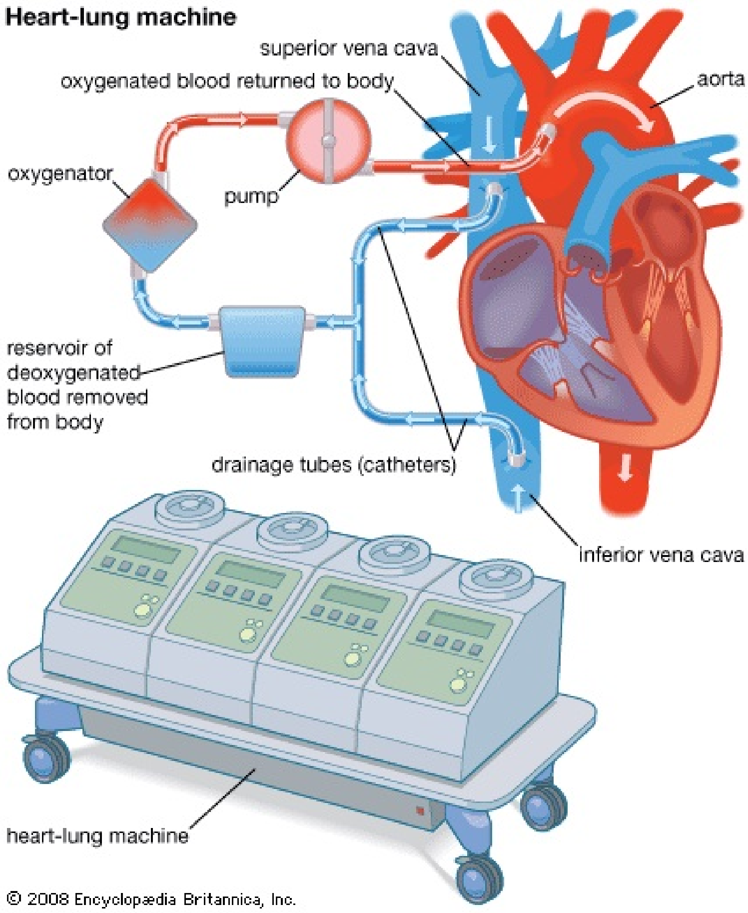

Figure 1.6: Heart lung machine

and are utilized for biomedical appliances. Oxygenator is an engineering device, used to oxygenate blood, known as heart-lung machine (Fig. 1.6). It is used in the open-heart surgery, which serves a dual purpose of heart and lung. During the operation impure blood is taken out of the body and passed into the heart-lung machine for the purification and oxygenated blood will be sent back to the body (Mishra and Pandey [84]).

Dialysis machine also works on the mechanism of peristalsis. Dialysis is a treatment that cleans and filters the blood by utilizing the dialysis machine (Fig. 1.7). It has been utilized from 1940 to treat people with kidney issues. Without dialysis, salts and other waste items will collect in the blood and poisons the body. This helps to keep our body in adjusting when the kidneys cannot do their work. It can help to keep the body running as commonly

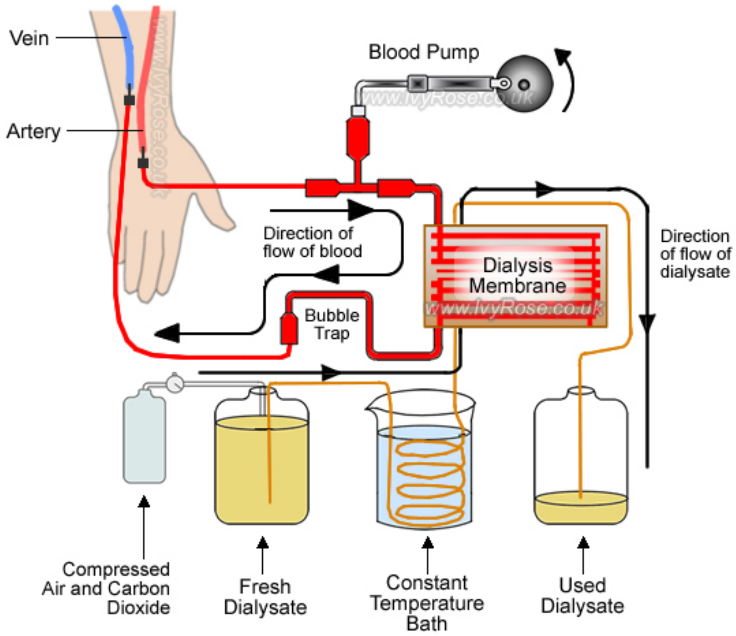

Figure 1.7

as could be permitted. Roller and finger pumps use this mechanism of peristalsis to pump the blood. Hence, many scientists and researchers have been showing core interest in peristaltic flow.

A non-biological application of peristalsis is the peristaltic pump (Fig. 1.8), which is used to move/clean/sterile of aggressive fluid through a tube without cross contamination between the exposed pump components and the fluid. As discussed by Jaffrin and Shapiro [49], the presence of viscous forces, one can produce effective pumping. In nuclear industry peristalsis avoids polluting of the outside environment during the exclusion of toxic liquid. Observations reveal that transportation of water in tall trees is due to peristalsis (Lightfoot [68]). The porous matrix of the trees assists this water flow.

The fluid mechanical study of peristalsis has received considerable attention in the last few decades mainly because of its relevance to industrial and physiological processes.

The relevance of peristaltic flow in physiology was brought out mainly through the works of Kill [54]. The study of the mechanism of peristaltic motion was first experimentally

Figure 1.8

examined by Latham [66]. These experimental results were in accordance with the theoretical results examined by Shapiro [133]. Burns and Parkes [18] considered the above experimental work and sinusoidal variations on the walls to investigate the flow of a viscous fluid through a pipe and a channel. A theoretical establishment of peristaltic stream developed by sinusoidal transverse waves of small amplitude for inertia-free Newtonian fluid was suggested by Fung and Yih [28]. They found that a backward motion in the mid region of the stream is generated when pumping in opposition to a positive pressure gradient is higher than a critical value. Later, Yin and Fung [29] extended this problem in the case of circular cylindrical pipe and who made the comparison of experimental and theoretical outcomes of peristaltic flow. Shapiro et al. [50] obtained the solution in the closed form considering a continuous train of peristaltic waves for low Reynolds number under large wavelength and arbitrarily chosen wave amplitude. They found that there were two major phenomena: trapping and reflux in physiology. A long wavelength approach to peristaltic movement was also carried by Zien and Ostrach [172]. Jaffrin and Shapiro [49] provided an elaborate review of the earlier literature regarding peristalsis. Bohme and

Friedrich [16] observed peristaltic transport mechanism of an incompressible visco-elastic fluid. Pozrikidis [105] investigated the flow in two dimensional channel with sinusoidal waves.

An experimental study of peristalsis was given by Weinberg et al. [169]. Since it is known (Patel et al. [99]) that human faeces behave rheologically like a power law fluid. Peristaltic transport of power law liquid with particular references to the motion of human faeces in colon investigated by Picologou et al. [103]. Manton [71] found an asymptotic growth in the stream in an axisymmetric pipe with lengthy peristaltic waves of uninformed shape and derived the important phenomena of trapping and reflux occurs with limitations. Kaimal [52] studied the peristaltic flow in an axisymmetric tube with uniformly distributed suspended particles, under low Reynolds number and long wavelength hypothesis. A numerical study of 2- dimensional peristaltic streams was made by Takabatake and Ayukawa [153]. Later, Tandon et al. [155] considered the inpact of microstructure and peripheral layer viscosity on creeping motion. Peristaltic transport of power law fluid in an axisymmetric tube under long wave length hypothesis is investigated by Radhakrishnamacharya [109]. Rath and Reese [117] studied creeping sinusoidal flow of non- Newtonian fluids containing small spherical particles. The effect of peristaltic motion on the movement of micro-organisms with a usage to spermatozoa transportation was explored by Shukla et al. [138]. A perturbation solution for peristaltic transport of a fluid-particle mixture for small amplitudes was given by Misra and Pandey [83].

The peristaltic pumping of Herschel-Bulkley fluid in a channel under long wavelength hypothesis and small Reynolds number was studied by Vajravelu et al. [166]. The peristaltic motion of Carreau fluid in an uniform tube is studied by Hakeem et al. [34]. Creeping sinusoidal flow of third-order fluid in an irregular conduit was analyzed by Haroun [36]. Radhakrishnamacharya and Sharma [112] considered the effect of viscosity variation on motion of a self propelling microorganism in a conduit with peristalsis. Nadeem et al. [88] studied the effect of peristaltic movement on heat and mass transfer for a third order fluid in a tube. Peristaltic pumping of a particle fluid suspension in a catheterized circular tube has been investigated by Medhavi [72]. Noreen et al. [92] considered the peristaltic flow of pseudoplastic fluid in an irregular channel. The impact of hydromagnetic field on peristaltic flow of a couple stress fluid in an inclined conduit was observed by Shit and Roy

[137].

In all the above investigations, the walls of the duct are assumed to be rigid. But, in most of the physiological situations, the walls are elastic in nature, i.e., walls get excited by the smooth muscle contractions whose tension controls its deformation.

Mittra and Prasad [86] analyzed the movement of Newtonian fluid under peristalsis to know the effects of the viscoelastic behavior of walls. The dynamic mechanism is presumed to be due to the imposition of moderate amplitude sinusoidal wave on the flexible walls of the channel. Srivastava and Srivastava [149] studied the peristaltic transport of Casson fluid. Radhakrishnamacharya and Srinivasulu [113] explored the influence of heat transfer on peristalsis considering the elasticity of the walls. Srinivasacharya et al. [145] investigated the influence of wall features on the creeping flow of a dusty fluid under long wave length hypothesis. The effect of sleep on peristaltic stream in an inclined conduit with wall properties has been investigated by Ramana Kumari and Radhakrishnamacharya [115]. The effect of magnetic field on the peristaltic transport of a couple stress fluid in a channel with wall properties was analyzed by Sankad and Radhakrishnamacharya [129]. Recently, Alemayehu and Radhakrishnamacharya [10], Akbar and Nadeem [7] and Tripathi and Beg [164] studied peristalsis under different conditions.

Theoretical study of viscous effects in peristaltic pumping was investigated by Provost and Schwarz [107]. Tokyo [161] developed a new mathematical model for the peristaltic motion in the esophagus. Obtained the manometric dimensions of luminal pressure in the esophagus.

It is known that many ducts in biological systems are having non-uniform cross section. In the human body, several small blood vessels, lymphatic vessels, intestines, ductus efferentes of the reproductive tract are generally observed to be of non-uniform cross section (Srivastava et al. [150]). Hence, Lee and Fung [67] studied the flow in non-uniform small blood vessels. Gupta and Seshadri [31] investigated peristaltic flow in non-uniform channels and tubes with particular reference to the flow of spermatic fluid in vasdeferens. Hasan et al. [37] extended the same problem with different wave forms. Radhakrishnamacharya and Radhkrishna Murthy [110] studied peristaltic transport in a non-uniform channel with heat transfer. Srinivasulu and Radhakrishnamacharya [146] studied the peristaltic motion of a Newtonian fluid in a non-uniform channel with wall effects. The peristaltic flow of blood under the effect of magnetic field in a non uniform channel was investigated by Mekheimer [75]. Sobh and Mady [143] studied the peristaltic motion of a Newtonian fluid in a non-uniform porous channel. Eytan et al. [27] analyzed asymmetric peristaltic flow in a non-uniform channel with particular application to human reproduction.

Another physiologically important phenomenon that this thesis deals with is a dispersion of a solute matter in a flowing fluid. We present the brief description of dispersion as follows.

1.4 Dispersion

A solution contains of a liquid, so-called the solvent, in which some stuff, named the solute, has dissolved. We consider a solution in which simple molecular dispersion takes place. The composition of the solution is characterized by its mass concentration C, which is the mass of dissolved matter per unit volume of liquid. One means by which the solute particles are dissolved and transported through the solvent is diffusion/dispersion. Therefore, dispersion is the process by which material is transported from one portion of a system to another as a result of random molecular motion (Fig. 1.9).

The consistent movement of the dissolvable molecules delivers a considerable number of collisions with a given huge solute particle. Therefore, pressure variations are created which in chance convey to the solute grain a jerky irregular path, named, a random walk. The result of this random walk is a net dislodgment of the molecule in some direction. The equivalent phenomenon occurs in the case of suspended particles (e.g. emulsions). This random motion is called Brownian motion, in honor of the English botanist Robert Brown (1828). Dispersion is a direct result of the random motion of the molecules in the direction of a gradient. Dispersion of soluble matter in laminar flow has biological applications such as drug and nutrient distribution in the body. Dispersion plays a vital role in many biological situations. Through dispersion, metabolites are swapped between a cell and its environment or among the tissues and blood stream.

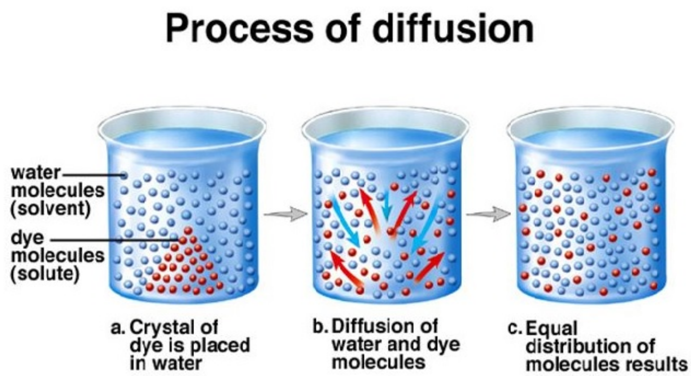

Figure 1.9

1.4.1 Fick's Law of Diffusion

Consider a solution in which simple molecular diffusion is occurring, the fluid being otherwise at rest. The mechanism of transport of the solute is governed only by concentration differences.

The material flux per unit area is known as the current density and is denoted by J. The classical theory of diffusion was invented more than one hundred years ago by a physiologist A. Fick in 1855. The first law of diffusion is that

$$Material flux = -\mathcal{D} \times concentration\ gradient,\ i.e.,$$

$$J = -\mathcal{D}\frac{\partial C}{\partial \mathcal{X}}, \tag{1.1}$$

where the concentration C varies from point to point and depends on the position $\mathcal{X}$ only and $\mathcal{D}$ is the diffusion coefficient. The diffusion coefficient is a characteristic of the solute of the fluid and in this case it is given by $\mathcal{D} = \frac{KT}{f}$, where K is the Boltzmann constant, T is the absolute temperature and f is a frictional coefficient which depends on the molecular size and shape and the viscosity of the fluid. For instance, for spherical fluids, Stokes' law says that $f = 6\pi\mu a$ where a is the radius of the molecule and μ is the viscosity of the fluid. The minus sign in equation (1.1) implies that the particle flow proceeds from a high concentration region to a low concentration region.

The dispersion of a solute flowing in a conduit has numerous applications in chemical, biomedical engineering, and physiological fluid dynamics. Taylor [156] was the first person, who proposed the basic theory on dispersion and investigated theoretically and experimentally that the dispersion of a solute is miscible with a liquid flowing through a channel. Dispersion plays an important role in physiological systems. For example, the knowledge of substances injected into a blood vessel is useful for many clinical and physiological purposes and also in the distribution of drugs in the body. It may also be useful in the investigation into the development of atherosclerotic lesions along the wall of modeled arterial bifurcation. Taylor [157, 158] suggested a simple method to study dispersion, analyzed the scattering of a solute matter in a solvent flowing under laminar conditions in a circular pipe. Taylor imposed certain restrictions in his analysis, which were later removed by Aris [11]. Numerous authors have studied dispersion in the flow of Newtonian and non-Newtonian fluids under different conditions following Taylor's approach. The effect of chemical response on scattering in non-Newtonian fluids were studied by Shukla et al. [139]. Chandra and Agarwal [5] analyzed dispersion in simple microfluid flows. Diffusion in the existence of a slip and chemical responses of flow in a porous tube has been studied by Mehta and Tiwari [73]. Philip and Chandra [19] studied the effects of heterogeneous and homogeneous responses on the scattering of a solute in simple microfluid. Hazra et al. [46] investigated the dispersion of a solute in oscillating flow of a non-Newtonian fluid in a channel. Zhangji et al. [171] considered the effects of peripheral layer on dispersion of soluble matter in Newton-dipolar stratified fluid. Bandyopadhyay and Mazumder [13] dealt with contaminant dispersion in unsteady generalized Couette flow. Yang et al. [170] considered experimental studies on the particle dispersion in a plane wake. Paul [102] analyzed the axial dispersion in pressure perturbed flow through an annular pipe oscillating around its axis.

Sarkar and Jayaraman [131, 132] considered the effect of wall absorption on scattering in oscillatory flow in an annulus. Nagarani et al. [90] considered the effect of boundary absorption on scattering in Casson fluid flow in a tube. Koo and Song [57] studied Taylor dispersion coefficients for longitudinal laminar flow in shell-and-tube exchangers.

Further, Paul [101] investigated scattering in unsteady Couette-Poiseuille flows. The analytical solution to 1- dimensional advection-diffusion equation with variable coefficients in semi-infinite media has been considered by Kumar et al. [62]. Dentz et al. [22] dealt with mixing, spreading and reaction in heterogeneous media. Similarly, Golder et al. [30] worked on mass transport in porous media. Jiang and Wu [51] studied transition rate transformation method for solving advection-dispersion equation. Kumar et al. [63] considered steady solute dispersion in composite porous medium between two parallel plates. Jaafar et al. [48] dealt with mathematical modeling of shear augmented dispersion of a solute in blood flow. Alemayehu and Radhakrishnamacharya [9, 10], Porta et al. [104], Ravikiran and Radhakrishnamacharya [121, 122, 123, 124], Hyat et al. [41, 43, 45] have considered dispersion of a solute in peristaltic flow of non-Newtonian fluids under different conditions.

Chemical reactions take place in most of the processes of dispersion of a solute. A description of both homogeneous and heterogeneous chemical reactions is given below.

1.5 First Order Chemical Reaction

A chemical response/reaction is a procedure that is generally characterized by a substance change in which the beginning materials (reactants) are not quite from the products. Chemical reactions have a tendency to include the movement of electrons, leading to the formation and breaking of chemical bonds. There are diverse varieties of chemical reactions and more than one way of classifying them. The order of response is well-defined as the amount of all the exponents of the reactants intricate in the rate constraint. It should be noted that all the particles shown in a chemical equation do not decide the value of order of reaction, but only those particles whose concentrations are changed are included in the determination of the order of a reaction. In other words, the number of the reacting particles whose concentration varies as an outcome of chemical reactions is termed as the order of reaction. For example, the reaction in which only one molecule undergoes a chemical change is called first order reaction. In the recent instants, liquid flows containing chemical response have been paying attention of engineers and scientists. Such flows have key importance in many processes like energy transfer in a wet cooling tower, evaporation of drying on the surface of a water body, producing electric power, flow in a desert cooler, food processing, groves of fruit trees, crop damage because of freezing, etc. There is always a molecular diffusion of species in the existence of a chemical response inside or at the boundary throughout numerous practical diffusive operations. There are two types of responses namely homogeneous and heterogeneous ([120]).

1.5.1 Homogeneous Chemical Reaction

Homogeneous reactions are chemical reactions in which the reactants are in the identical phase. A response among two gases, two liquids or two solids is homogeneous. The reactions between gases (e.g. the combination of common household gas and oxygen to produce a flame) and the reactions between liquids or substances dissolved in liquids can be named as homogeneous chemical reactions. From a theoretical standpoint, homogeneous reactions are the simplest type of reactions because the chemical changes that take place are exclusively dependent on the nature of the interactions of the reacting substances. The smog formation is a significant example, representing a first order homogeneous chemical reaction.

1.5.2 Heterogeneous Chemical Reaction

Heterogeneous reaction is a chemical reaction in which the reactants occur in two or more phases (i.e. solid and gas, solid and liquid, two immiscible liquids) or in which one or more reactants experience chemical change at boundary, for instance, on the surface of a solid catalyst. The reaction of metals with acids, the electrochemical changes that occur in batteries and electrolytic cells, and the phenomena of corrosion are part of the subject of heterogeneous reactions. By far the majority of the researches of heterogeneous reactions are devoted to heterogeneous catalysis (e.g. the reactions between gases or liquids accelerated by solids). Practical appliances of heterogeneous responses are in catalytic converters, fuel cells and chemical vapor deposition among others.

Chemical responses usually take place during dispersal of a solute matter in a fluid. This is the reason why some investigators dealing with dispersion considered chemical response in their study. To mention a few examples, Gupta and Gupta [32] discussed effect of homogeneous and heterogeneous responses on the scattering of a solute in the laminar flow between two plates. Dutta et al. [23] studied scattering of a solute in a non-Newtonian liquid with the simultaneous chemical response. Further, Rao and Padma [93, 95] considered homogeneous and heterogeneous chemical responses on the scattering of a solute in MHD Couette flow. Padma and Rao [94] dealt with the influence of homogeneous and heterogeneous responses on the scattering of a solute in laminar flow between two parallel porous plates. The impacts of chemical response, heat and mass transfer on MHD flow, along a vertical porous wall discussed by Ahmed and Chamkha [6]. Saini et al. [127] examined the effects of first order chemical response on the dispersal coefficient associated with laminar flow through a circular tube. Effect of first order chemical response on gravitational instability in a porous medium is discussed by Kim and Choi [55].

Further, characteristics such as magneto-hydrodynamics and porous medium have been considered in this thesis. The brief description of each of them is given below.

1.6 Magnetohydrodynamics (MHD)

The study of the interaction of electrically conducting fluid flow with a magnetic field is called magneto-hydrodynamics (MHD). The movement of conducting fluid generates electric currents across the magnetic field that leads to the formation of mechanical forces and modify the motion of the fluid.

The flow of blood takes place in two layers. One in the plasma layer which is near the wall and another one is the core layer which consists of a suspension of cells in the plasma. The core is treated as magnetic field because red blood cells have iron, which is magnetic in nature. The magnetism affects the human body through the nervous system, circulatory system and the endocrine system.

For MHD flow, there is an extra term due to MHD body force, namely, $\vec{J} \times \vec{B}$ in the momentum equation.

The basic equations that govern the flow influenced by MHD (after ignoring the displacement currents) as:

$$\nabla \cdot \vec{B} = 0, \ \nabla \times \vec{B} = \mu_m \vec{J}, \ \nabla \cdot \vec{E} = -\frac{\partial \vec{B}}{\partial t} \text{ and } \vec{J} = \sigma \left(\vec{E} + \vec{q} \times \vec{B} \right) \tag{1.2}$$

Which is the Generalized Ohm's law and Maxwell's equation.

The velocity of the fluid is $\vec{q}$, the electric current density is $\vec{J}$, the total magnetic field is $\vec{B} = \left(\vec{B}_0 + \vec{B}_1\right)$, the induced magnetic field is $\vec{B}_1$ $\left(\text{and } \vec{B}_1 \ll \vec{B}_0\right)$, the Lorentz's force is $\vec{J} \times \vec{B}$, acting on the fluid, electrical conductivity is σ, the magnetic permeability is μ_m and electric field is $\vec{E}$.

It is pressumed that, the imposed and induced electric field is minute, the magnetic Reynolds number is low and μ_m is constant throughout the flow field. Hence the force simplifies as:

$$\vec{J} \times \vec{B} = -\sigma {B_0}^2 \mathfrak{U}. \tag{1.3}$$

The applications of magneto-hydrodynamics are very broad, ranging from astrophysics and plasma physics to drug targeting. The principle of magnetic field is also applied in medical field in the form of a device called Magnetic Resonance Imaging (MRI scanning - Fig 1.10), which is widely used for diagnosis of diseases of brain and other parts of the body. Further, the effect of magnetic field on fluid flows finds applications in devices such as Magnetohydrodynamic (MHD) power producers, heating of aerodynamic, MHD pumps, crude oil purification, etc. Moreover, many physiological fluids possess electrically conducting properties and hence different effects could be observed in fluid flow, in the existance of magnetic field.

Motivated by this, Sud et al. [152] considered the magnetic effect on pumping action of the blood. Prasad Rao et al. [106] studied free convection in hydrodynamic flows in a vertical wavy channel. Srivastava and Agrawal [148] have observed that blood constitutes of plasma wherein red cells occurs in suspension. They considered blood as an electrically conducting fluid. Radhakrishnamacharya and Radhakrishna Murthy [111] examined the interaction of heat flow and peristalsis of an incompressible viscous liquid moving inside a 2-dimensional conduit. RatishKumar and Naidu [119] discussed a numerical study of

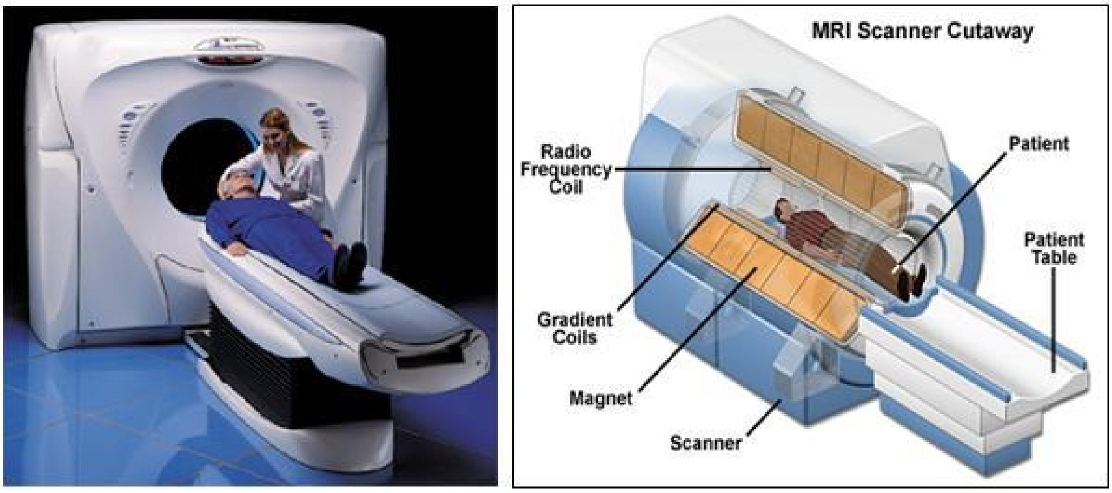

Figure 1.10

magnetic effects in peristaltic flows. Mekheimer [75] considered creeping stream of blood under the effect of a magnetic field in a non-uniform channel. Kim [56] observed the transfer of mass and heat in MHD-micropolar fluid over a vertical moving porous plate in a permeable medium. Mekheimer [77] dealt with the peristaltic movement of a magneto-micropolar fluid under the effect of induced magnetic field. The influence of wall characterstics and magnetic field on peristaltic transport through a porous medium has been explored by Kothandapani and Srinivas [60]. Recently, Many scholars studied MHD effects on various fluids under different limitations (Hayat et al. [39], Elmaboud [26], Akbar and Nadeem [7], Abd-Alla et al. [2], Kothandapani et al. [58]).

1.7 Porous Media

Porous medium is formed by many relatively closely packed particles or solid matrix with its void filled with fluids. A porous medium is a material containing pores or spaces in between the solid matter through which gas or liquid can pass. The human lung, bile duct, gallbladder with stones, small blood vessels, sandstone, beach sand, limestone are some of the examples of natural porous media (Figs. 1.11, 1.12, 1.13, 1.14, 1.15, 1.16). Moreover, movement of underground water, liquid filtration and water discharge in river beds are a limited example of flow through a permeable medium.

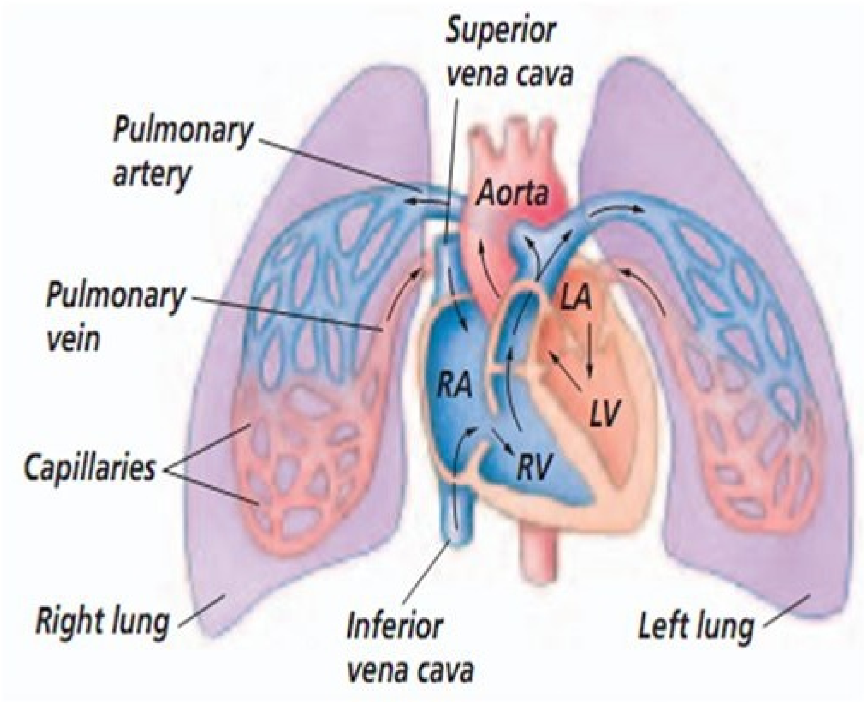

Figure 1.11

A peristaltic stream with a porous intermediate has attained significance in the current decade because of its practical applications mainly in biomechanics and geophysical fluid dynamics. Even in some pathological situations like: transportation of fluids in the kidneys, in the lungs, gallbladder with stones, small blood vessels and tissues, cartilage, bones and allocation of fatty cholesterol can be well thoughtout as a permeable medium. The proper functioning of these depends on the stream of blood, nutrients, etc., through them. The oil reservoirs are mainly composed of limestone and sandstone wherein the oil is trapped. With the knowledge of flow through permeable media. Oil extraction from the oil refinery can be enhanced, many medical conditions like tumor growth and their treatment can be well understood.

Terrill [159] studied laminar flow in a porous tube. Criskysikopoulos et al. [21] analyzed the one dimensional solute movement through a permeable medium with variable retardation factor. Pal [96] considered the influence of chemical response on the diffusion of a

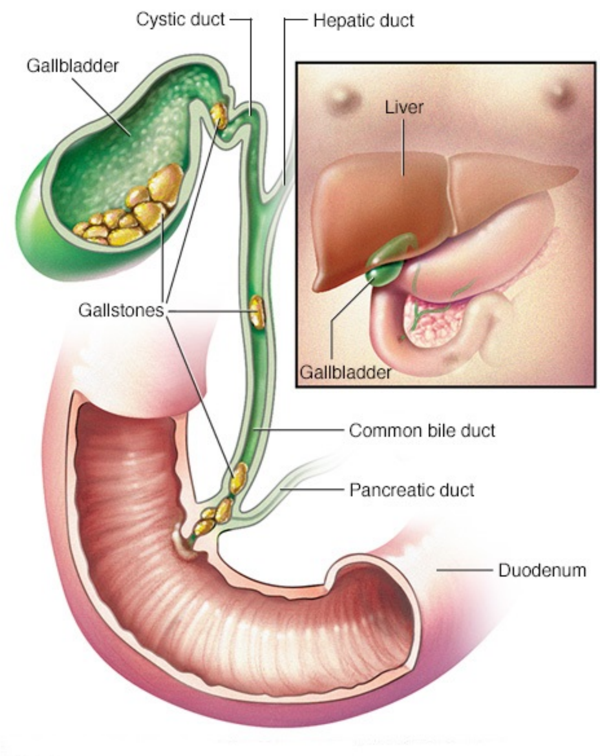

Figure 1.12

Figure 1.13

Figure 1.14

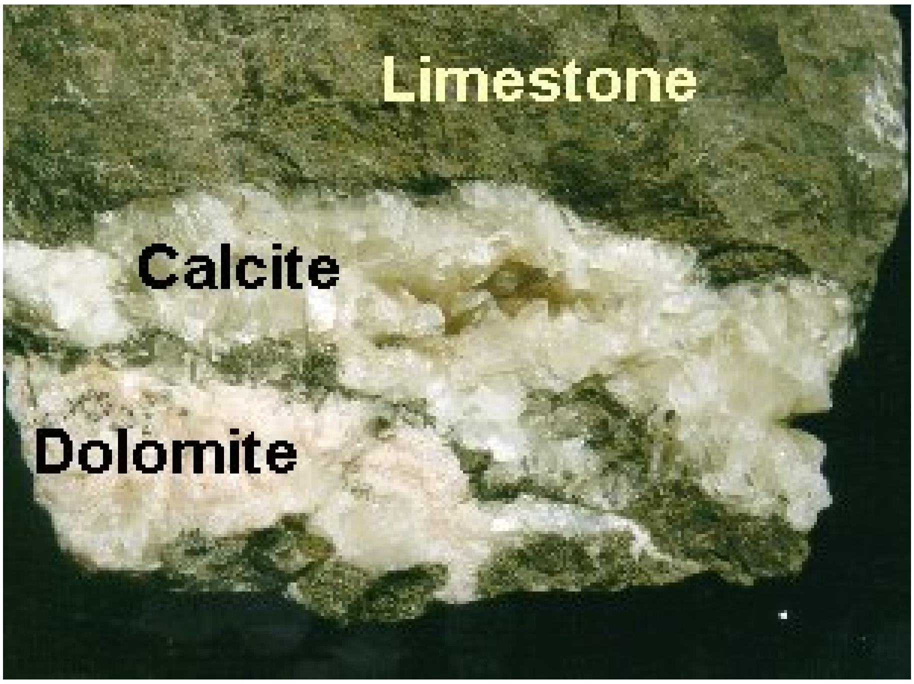

Figure 1.15

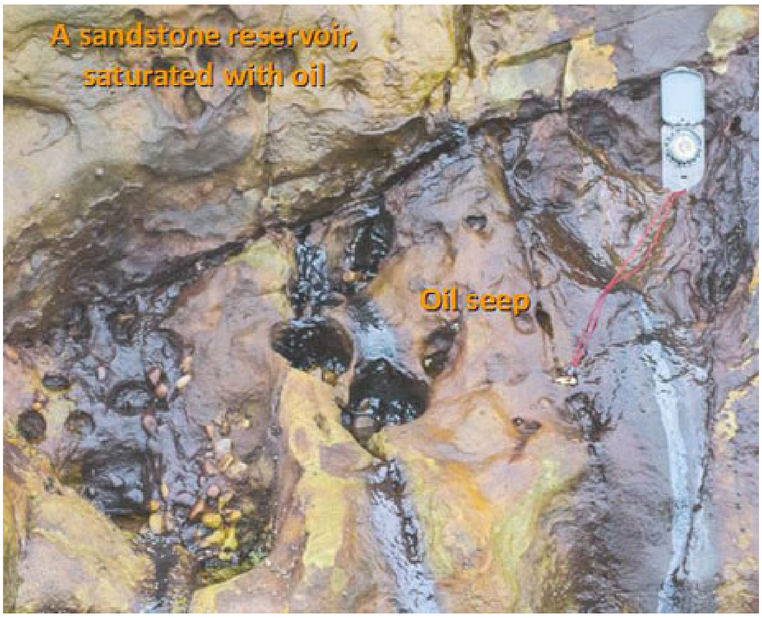

Figure 1.16

solute in a permeable medium. Shehawey and Sebaei [136] explored peristaltic movement with a permeable medium in a cylindrical tube. Quintard et al. [108] investigated scattering in heterogeneous porous media. Rao and Mishra [116] considered peristaltic pumping of a power law liquid in a porous tube. Hayat et al. [40] analyzed a mathematical model of peristalsis in tubes through a porous medium. Misra et al. [82] carried out peristaltic pumping of a physiological liquid in an asymmetric porous channel under external magnetic field. Sobh and Mady [143] considered creeping flow through a permeable medium in a non-uniform channel. Khan and Ellahi [53] discussed an exact solution for oscillatory flows of generalized Oldroyd-B fluid through a porous medium in a rotating frame. Khan et al. [4] studied the peristaltic transport of a Jeffrey fluid with variable viscosity through a porous medium in an asymmetric channel. Nadeem et al. [89] analyzed the creeping sinusoidal flow of nano-fluid through eccentric tubes comprising permeable medium. A mathematical study of the peristaltic pumping of viscoelastic liquid using the generalized fractional Burger's model through a non-uniform channel is presented by Tripathi and Beg [162]. Abed-Alla and Abo-Dahab [1] studied the effects of rotation and magnetic field on the peristaltic flow of a Jeffrey fluid in a symmetric channel through a permeable medium. Motivated by this, several investigators considered the effect of slip in various fluids flows under different limitations (Bhatt and Sacheti [15], Terrill [159], Kwang et al. [65], Mehta and Tiwari [73]. Ashgar et al. [12], Sobh [140], Srinivas et al. [144], Chaube et al. [20], Tripathi et al. [165], Akram [8], and Gurju et al. [33]).

Many physiological fluids like blood, chyme exhibit the behavior of Newtonian and non-Newtonian fluids. We describe below the relevant concepts and governing equations for an incompressible viscous fluid and couple stress fluid used in this thesis.

1.8 Classification of Fluids

Depending on the variation of strain rate with the stress within a matter, the viscosity can be classified as linear or non-linear. The matter exhibiting a relationship weherein stress is linearly comparative to the strain rate is termed Newtonian. In this contrast, a material exhibiting a non-linear relationship between the stress and the strain rate is termed non-Newtonian.

1.8.1 Newtonian Fluid

Biofluids are the fluids present in the ducts of the living body, which are treated either as Newtonian or non-Newtonian fluids depending on the physiological circumstances. Extensive research work has been carried out on the physiological liquid flow, during the last few decades, assuming the fluid under peristaltic motion to behave as a Newtonian fluid with constant viscosity. Newtonian behavior has been noticed in most of liquids with simple molecular structures and all gases.

Basic Equations

The constitute equations of motion characterizing an incompressible Newtonian fluid flow are given as:

$$\nabla \cdot \vec{q} = 0, \tag{1.4}$$

$$-\nabla P + \mu \nabla \times \nabla \times \vec{q} = \rho \left[\frac{\partial \vec{q}}{\partial t} + \vec{q} \cdot \nabla \vec{q} \right], \tag{1.5}$$

where the velocity vector is $\vec{q}$, the pressure is P, the density is ρ , the time is t, the coefficient of viscosity is μ.

The equation (1.4) and (1.5) represents the principles of conservation of mass and linear momentum.

The constitutive equation containing the stress tensor t_{ij} and rate of deformation tensor d_{ij} is given as:

$$t_{ij} = -P\delta_{ij} + 2\mu d_{ij}, \tag{1.6}$$

where δ_{ij} the Kronecker delta.

A huge work covering on mathematical and experimental models in a Newtonian or non-Newtonian fluid in a conduit has been carried out. Most of the researchers examined the fluid to behave like a viscous fluid with constant viscosity for physiological peristalsis including the flow of blood in arterioles. Gupta and Seshadri [31] investigated the transportation of a Newtonian fluid under peristalsis. The peristaltic transport of an incompressible generalized Newtonian liquid in a planar conduit has been explored by Misery et al. [79]. Naby and Misery [3] examined the impacts of an endoscope on the peristaltic flow of generalized Newtonian liquid. A Newtonian fluid in an irregular conduit was considered by Mishra and Rao [80] for the peristaltic movement analysis. The wall compliance on the creeping flow of a Newtonian liquid in an irregular channel has been considered by Haroun [35]. Some investigators studied creeping sinusoidal flow of an incompressible and viscous fluid with different limitations have been reported in references (Ebaid [24], Hayat and Nasir [38], Kothandapani and Srinivas [59], Raghunath Rao [114]).

1.8.2 Non-Newtonian Fluid

Non-Newtonian fluids cannot be explained with a single constitutive equation between stress and strain rate, but their constitutive equations lead to complicated mathematical problems. Thus the mathematicians, physicists, researchers are challenged in modeling, analyzing and solving the non-Newtonian fluid flows

Through the investigations, it is accepted that blood in tiny arteries and liquids in the lymphatic vessels and in the digestive system, urine under certain pathological conditions, etc. behave like non-Newtonian liquids. Al though the solution of non-Newtonian liquids is complex due to the appearance of the non-linear term, blood flow in human body, alloys and metals in industries, mercury amalgams and lubrication with heavy oils and greases in machines, are few examples of flow of non-Newtonian liquids that show us how important is the study of non-Newtonian fluids ([120]).

The following Non-Newtonian fluid model study has been made in this thesis:

Couple Stress Fluid

The discrepancy of the real fluids compared with that of the behavior of Newtonian fluid is well explained by the couple stress fluid theory. The equations that govern the couple stress fluid motion are none other than the Navier Stokes equations. Stokes [151] was the first person, who introduced couple stress fluid in 1966. Later, many researchers of the fluid dynamics concentrated on the study of couple stress fluid flow model. This model defines the rotation field in terms of the velocity field, i.e., the rotation vorticity vector ($\vec{\omega}$) is equal to one-half of the curl of the velocity ($\vec{q}$) (i.e. vorticity). Further, this theory takes into account all the important features and effects of the couple stresses, which results the Navier-Stokes equations.

Basic Equations

The equations of motion characterizing an incompressible couple stress fluid flow (Stokes [151]) after neglecting body couples and body forces are given as:

$$\nabla \cdot \vec{q} = 0, \tag{1.7}$$

$$-\nabla P - \mu \nabla \times \nabla \times \vec{q} - \eta \nabla \times \nabla \times \nabla \times \nabla \times \vec{q} = \rho \left[\frac{\partial \vec{q}}{\partial t} + \vec{q} \cdot \nabla \vec{q} \right], \tag{1.8}$$

where the velocity vector is $\vec{q}$, the pressure is P, the density is ρ , the time is t, the coefficient of viscosity is μ and the couple stress viscosity is η.

The equations (1.7)and (1.8) respectively represent the principles of conservation of mass and linear momentum.

The constitutive equation containing the stress tensor t_{ij} and deformation rate tensor d_{ij} is specified as:

$$t_{ij} = -P\delta_{ij} + +2\mu d_{ij} + \lambda(\nabla\cdot\vec{q})\delta_{ij} - \frac{1}{2}\varepsilon_{ijk}(m_{,k} + 4\eta_1\omega_{k,rr}), \tag{1.9}$$

For the couple stress tensor m_{ij}, the linear constitutive relation is observed as:

$$m_{ij} = \frac{1}{3}m\delta_{ij} + 4\eta_1\omega_{j,i} + 4\eta'\omega_{i,j}, \tag{1.10}$$

where the spin tensor is $\omega_{i,j}$, rate of deformation tensor is d_{ij}, and trace of the couple stress tensor is m. The viscosity coefficients are denoted by λ and μ, the couple stress viscosity coefficients denoted by η_1, η'.

These constants are bounded by the following inequalities:

$$3\lambda + 2\mu \geq 0; \quad \mu \geq 0; \quad \eta_1 \geq 0; \quad |\ \eta_1'\ | \leq \eta_1. \tag{1.11}$$

Here, $l = \sqrt{\frac{\eta_1}{\mu}}$ - the length constraint that measures the polarity of the fluid model and for non-polar fluids $l = 0$.

At the points on the boundary, the condition to be satisfied by the field vector $\vec{q}$ is the hyper-stick condition or condition of super adherence, which means that the velocity vector $\vec{q}$ and the effect of couple stresses on the tangential component of the spin vector $\vec{\omega} = \frac{1}{2}\nabla\times\vec{q}$ can be prescribed so as to synchronize with their respective values on the boundary.

As the couple stress fluid possesses the mechanism that explains complex rheological fluids as seen in blood and liquid crystals. The study of couple stress fluid has gained importance in the recent years. Couple stress fluid is a fluid consisting of rigid, randomly oriented particles suspended in a viscous medium, such as blood, lubricants containing small amount of high polymer additive, electro-rhelogical fluids and synthetic fluids. The main feature of couple stresses is to introduce a size dependent effect. Numerous research works pertaining to couple stress fluid are brought out by Srivastava [147]. The research carried on this fluid is much helpful in many physiological problems. The transport of this liquid under peristalsis has been analyzed by Shehawey and Mekheimer [134]. Kothandapani and Srinivas [59] examined the MHD creeping flow of this fluid with heat and compliant wall. Pandey and Chaube [98] gave a report on the motion of this fluid within a conduit having wall features with peristalsis. They showed that the boundary velocity of the fluid reduces with gains in couple stress constraint. The couple stress fluid was analyzed for creeping flow to know the relevance in hemodynamics by Maiti and Misra [70]. Some studies on the peristaltic transport of couple stress fluid have been reported in references (Valanis and Sun [167], Sagayamary and Devanathan [126], Mekheimer [74, 77], Sobh [140], Bujurke and Jayaraman [17], Wang et al. [168])

1.9 Problem statement

The liquids existing in the ducts of living being can be categorized as Newtonian and non-Newtonian liquids based on their behavior. It is considered that the blood and other physiological liquids exhibit Newtonian as well as non-Newtonian behaviors. Several investigators have contributed in this regard. But, the dispersion of a solute substance and the flow of an incompressible viscous fluid and couple stress fluid with wall features have not been considered. Thus, in view of studying an incompressible viscous fluid and couple stress fluid with wall properties, the following research issues have been considered.

This necessity has led to the following research issues:

What is the effect of peristalsis on dispersion of an incompressible viscous fluid with wall features? What effect do the wall and chemical response on the peristaltic pumping of an incompressible viscous fluid in a permeable medium? What might be the effect of MHD on this flow? In addition to these, what might be the effects of the above studies when a non-Newtonian fluid is taken into consideration instead of the Newtonian fluid?

1.10 Objective of the research

The objective of the thesis is to explore peristalsis and dispersion of a solute substance with wall features by the analytical method, and assess appropriate conclusions when applied to the peristaltic flow issues. The mathematical modeling is based on some suppositions leading to tractable analytical solutions of the problem to examine the relation between constraints.

The core objective is to study the interaction of peristalsis and dispersion on an incompressible viscous fluid and couple stress fluid models to examine the MHD, porosity, chemical response rate effects in a uniform channel having compliant walls. The flow is modeled by taking into consideration of long wavelength hypothesis, Taylor's procedure and twistable periphery conditions.

1.11 Outline of the Thesis

The first chapter is introductory, deals with several characteristics of the fluid and the relevant literature survey, thus explaining the reason for consideration of the problems involved in the following chapters of the thesis and the basic equations of the fluid model.

An incompressible viscous fluid and couple stress fluid models have been used since they are known to be better models for physiological fluids, particularly, blood, chyme, bile. Keeping these things in mind, the following problems have been considered in chapters 2 - 7 of the thesis.

Chapters 2 to 4 consider the effect of peristalsis on dispersion of a solute in an incompressible and viscous fluid flow with wall features wherein chapters 5 to 7 deal with dispersion of a solute in peristaltic motion of a couple stress fluid with wall features under different limitations. For the analysis, long wavelength hypothesis, Taylor's procedure and twistable periphery conditions are considered.

Chapter 2 studies the scattering of a solute matter in the peristaltic transport of an incompressible and viscous fluid in a uniform channel having wall properties. Long wavelength hypothesis, Taylor's procedure and twistable periphery conditions at the flexible walls are used to find a closed form solution for the average effective scattering coefficient in the presence of simultaneous homogeneous and heterogeneous chemical reactions. The effects of various pertinent constraints on the effective scattering coefficient are discussed. It is seen that average scattering ascends with an amplitude ratio, which implies that scattering is high in the existence of peristalsis. It also increases with the rigidity, stiffness and deceptive nature of the walls. Further, dispersion descends with heterogeneous and homogeneous chemical response rates.

The effectiveness of the analytical expression of the mean scattering coefficient for the peristaltic pumping of an incompressible and viscous fluid in a uniform porous channel with elastic wall is analyzed and assessed in chapter 3. Using dynamic boundary conditions, Taylor's procedure and long wavelength hypothesis, the analytic solution has been computed. The influence of permeability constraint, peristalsis through amplitude ratio, rigidness, stiffness, damping characteristic of wall, heterogeneous and homogeneous response rates on scattering coefficient have been examined through graphs. It is noticed that peristalsis enhances scattering of a solute. It is also revealed that scattering amplifies with the permeability and wall constraints. Further, it falls with homogeneous response and heterogeneous response rates.

Chapter 4, presents analytical results for the dispersion of a solute matter in magnetohydrodynamic (MHD) peristaltic motion of a viscous fluid with wall properties. The magnetic field is applied uniformly at right angles to the channel wall. Following the same procedure as in the previous chapters, the solution for the effective scattering coefficient has been determined analytically. The effects of various relevant constraints are discussed. It is witnessed that scattering rises with peristalsis, permeability and wall characteristics. Further, scattering fall down with homogenous response and heterogeneous response rates.

Chapter 5 reports the dispersion and the creeping sinusoidal flow of an incompressible couple stress fluid in a uniform channel having compliant walls. The equations governing the flow have been linearized by long wavelength hypothesis and mathematical expression of the scattering coefficient has been found using Taylor's procedure and dynamic border conditions of the flexible wall. The elastic wall features on scattering coefficient with peristalsis has been studied through graphs. It is found that rigidness, stiffness and dissipative nature of the wall enhance the scattering. It is also noted that scattering coefficient increases with amplitude ratio and couple stress constraint. Conversely, it is found to decrease with homogeneous and heterogeneous response rates.

Chapter 6 concentrates on scattering of a solute matter in the creeping sinusoidal flow of an incompressible and couple stress fluid through a permeable medium with wall properties. Long wavelength hypothesis, Taylor's procedure and dynamic boarder conditions have been applied to obtain the average effective scattering coefficient in the existence of heterogeneous-homogeneous chemical responses. The effects of various pertinent constraints on the scattering coefficient are presented graphically. It is examined that average effective scattering coefficient increases with the amplitude ratio, which clears that scattering is high in the existence of peristalsis. It is also noticed that scattering rises with the porosity and wall constraints. Further, it is found to drop with couple stress constraint, homogeneous and heterogeneous response rates.

In chapter 7, an attempt has been made to investigate the diffusion of a solute in the magnetohydrodynamic (MHD) creeping sinusoidal flow of a couple stress fluid having wall properties. Considering the flexible effects of deformable boundaries, the relevant stream equations of motion have been solved under long wavelength hypothesis. Taylor's procedure and dynamic periphery circumstances at the elastic walls have been used to find a closed form expression for effective scattering coefficient. It is witnessed that the scattering increases with rigidity, stiffness, deceptive nature of the walls. Conversely, it reduces with magnetic constraint, couple stress constraint, homogeneous and heterogeneous chemical response rates. It can also be viewed that the occurrence of peristalsis, enhances scattering of a solute.

Finally, chapter eight gives the main conclusions and scope for future work.

Part - I

Peristalsis and Dispersion of a Solute in an Incompressible Viscous Fluid with Chemical Reactions and Wall Effects

Chapter 2

Effect of Chemical Reactions on Dispersion of a Solute in Peristaltic Motion of an Incompressible Viscous Fluid with Wall Properties

2.1 Introduction

Peristaltic motion is a well-known natural phenomenon of fluid mixing and movement that take place in biological tracts. The mechanism behind this is the progressive wave moving along the boundaries of the tract from the region of low pressure to high pressure through driving action studied by Yin and Fung [29]. In particular, it occurs in many physiological situations like transport of mixture of food grains and liquids in the esophagus, movement of urine through the ureter, driving blood in small blood vessels, etc. This process appears in many industrial systems to force/drive corrosive and sanitary fluids. Several researchers have studied many liquids with peristalsis under different circumstances (Fung and Yih [28], Shapiro et al. [50], Shehawey and sebaei [136], Radhakrishnamacharya [109], Tripathi and Beg [165], Misra and Pandey [85], Takagi and Balmforth [154]). Mittra and Prasad [86] have studied the wall effects on Poiseuille flow with peristalsis. In addition, several researchers have explored the wall effects on non- Newtonian fluids in peristalsis (Muttu et al. [87], Sankad and Radhakrishnamacharya [128]).

Dispersion is a mechanism that enhances the rate of broadening of a solute cloud in flow through a tube or channel and which can be utilized as an effective means to accomplish mixing or diluting. Dispersion plays a central task in chyme transport and other applications like environmental pollutant transportation, chromatographic separation, the mixing and transport of drugs or toxic substances in physiological structures (Ng [91]). The dispersion of a solute in a solvent flowing in a channel has wide applications in physiological fluid dynamics, biomedical and chemical industries. The basic theory of dispersion was first proposed by Taylor [156, 157, 158] and he further discussed the dispersion of a solute in a circular pipe with an incompressible viscous fluid through laminar flow. Taylor investigated that, the solute disperses with an equivalent average effective dispersion coefficient, and the dispersion depends on the radius of the tube, coefficient of molecular diffusion and average speed of the flow, under the hypothesis that the solute material does not chemically react with the fluid. Aris [11], Padma and Rao [93], Gupta and Gupta [32], Rao and Padma [94, 95], and other several investigators have investigated the dispersion of a solute in viscous fluid, under different limitations. Furthermore, Chandra and Agarwal [5], Philip and Chandra [19], Dutta et al. [23], Hayat et al. [41, 45], Alemayehu and Radhakrishnamacharya [10], and Ravikiran and Radhakrishnamacharya [121] extended this analysis to non Newtonian fluids. Several studies have been carried out on the dispersion with chemical reactions for Newtonian and non-Newtonian fluids.

Diffusion and peristalsis are more essential characteristics in bio-medical, natural and chemical processes. The liquids present in the ducts of living being can be classified as Newtonian and non-Newtonian fluids based on their behavior. The impact of simultaneous homogeneous, heterogeneous reactions with peristalsis of an incompressible viscous fluid with wall properties has not received much attention. Peristalsis may have significant effects on the dispersion of a solute in fluid flow. Hence, in this chapter, we have considered a mathematical model to study the peristaltic pumping of Newtonian fluid with wall features and chemical reactions through δ-approximation, conditions of Taylor's limit and dynamic boundary conditions. The analytical expression for the mean effective scattering coefficient has been obtained and results are analyzed for different values of relevant constraints through graphs.

2.2 Formulation of the Problem

We have considered peristaltic pumping of an incompressible viscous fluid in the 2- dimensional compliant wall channel, the Cartesian coordinates (x, y) with x- axis at the centre of the fluid flow and the homogeneous, heterogeneous reaction effects in the flow analysis. The peristaltic wave with speed c produces the flow travelling along the walls of the channel. Figure 2.1 shows the travelling waves.

The wave shape is given by the subsequent equation as:

$$\mathcal{Y} = \pm h = \pm \left[d + a \sin \frac{2\pi}{\lambda} (\mathcal{X} - ct) \right], \tag{2.1}$$

where the speed is c, the amplitude is a, the wavelength of the wave is λ, and the half width of the channel is d.

The relating flow equations (Gupta and Seshadri [31]) of the present issue as:

$$\frac{\partial \mathcal{U}}{\partial \mathcal{X}} + \frac{\partial \mathcal{V}}{\partial \mathcal{Y}} = 0, \tag{2.2}$$

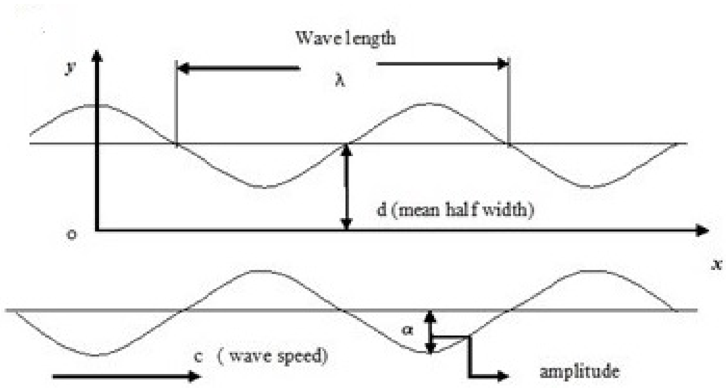

Figure 2.1: Geometry of the problem

$$-\frac{\partial p}{\partial \mathcal{X}}+\mu\left(\frac{\partial^2}{\partial \mathcal{X}^2}+\frac{\partial^2}{\partial \mathcal{Y}^2}\right)\mathcal{U}=\rho\left[\frac{\partial}{\partial t}+\mathcal{U}\frac{\partial}{\partial \mathcal{X}}+\mathcal{V}\frac{\partial}{\partial \mathcal{Y}}\right]\mathcal{U}, \tag{2.3}$$

$$-\frac{\partial p}{\partial \mathcal{Y}}+\mu\left(\frac{\partial^2}{\partial \mathcal{X}^2}+\frac{\partial^2}{\partial \mathcal{Y}^2}\right)\mathcal{V}=\rho\left[\frac{\partial}{\partial t}+\mathcal{U}\frac{\partial}{\partial \mathcal{X}}+\mathcal{V}\frac{\partial}{\partial \mathcal{Y}}\right]\mathcal{V}, \tag{2.4}$$

where the fluid density is ρ, the pressure is p, the viscosity coefficient is μ, the velocity component in the $\mathcal{X}$ direction is $\mathcal{U}$, velocity component in $\mathcal{Y}$ direction is $\mathcal{V}$.

Referring Mittra and Prasad [86], the condition of the flexible wall movement is specified as:

$$\mathcal{L}(h)=p-p_0, \tag{2.5}$$

where the movement of the stretched membrane by the damping force is $\mathcal{L}$ and is intended by the subsequent equation:

$$\mathcal{L}=-\mathcal{T}\frac{\partial^2}{\partial \mathcal{X}^2}+m\frac{\partial^2}{\partial t^2}+\mathbf{C}\frac{\partial}{\partial t}. \tag{2.6}$$

Here, the coefficient of sticky damping force is $\mathbf{C}$, the mass per/area is m, and the membrane tension is $\mathcal{T}$.

2.3 Method of Solution

Under long - wavelength hypothesis and referring Alemayehu and Radhakrishnamacharya [9], the equations (2.2) to (2.4) yield as:

$$\frac{\partial \mathcal{U}}{\partial \mathcal{X}} + \frac{\partial \mathcal{V}}{\partial \mathcal{Y}} = 0, \tag{2.7}$$

$$-\frac{\partial p}{\partial \mathcal{X}} + \mu \frac{\partial^2 \mathcal{U}}{\partial \mathcal{Y}^2} = 0, \tag{2.8}$$

$$-\frac{\partial p}{\partial \mathcal{Y}} = 0. \tag{2.9}$$

The appropriate periphery conditions are specified as:

$$\mathcal{U} = 0, \ \text{ at } \quad \mathcal{Y} = \pm h. \tag{2.10}$$

It is presumed that $p_0 = 0$ and the channel walls are inextensible; therefore, the straight displacement of the wall is zero and only lateral movement takes place, and from equation (2.5), (2.6) and (2.8), we get

$$\frac{\partial}{\partial \mathcal{X}} \mathcal{L}(h) = \mu \frac{\partial^2 \mathcal{U}}{\partial \mathcal{Y}^2} \quad \text{at} \quad \mathcal{Y} = \pm h, \tag{2.11}$$

where

$$\frac{\partial}{\partial \mathcal{X}} \mathcal{L}(h) = \frac{\partial p}{\partial \mathcal{X}} = -\mathcal{T} \frac{\partial^3 h}{\partial \mathcal{X}^3} + m \frac{\partial^3 h}{\partial \mathcal{X} \partial t^2} + \mathsf{C} \frac{\partial^2 h}{\partial \mathcal{X} \partial t}. \tag{2.12}$$

After solving equations (2.8) and (2.9) with the conditions (2.10) and (2.11), we obtain

$$\mathcal{U}(\mathcal{Y}) = \frac{1}{2\mu} \left(\frac{\partial p}{\partial \mathcal{X}} \right) \left(\mathcal{Y}^2 - h^2 \right), \tag{2.13}$$

The mean velocity is specified as:

$$\bar{\mathcal{U}} = \frac{1}{2h}\int_{-h}^{h} \mathcal{U}(\mathcal{Y})dy. \tag{2.14}$$

Equations (2.13) and (2.14) yield as:

$$\bar{\mathcal{U}} = -\frac{1}{\mu}\left(\frac{\partial p}{\partial \mathcal{X}}\right)\frac{h^2}{3}. \tag{2.15}$$

If convection is across the plane moving with the mean speed of the flow, then relative to this plane, the fluid velocity is given by the condition (Alemayehu and Radhakrishnamacharya [10], Sobh [142]).

$$\mathcal{U}_{\mathcal{X}} = \mathcal{U} - \bar{\mathcal{U}}. \tag{2.16}$$

From equations (2.13), (2.15) and (2.16), we find

$$\mathcal{U}_{\mathcal{X}} = \frac{1}{2\mu}\left(\frac{\partial p}{\partial \mathcal{X}}\right)\left(\mathcal{Y}^2 - \frac{h^2}{3}\right), \tag{2.17}$$

where

$$\mathcal{P}' = \frac{\partial p}{\partial \mathcal{X}} = -\mathcal{T}\frac{\partial^3 h}{\partial \mathcal{X}^3} + m\frac{\partial^3 h}{\partial \mathcal{X}\partial t^2} + \mathsf{C}\frac{\partial^2 h}{\partial \mathcal{X}\partial t}.$$

2.4 Simultaneous homogeneous and heterogeneous chemical reactions with diffusion

The first order irreversible reaction model in the peristaltic pumping of viscous fluid flow under isothermal conditions (Taylor [156], Gupta and Gupta [32]) is considered as:

$$\frac{\partial C}{\partial t} + \mathcal{U}\frac{\partial C}{\partial \mathcal{X}} = \mathcal{D}\left(\frac{\partial^2 C}{\partial \mathcal{X}^2} + \frac{\partial^2 C}{\partial \mathcal{Y}^2}\right) - k_1 C. \tag{2.18}$$

Using Taylor's approximation $\frac{\partial^2 C}{\partial x^2} \leq \frac{\partial^2 C}{\partial y^2}$, the equation (2.18) is expressed as:

$$\frac{\partial C}{\partial t} + u\frac{\partial C}{\partial \mathcal{X}} = D\frac{\partial^2 C}{\partial \mathcal{Y}^2} - k_1 C. \tag{2.19}$$

In the above equation, concentration of the fluid is C, the molecular diffusion coefficient is $\mathcal{D}$ and the rate constant of first order chemical response is k_1.

For the regular estimations of physiologically essential parameters of this issue, it is normal that $\bar{\mathcal{U}} \approx C$ (Alemayehu and Radhakrishnamacharya [10]).

Utilizing this condition $\bar{\mathcal{U}} \approx C$, with below specified dimensionless quantities,

$$\theta = \frac{t}{\bar{t}}, \quad \bar{t} = \frac{\lambda}{\bar{\mathcal{U}}}, \quad \eta = \frac{\mathcal{Y}}{d}, \quad \xi = \frac{(\mathcal{X} - \bar{\mathcal{U}}t)}{\lambda}, \quad \mathcal{H} = \frac{h}{d}, \quad \mathcal{P} = \frac{d^2}{\mu c \lambda}\mathcal{P}'. \tag{2.20}$$

Equations (2.12), (2.17) and (2.19) reduce to

$$\mathcal{P} = -\varepsilon\left[(\mathcal{E}_1 + \mathcal{E}_2)(2\pi)^3\cos(2\pi\xi) - \mathcal{E}_3(2\pi)^2\sin(2\pi\xi)\right], \tag{2.21}$$

$$\mathcal{U}_{\mathcal{X}} = \frac{d^2}{2\mu}\frac{\partial p}{\partial \mathcal{X}}\left(\eta^2 - \frac{H^2}{3}\right), \tag{2.22}$$

$$\frac{\partial^2 C}{\partial \eta^2} - \frac{k_1 d^2}{\mathcal{D}}C = \frac{d^2}{\lambda \mathcal{D}}\mathcal{U}_{\mathcal{X}}\frac{\partial C}{\partial \xi}, \tag{2.23}$$

where
the amplitude ratio is $\varepsilon\left(= \frac{a}{d}\right)$, the rigidity is $\mathcal{E}_1\left(= -\frac{\mathcal{T}d^3}{\lambda^3\mu\mathbf{c}}\right)$, the stiffness is $\mathcal{E}_2 = \left(\frac{m\mathbf{c}d^3}{\lambda^3\mu}\right)$, the viscous damping force in the wall is $\mathcal{E}_3 = \left(\frac{\mathbf{c}d^3}{\mu\lambda^2}\right)$.

Below, we discuss the diffusion with first order reaction taking place in the mass of the fluid medium and at the walls of the channel, the walls are catalytic to chemical reaction. Hence, the boundary conditions at the walls (Philip and Chandra [19]) are expressed by the following equations:

$$0=\mathcal{F}C+\frac{\partial C}{\partial \mathcal{Y}} \quad \text{at} \quad \mathcal{Y}=[a\sin\frac{2\pi}{\lambda}(\mathcal{X}-\bar{\mathcal{U}}t)+d]=h, \tag{2.24}$$

$$0=-\mathcal{F}C+\frac{\partial C}{\partial \mathcal{Y}} \quad \text{at} \quad \mathcal{Y}=-[a\sin\frac{2\pi}{\lambda}(\mathcal{X}-\bar{\mathcal{U}}t)+d]=-h. \tag{2.25}$$

If we use the equation (2.20), the conditions (2.24) and (2.25) reduces to

$$0=\beta C+\frac{\partial C}{\partial \eta} \quad \text{at} \quad \eta=[\varepsilon\sin(2\pi\xi)+1]=\mathcal{H}, \tag{2.26}$$

$$0=-\beta C+\frac{\partial C}{\partial \eta} \quad \text{at} \quad \eta=-[\varepsilon\sin(2\pi\xi)+1]=-\mathcal{H}, \tag{2.27}$$

where the heterogeneous response rate parameter corresponding to the catalytic response at the walls is $\beta=\mathcal{F}d$.

Assuming that $\frac{\partial C}{\partial \xi}$ is independent of η at any cross section, we obtain the concentration of the solute C as follows:

$$C(\eta)=-\frac{d^4}{2\lambda\mu\mathcal{D}}\frac{\partial C}{\partial \xi}\frac{\partial p}{\partial \mathcal{X}}\Big[\frac{A_1}{A_2}\cosh(\alpha\eta)+\frac{\mathcal{H}^2}{3\alpha^2}-\frac{\eta^2}{\alpha^2}-\frac{2}{\alpha^4}\Big], \tag{2.28}$$

where $A_1=\alpha\sinh\alpha\mathcal{H}+\beta\cosh\alpha\mathcal{H}, \quad A_2=\left(\frac{2\mathcal{H}}{\alpha^2}+\frac{2\beta\mathcal{H}^2}{3\alpha^2}+\frac{2\beta}{\alpha^4}\right).$

The volumetric rate $\mathcal{Q}$ is defined as the rate in which the solute is pumping across a section of channel per unit breadth.

$$\mathcal{Q}=\int_{-\mathcal{H}}^{\mathcal{H}} C\,\mathcal{U}_{\mathcal{X}}d\eta. \tag{2.29}$$

Using equations (2.22) and (2.28) in equation (2.29), we get

$$\mathcal{Q}=-2\frac{d^6}{\lambda\mu^2\mathcal{D}}\frac{\partial C}{\partial \xi}\mathcal{G}(\xi,\alpha,\beta,\varepsilon,\mathcal{E}_1,\mathcal{E}_2,\mathcal{E}_3), \tag{2.30}$$

where

$$\mathcal{G}(\xi,\alpha,\beta,\varepsilon,\mathcal{E}_1,\mathcal{E}_2,\mathcal{E}_3) = \\ \left[\mathcal{P}\frac{A_2}{2A_1}\left(\frac{\mathcal{H}^2}{3\alpha}\sinh\alpha\mathcal{H} - \frac{\mathcal{H}}{\alpha^2}\cosh\alpha\mathcal{H} + \frac{1}{\alpha^3}\sinh\alpha\mathcal{H}\right) - \mathcal{P}\frac{\mathcal{H}^5}{45\alpha^2}\right]. \quad (2.31)$$

Glancing at equation (2.30) with Fick's law of diffusion, the scattering coefficient $\mathcal{D}^*$ was calculated such that the solute disperses near to the plane moving with the typical speed of the flow and is specified as:

$$\mathcal{D}^* = 2\frac{d^6}{\mu^2\mathcal{D}}\mathcal{G}(\xi,\alpha,\beta,\varepsilon,\mathcal{E}_1,\mathcal{E}_2,\mathcal{E}_3). \quad (2.32)$$

Let $\bar{\mathcal{G}}$ be the mean of $\mathcal{G}$ and is attained by the succeeding equation:

$$\bar{\mathcal{G}} = \int_0^1 \mathcal{G}(\xi,\alpha,\beta,\varepsilon,\mathcal{E}_1,\mathcal{E}_2,\mathcal{E}_3)d\xi. \quad (2.33)$$

2.5 Outcomes and Discussion

This segment is prepared to investigate the impacts of different constraints on the concentration. The mean effective dispersion coefficient was observed through the function $\bar{\mathcal{G}}(\xi,\alpha,\beta,\varepsilon,\mathcal{E}_1,\mathcal{E}_2,\mathcal{E}_3)$ for simultaneous homogeneous, heterogeneous reactions given by equation (2.33). $\bar{\mathcal{G}}$ was computed by the software MATHEMATICA and end results are presented graphically. The penetrating constraints present in this argument are the amplitude ratio (ε), the homogeneous reaction rate (α), the heterogeneous reaction rate (β), the rigidity ($\mathcal{E}_1$), the stiffness ($\mathcal{E}_2$), and the viscous damping force ($\mathcal{E}_3$). We may ensure that $\mathcal{E}_1, \mathcal{E}_2$ and $\mathcal{E}_3$ cannot be zero all together.

We have considered the Figs. 2.2, 2.3, 2.4, and 2.5 for the impact of the rigidity parameter ($\mathcal{E}_1$) of the elastic wall on the mean effective dispersion coefficient ($\bar{\mathcal{G}}$). Dispersion enhances with increase in wall rigidity ($\mathcal{E}_1$) in the cases of (a) without stiffness in the wall ($\mathcal{E}_2$=0) and perfectly elastic wall ($\mathcal{E}_3$=0) (Figs. 2.2, 2.4); (b) with stiffness in the wall ($\mathcal{E}_2 \neq$0) and dissipative wall ($\mathcal{E}_3 \neq$0) (Figs. 2.3, 2.5). It is observed that $\bar{\mathcal{G}}$ increases with the stiffness ($\mathcal{E}_2$) when the wall is dissipative in nature ($\mathcal{E}_3 \neq 0$) (Figs. 2.7, 2.8). Further, it is noted that boost in viscous damping force ($\mathcal{E}_3$) increases $\bar{\mathcal{G}}$ for both the cases of without stiffness in the wall ($\mathcal{E}_2 = 0$) (Figs. 2.10, 2.12) and stiffness in the wall ($\mathcal{E}_2 \neq 0$) (Figs. 2.11, 2.13). This understanding might be derived to the truths that the increment in the flexibility of the channel walls helps the stream moment which causes to enhance the scattering. It is also noticed that dispersion is more in presence of stiffness in the wall as compared to without stiffness in the wall. These results are in agreement with the results of Ravikiran and Radhakrishnamacharya [122, 123]. Furthermore, the effective dispersion coefficient enhances with an increase in the amplitude ratio (ε) (Figs. 2.6, 2.9, 2.14). As already known, the increment in the amplitude ratio is the expansion in the amplitude of the wave across the channel and this cause to increase the fluid velocity within the channel and consequently dispersion may enhance. This outcome concurs with that of Sobh [142], Alemayehu and Radhakrishnamacharya [9, 10].

Diffusion reduces with homogeneous response rate (α) (Figs. 2.2, 2.3, 2.7, 2.10, 2.11) and heterogeneous response rate (β) (Fig. 2.4, 2.5, 2.8, 2.12, 2.13). This result is consistent with the arguments of Gupta and Gupta [32], Sobh [142], Alemayehu and Radhakrishnamacharya [9], Hayat et al. [45], Ravikiran and Radhakrishnamacharya [122].

2.6 Conclusion

The present study investigates the effect of compliant wall and chemical reactions on Newtonian fluid with peristalsis. It is observed that, the concentration profile ($\bar{\mathcal{G}}$) amplifies with an increase in amplitude ratio and wall constraints. Furthermore, opposite behaviors of heterogeneous response and homogeneous response rate constraints are observed on $\bar{\mathcal{G}}$. Finally, it concludes that amplitude ratio, wall constraints favor the scattering and peristaltic flow increases the dispersion.

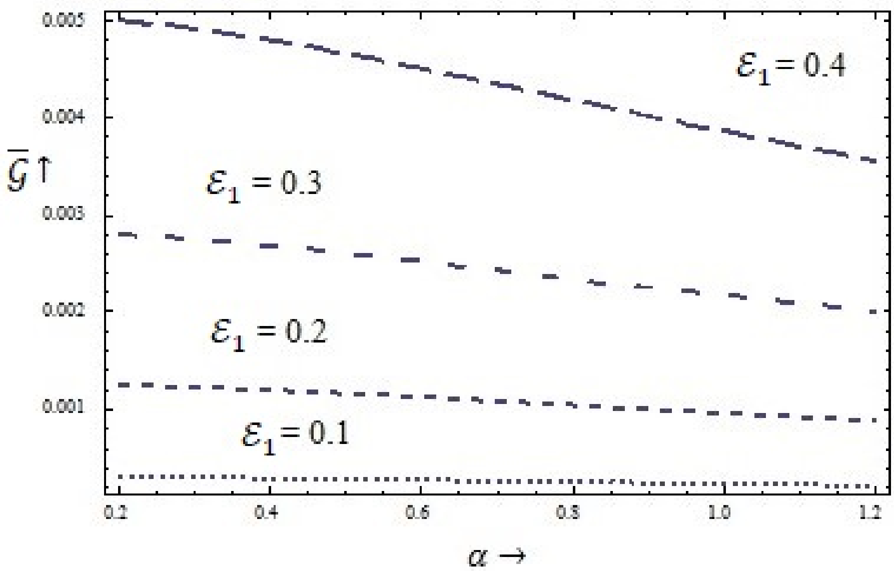

Figure 2.2: Illustration of scattering coefficient $\bar{\mathcal{G}}$ with $\mathcal{E}_1$ with $\varepsilon = 0.2$, $\beta = 5.0$, $\mathcal{E}_2 = 0.0$, $\mathcal{E}_3 = 0.00$.

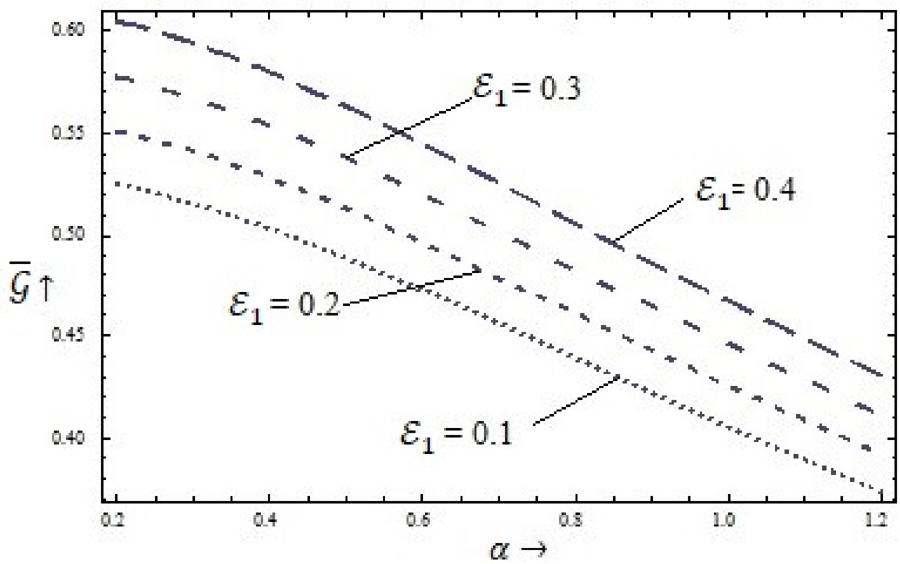

Figure 2.3: Illustration of scattering coefficient $\bar{\mathcal{G}}$ with $\mathcal{E}_1$ with $\varepsilon = 0.2$, $\beta = 5.0$, $\mathcal{E}_2 = 4.0$, $\mathcal{E}_3 = 0.06$.

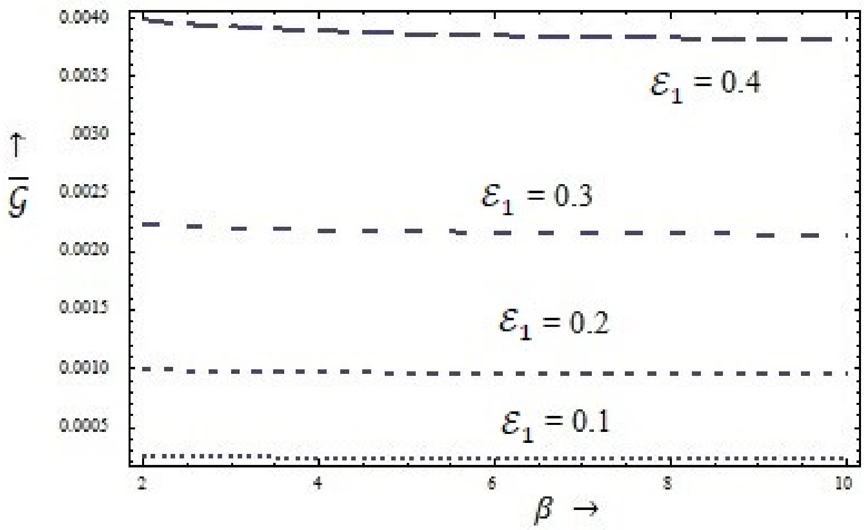

Figure 2.4: Illustration of scattering coefficient $\bar{\mathcal{G}}$ with $\mathcal{E}_1$ with $\varepsilon = 0.2$, $\alpha = 1.0$, $\mathcal{E}_2 = 0.0$, $\mathcal{E}_3 = 0.00$.

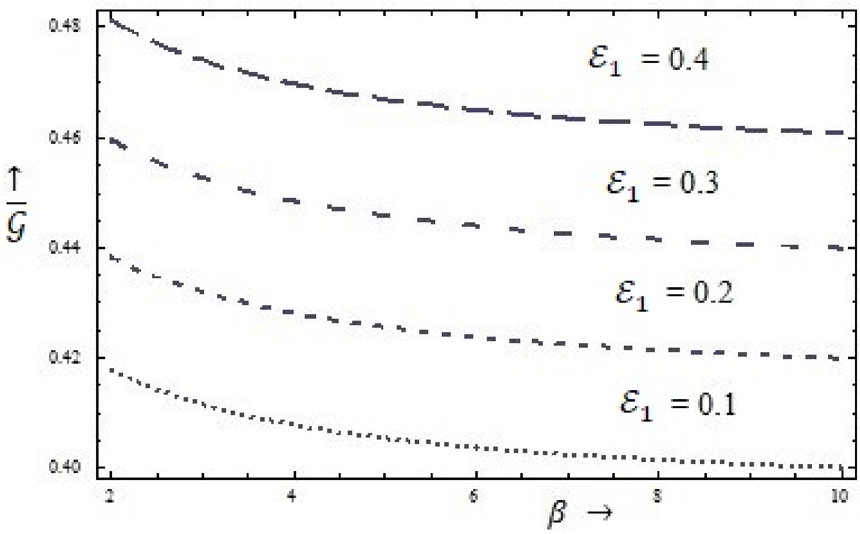

Figure 2.5: Illustration of scattering coefficient $\bar{\mathcal{G}}$ with $\mathcal{E}_1$ with $\varepsilon = 0.2$, $\alpha = 1.0$, $\mathcal{E}_2 = 4.0$, $\mathcal{E}_3 = 0.06$.

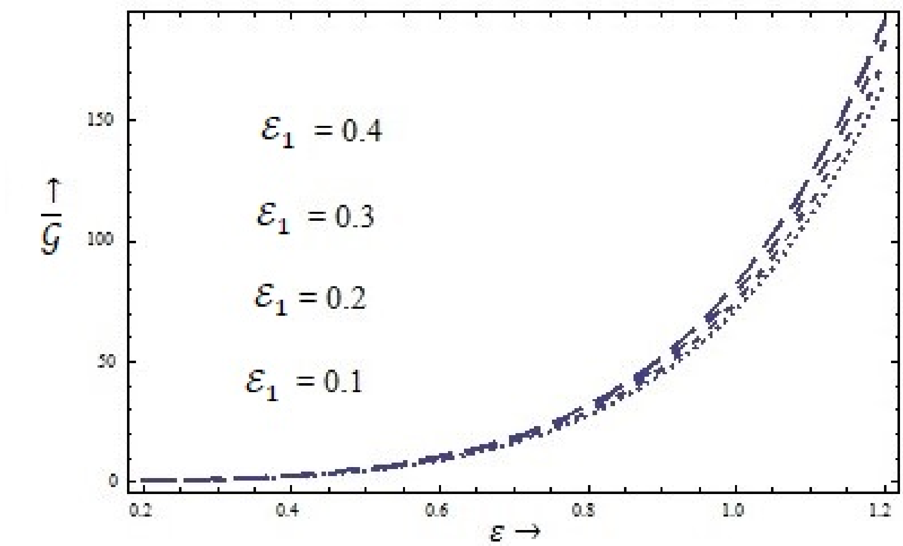

Figure 2.6: Illustration of scattering coefficient $\bar{\mathcal{G}}$ with $\mathcal{E}_1$ with $\alpha = 1.0$, $\beta = 5.0$ $\mathcal{E}_2 = 4.0$, $\mathcal{E}_3 = 0.00$.

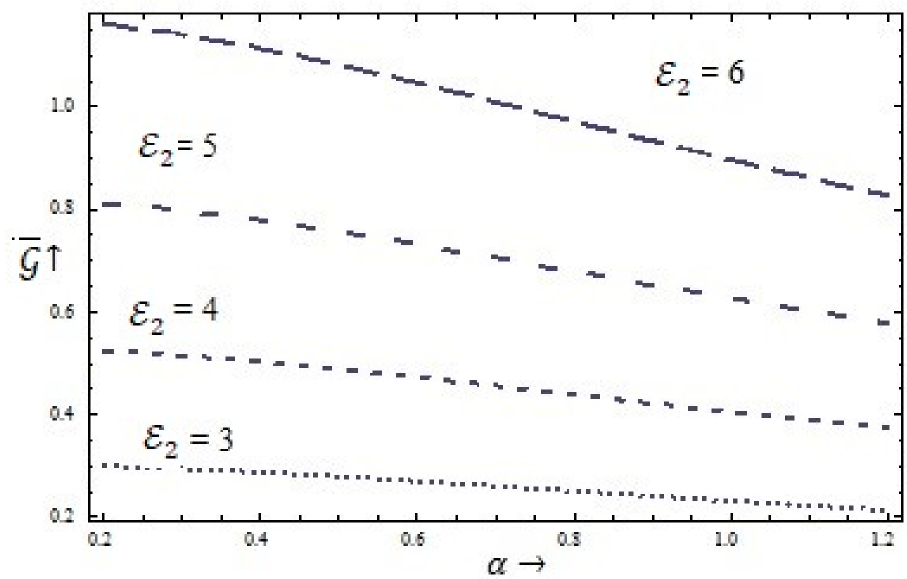

Figure 2.7: Illustration of scattering coefficient $\bar{\mathcal{G}}$ with $\mathcal{E}_2$ with $\varepsilon = 0.2$, $\beta = 5.0$, $\mathcal{E}_1 = 0.1$, $\mathcal{E}_3 = 0.06$.

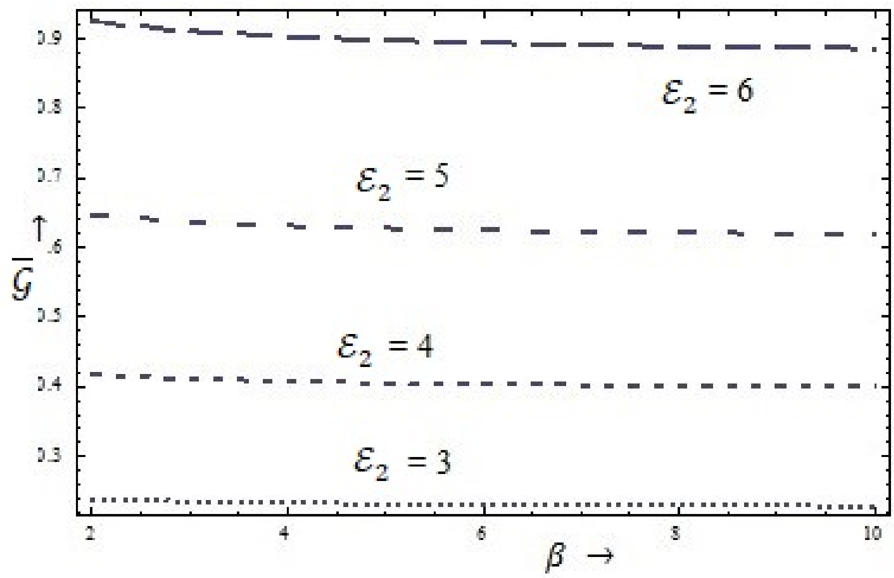

Figure 2.8: Illustration of scattering coefficient $\bar{\mathcal{G}}$ with $\mathcal{E}_2$ with $\varepsilon = 0.2$, $\alpha = 1.0$, $\mathcal{E}_1 = 0.1$, $\mathcal{E}_3 = 0.06$.

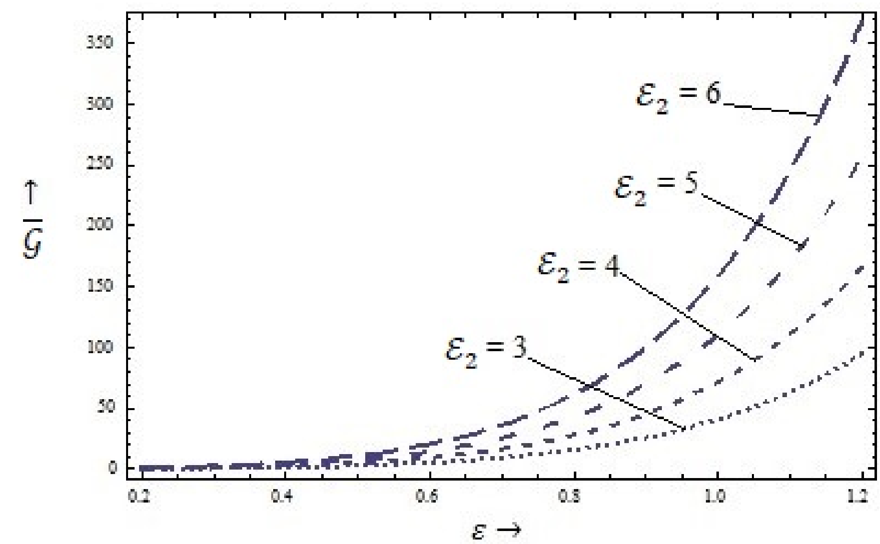

Figure 2.9: Illustration of scattering coefficient $\bar{\mathcal{G}}$ with $\mathcal{E}_2$ with $\alpha = 1.0$, $\beta = 5.0$ $\mathcal{E}_1 = 0.1$, $\mathcal{E}_3 = 0.06$.

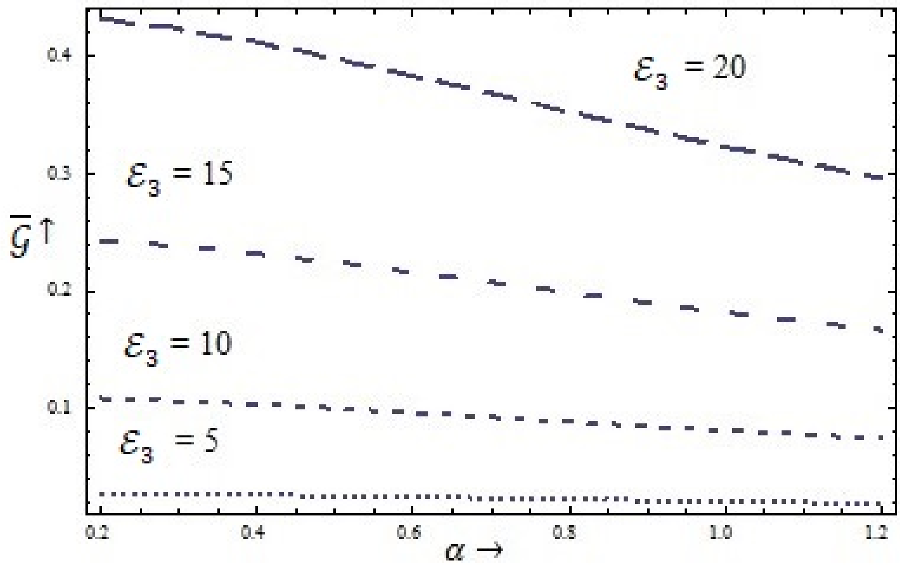

Figure 2.10: Illustration of scattering coefficient $\bar{\mathcal{G}}$ with $\mathcal{E}_3$ with $\varepsilon = 0.2$, $\beta = 5.0$, $\mathcal{E}_1 = 0.1$, $\mathcal{E}_2 = 0.00$.

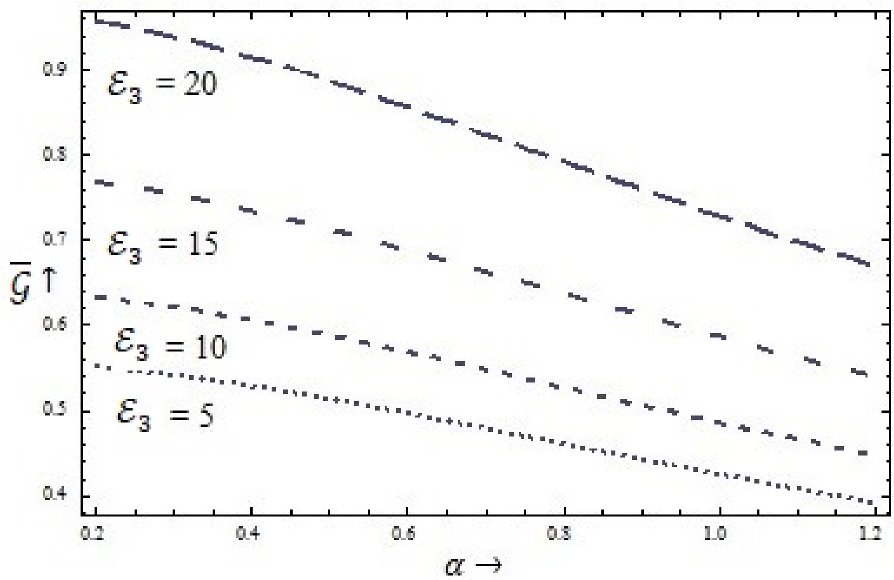

Figure 2.11: Illustration of scattering coefficient $\bar{\mathcal{G}}$ with $\mathcal{E}_3$ with $\varepsilon = 0.2$, $\beta = 5.0$, $\mathcal{E}_1 = 0.1$, $\mathcal{E}_2 = 4.0$.

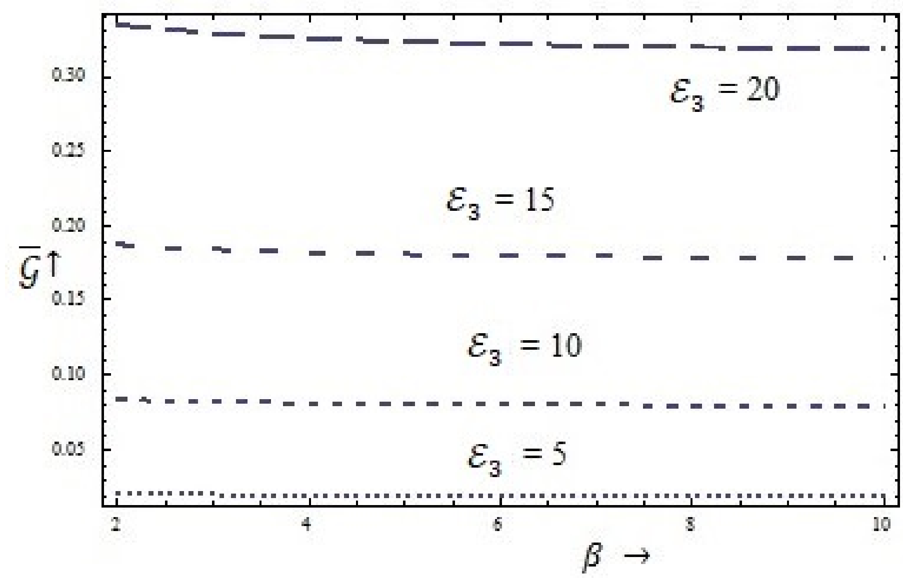

Figure 2.12: Illustration of scattering coefficient $\bar{\mathcal{G}}$ with $\mathcal{E}_3$ with $\varepsilon = 0.2$, $\alpha = 1.0$, $\mathcal{E}_1 = 0.1$, $\mathcal{E}_2 = 0.00$.

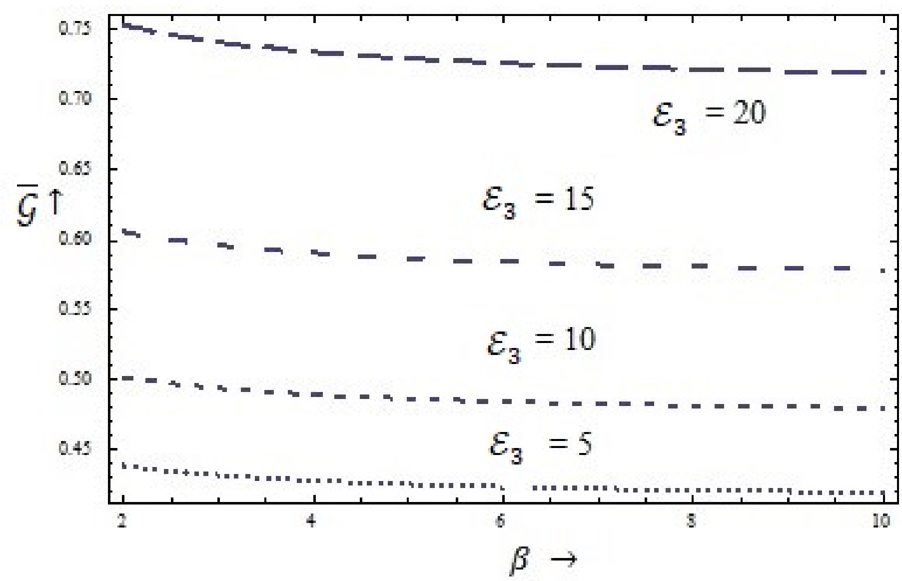

Figure 2.13: Illustration of scattering coefficient $\bar{\mathcal{G}}$ with $\mathcal{E}_3$ with $\varepsilon = 0.2$, $\alpha = 1.0$, $\mathcal{E}_1 = 0.1$, $\mathcal{E}_2 = 4.0$.

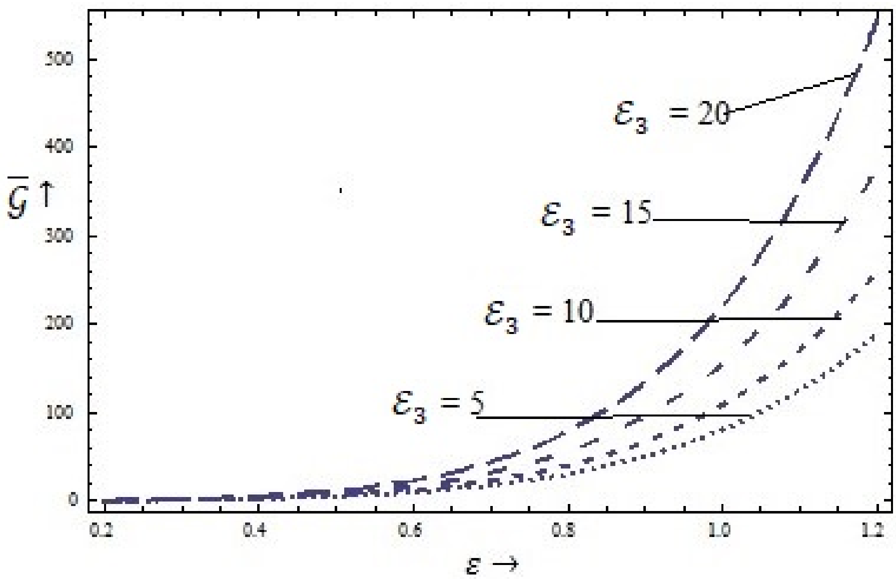

Figure 2.14: Illustration of scattering coefficient $\bar{\mathcal{G}}$ with $\mathcal{E}_3$ with $\alpha = 1.0$, $\beta = 5.0$ $\mathcal{E}_1 = 0.1$, $\mathcal{E}_2 = 4.0$.

Chapter 3

Peristaltic Pumping of an Incompressible Viscous Fluid in a Porous Medium with Wall Effects and Chemical Reactions

3.1 Introduction

In the chapter 2, we have explored the influence of wall features on dispersion of a solute in peristaltic pumping of a viscous fluid. A permeable medium is a material containing pores or spaces between solid matter wherein gas and liquid can pass through. As most of the tissues in the body are deformable porous media, in the recent years, studies involving flow past a porous media has gained significant interest, to understand various medical conditions (viz., tumor growth) and treatments (injections). Flow through a permeable medium has several applications in Geo-fluid dynamics, physiological fluid dynamics and engineering sciences. The study of flow in permeable media is an immensely vital role in understanding the transport process in kidneys, lungs, gallbladder with stones. The flow of blood in the micro vessels of a lung which may be treated as a channel bounded by two thin, porous layers (Misra and Ghosh [81]). The proper functioning of such things depends on the flow of blood and nutrients. The study of peristaltic movement past a permeable medium was first presented by Shehawey et al. [135]. Since, then many researchers have been working on the peristaltic transport in porous media.

An mentioned above and in chapter 1 (section 1.7), several investigators have worked on different Newtonian and non-Newtonian liquids with permeable medium. To the best of our knowledge, no attempt has yet been reported to discuss the impact of simultaneous homogeneous and heterogeneous chemical responses on a peristaltic stream of an incompressible viscous fluid through a porous medium with wall effects. It is realized that porosity and peristalsis may have a significant effect on the scattering of a solute in liquid streams. Therefore, in this chapter, the peristaltic pumping of an incompressible viscous fluid in a porous medium with wall effects and chemical reactions have been considered. Utilizing long wavelength hypothesis, Taylor's limiting condition and dynamic periphery limitation, the analytic expression for mean effective scattering coefficient in case of chemical reactions has been derived and the impacts of many physical constraints on it are discussed through graphs.

3.2 Formulation of the problem

Consider the flow of an incompressible viscous liquid through a permeable medium with peristalsis in a uniform channel. Figure 3.1 depicts the wave shape.

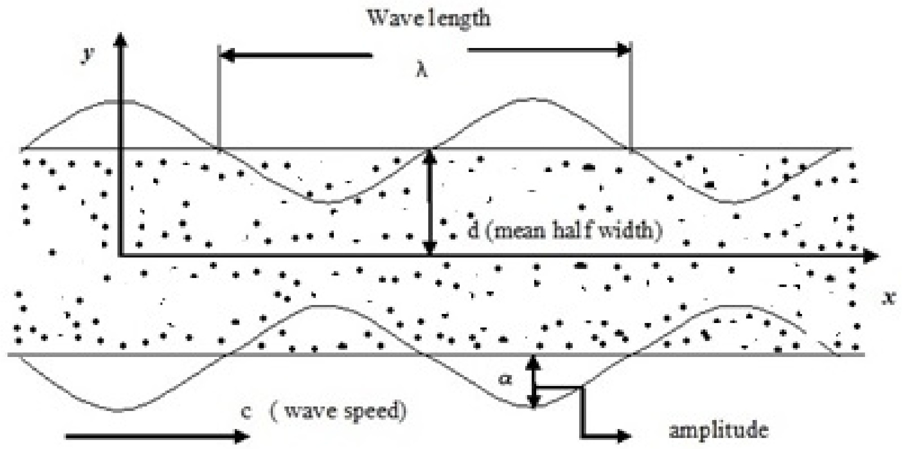

Figure 3.1: Geometry of the problem.

The equation of wave shape is considered same as in the previous chapter (Eqn. 2.1). The basic equations (Gupta and Seshadri [31]) govern the flow of the current problem are as follows:

$$\frac{\partial \mathcal{U}}{\partial \mathcal{X}} + \frac{\partial \mathcal{V}}{\partial \mathcal{Y}} = 0, \tag{3.1}$$

$$-\frac{\partial p}{\partial \mathcal{X}} + \mu \left(\frac{\partial^2}{\partial \mathcal{X}^2} + \frac{\partial^2}{\partial \mathcal{Y}^2} \right) \mathcal{U} - \frac{\mu}{\bar{k}} \mathcal{U} = \rho \left[\frac{\partial}{\partial t} + \mathcal{U} \frac{\partial}{\partial \mathcal{X}} + \mathcal{V} \frac{\partial}{\partial \mathcal{Y}} \right] \mathcal{U}, \tag{3.2}$$

$$-\frac{\partial p}{\partial \mathcal{Y}} + \mu \left(\frac{\partial^2}{\partial \mathcal{X}^2} + \frac{\partial^2}{\partial \mathcal{Y}^2} \right) \mathcal{V} - \frac{\mu}{\bar{k}} \mathcal{V} = \rho \left[\frac{\partial}{\partial t} + \mathcal{U} \frac{\partial}{\partial \mathcal{X}} + \mathcal{V} \frac{\partial}{\partial \mathcal{Y}} \right] \mathcal{V}, \tag{3.3}$$

where density is ρ, pressure is p, viscosity coefficient is μ, velocity component in the $\mathcal{X}$, $\mathcal{Y}$ direction are $\mathcal{U}$, $\mathcal{V}$ respectively, porosity component is $\bar{k}$.

Condition of the flexible wall movement (Mittra and Prasad [86]) is specified as:

$$\mathcal{L}(h) = p - p_0, \tag{3.4}$$

where the movement of the stretched membrane by the damping force is $\mathcal{L}$ and is intended by the subsequent equation:

$$\mathcal{L} = -\mathcal{T}\frac{\partial^2}{\partial \mathcal{X}^2} + m\frac{\partial^2}{\partial t^2} + \mathsf{C}\frac{\partial}{\partial t}. \tag{3.5}$$

Here the mass per/ area is m, the tension in the membrane is $\mathcal{T}$, and the coefficient of sticky damping force is C.

3.3 Method of Solution

After solving the equations (3.1) to (3.3) under long - wavelength hypothesis (Alemayehu and Radhakrishnamacharya [10]), we get

$$\frac{\partial \mathcal{U}}{\partial \mathcal{X}} + \frac{\partial \mathcal{V}}{\partial \mathcal{Y}} = 0, \tag{3.6}$$

$$-\frac{\partial p}{\partial \mathcal{X}} + \mu\frac{\partial^2 \mathcal{U}}{\partial \mathcal{Y}^2} - \frac{\mu}{\bar{k}}\mathcal{U} = 0, \tag{3.7}$$

$$\frac{\partial p}{\partial \mathcal{Y}} = 0. \tag{3.8}$$

The allied border conditions are given as:

$$\mathcal{U} = 0 \ \text{ at } \quad \mathcal{Y} = \pm h. \tag{3.9}$$

From equation (3.4), (3.5) and (3.7), active periphery conditions at the stretchy walls (Mittra and Prasad [86]) are specified as:

$$\frac{\partial}{\partial x}\mathcal{L}(h) = \mu \frac{\partial^2 \mathcal{U}}{\partial \mathcal{Y}^2} - \frac{\mu}{\bar{k}}\mathcal{U} \quad \text{at} \quad \mathcal{Y} = \pm h, \tag{3.10}$$

where

$$\frac{\partial}{\partial x}\mathcal{L}(h) = \frac{\partial p}{\partial \mathcal{X}} = -\mathcal{T}\frac{\partial^3 h}{\partial \mathcal{X}^3} + m\frac{\partial^3 h}{\partial \mathcal{X}\partial t^2} + \mathsf{C}\frac{\partial^2 h}{\partial \mathcal{X}\partial t} = \mathcal{P}'. \tag{3.11}$$

After solving the equations (3.7) to (3.8) with equations (3.9) and (3.10), we get

$$\mathcal{U}(\mathcal{Y}) = \frac{1}{\mu m_1^2}\frac{\partial p}{\partial \mathcal{X}}\left[\frac{\cosh(m_1\mathcal{Y})}{\cosh(m_1 h)} - 1\right]. \tag{3.12}$$

The mean speed is specied as:

$$\bar{\mathcal{U}}(\mathcal{Y}) = \frac{1}{2h}\int_{-h}^{h}\mathcal{U}(\mathcal{Y})d\mathcal{Y}. \tag{3.13}$$

Equations (3.12) and (3.13) yield as:

$$\bar{\mathcal{U}} = \frac{1}{\mu m_1^2}\frac{\partial p}{\partial \mathcal{X}}\left[\frac{\sinh(m_1 h)}{m_1 h \sinh(m_1 h)} - 1\right]. \tag{3.14}$$

Utilizing Alemayehu and Radhakrishnamacharya [10], the liquid speed is given by the equation:

$$\mathcal{U}_{\mathcal{X}} = \mathcal{U} - \bar{\mathcal{U}}. \tag{3.15}$$

Equations (3.12), (3.14) and (3.15), we obtaion

$$\mathcal{U}_{\mathcal{X}} = \frac{1}{\mu m_1^2}\frac{\partial p}{\partial \mathcal{X}}\left[B_1' \cosh(m_1\mathcal{Y}) - B_2'\right], \tag{3.16}$$

where

$$\frac{\partial p}{\partial \mathcal{X}} = m\frac{\partial^3 h}{\partial \mathcal{X}\partial t^2} + c\frac{\partial^2 h}{\partial \mathcal{X}\partial t} - \mathcal{T}\frac{\partial^3 h}{\partial \mathcal{X}^3}, \quad m_1 = \sqrt{\frac{1}{\bar{k}}}, \quad B_1' = \frac{1}{\cosh(m_1 h)},$$
$$B_2' = \frac{\sinh(m_1 h)}{m_1 h \cosh(m_1 h)}.$$

3.4 Simultaneous homogeneous and heterogeneous chemical reactions with diffusion

Following $\frac{\partial^2 C}{\partial x^2} \leq \frac{\partial^2 C}{\partial y^2}$ (Taylor [156], Gupta and Gupta [32]), the dispersion equation for the concentration C of the substance for the present issue under isothermal conditions is expressed as:

$$\mathcal{D}\frac{\partial^2 C}{\partial \mathcal{Y}^2} - k_1 C = \mathcal{U}\frac{\partial C}{\partial \mathcal{X}} + \frac{\partial C}{\partial t}. \tag{3.17}$$

Here, the rate constant of first order chemical response is k_1, the molecular diffusion coefficient is $\mathcal{D}$ and liquid concentration is C.

The dimensionless quantities are specified as:

$$\theta = \frac{t}{\bar{t}}, \bar{t} = \frac{\lambda}{\bar{\mathcal{U}}}, \eta = \frac{\mathcal{Y}}{d}, \xi = \frac{(\mathcal{X} - \bar{\mathcal{U}}t)}{\lambda}, \mathcal{H} = \frac{h}{d}, \mathcal{P} = \frac{d^2}{\mu c}\mathcal{P}', k = \frac{\bar{k}}{d^2}. \tag{3.18}$$

For the regular estimations of physiologically essential parameters of this issue, it is normal that $\bar{\mathcal{U}} \approx C$ (Alemayehu and Radhakrishnamacharya [10]).

To proceed further, we use $\bar{\mathcal{U}} \approx C$ in (3.17), equations (3.11), (3.16) and (3.17) are non-dimensionalized as:

$$\mathcal{P} = -\varepsilon\left[(\mathcal{E}_1 + \mathcal{E}_2)(2\pi)^3\cos(2\pi\xi) - \mathcal{E}_3(2\pi)^2\sin(2\pi\xi)\right], \tag{3.19}$$

$$\mathcal{U}_{\mathcal{X}} = \frac{d^2}{\mu m^2}\mathcal{P}\left[B_1\cosh(m\eta) - B_2\right], \tag{3.20}$$

$$\frac{\partial^2 C}{\partial \eta^2} - \frac{k_1 d^2}{\mathcal{D}} C = \frac{d^2}{\lambda \mathcal{D}} \mathcal{U}_{\mathcal{X}} \frac{\partial C}{\partial \xi}, \tag{3.21}$$

where

the amplitude ratio is $\varepsilon \left(= \frac{a}{d}\right)$, the rigidity is $\mathcal{E}_1 \left(= -\frac{\mathcal{T} d^3}{\lambda^3 \mu \mathbf{c}}\right)$, the stiffness is $\mathcal{E}_2 = \left(\frac{m \mathbf{c} d^3}{\lambda^3 \mu}\right)$, the viscous damping force in the wall is $\mathcal{E}_3 = \left(\frac{\mathbf{c} d^3}{\mu \lambda^2}\right)$,

The dispersion with first- order irreversible chemical response occur in the mass of the liquid and at the channel walls.

Referring Philip and Chandra [19], the wall conditions are specified as:

$$0 = \mathcal{F} C + \frac{\partial C}{\partial \mathcal{Y}} \quad \text{at} \quad \mathcal{Y} = [a \sin \frac{2\pi}{\lambda} (\mathcal{X} - \bar{\mathcal{U}} t) + d] = h, \tag{3.22}$$

$$0 = -\mathcal{F} C + \frac{\partial C}{\partial \mathcal{Y}} \quad \text{at} \quad \mathcal{Y} = -[a \sin \frac{2\pi}{\lambda} (\mathcal{X} - \bar{\mathcal{U}} t) + d] = -h. \tag{3.23}$$

From equations (3.18), (3.22) and (3.23), we get

$$0 = \beta C + \frac{\partial C}{\partial \eta} \quad \text{at} \quad \eta = [\varepsilon \sin(2\pi\xi) + 1] = \mathcal{H}, \tag{3.24}$$

$$0 = -\beta C + \frac{\partial C}{\partial \eta} \quad \text{at} \quad \eta = -[\varepsilon \sin(2\pi\xi) + 1] = -\mathcal{H}, \tag{3.25}$$

where the heterogeneous response rate constraint is $\beta = \mathcal{F} d$, relating to catalytic reaction at the walls.

From equations (3.24), (3.25) the primitive of equation (3.21) as follows:

$$C(\eta) = -\frac{d^4}{\lambda \mu \mathcal{D} m^2} \frac{\partial C}{\partial \xi} \mathcal{P} \Big[B_4 \cosh(m\eta) - B_5 \cosh(\alpha\eta) + B_6 - B_7 \cosh(\alpha\eta) \Big]. \tag{3.26}$$

and $\alpha=\sqrt{\frac{k_1}{\mathcal{D}}d^2},\ m=m_1d=\sqrt{\frac{1}{k}}.$

As expressed in chapter 2, the volumetric flow rate $\mathcal{Q}$ is specified as:

$$\mathcal{Q}=\int_{-\mathcal{H}}^{\mathcal{H}} C\mathcal{U}_{\mathcal{X}}d\eta. \tag{3.27}$$

Using equations (3.20) and (3.26) in equation (3.27), we get

$$\mathcal{Q}=-2\frac{d^6}{\lambda\mu^2\mathcal{D}}\frac{\partial C}{\partial\xi}\mathcal{G}(\xi,\alpha,\beta,\varepsilon,\mathcal{E}_1,\mathcal{E}_2,\mathcal{E}_3,k), \tag{3.28}$$

where

$$\begin{aligned}\mathcal{G}(\xi,\alpha,\beta,\varepsilon,\mathcal{E}_1,\mathcal{E}_2,\mathcal{E}_3,k)&=\\ -\frac{\mathcal{P}^2}{m^4}\Big[\frac{B_1B_4}{2}B_8-(B_1B_5+B_1B_7)B_9+(B_1B_6-B_2B_4)B_{10}+&\\ (B_2B_5+B_2B_7)B_{11}-B_2B_6\mathcal{H}\Big],&\end{aligned} \tag{3.29}$$

$$\begin{gathered}B_1=\frac{1}{\cosh m\mathcal{H}},B_2=\frac{\sinh m\mathcal{H}}{m\mathcal{H}\cosh m\mathcal{H}},B_3=\frac{\sinh m\mathcal{H}}{\alpha\sinh\alpha\mathcal{H}},\\ B_4=\frac{1}{(m^2-\alpha^2)\cosh m\mathcal{H}},B_6=\frac{\sinh m\mathcal{H}}{m\mathcal{H}\alpha^2\cosh m\mathcal{H}},\alpha=\sqrt{\frac{k_1}{\mathcal{D}}}d,\\ B_5=\frac{m\sinh m\mathcal{H}+\beta\cosh m\mathcal{H}}{(m^2-\alpha^2)\cosh m\mathcal{H}(\alpha\sinh\alpha\mathcal{H}+\beta\cosh\alpha\mathcal{H})},B_{10}=\frac{\sinh m\mathcal{H}}{m},\\ B_7=\frac{\beta\sinh m\mathcal{H}}{m\mathcal{H}\alpha^2\cosh m\mathcal{H}(\alpha\sinh\alpha\mathcal{H}+\beta\cosh\alpha\mathcal{H})},\\ B_8=\frac{2m\mathcal{H}+\sinh 2m\mathcal{H}}{2m},\\ B_9=\frac{m\sinh m\mathcal{H}\cosh\alpha\mathcal{H}-\alpha\cosh m\mathcal{H}\sinh\alpha\mathcal{H}}{(m^2-\alpha^2)},B_{11}=\frac{\sinh\alpha\mathcal{H}}{\alpha},\end{gathered}$$

Glancing at equation (3.28) with Fick's bylaw of dispersion, the scattering coefficient $\mathcal{D}^*$

was intended such that the solute disperses near to the plane moving with the typical speed of the flow and is specified as:

$$\mathcal{D}^* = 2\frac{d^6}{\mu^2\mathcal{D}}\mathcal{G}(\xi,\alpha,\beta,\varepsilon,\mathcal{E}_1,\mathcal{E}_2,\mathcal{E}_3,k). \tag{3.30}$$

Let $\bar{\mathcal{G}}$ be the mean of $\mathcal{G}$ and is attained by the succeeding equation:

$$\bar{\mathcal{G}} = \int_0^1 \mathcal{G}(\xi,\alpha,\beta,\varepsilon,\mathcal{E}_1,\mathcal{E}_2,\mathcal{E}_3,k)d\xi, \tag{3.31}$$

3.5 Outcomes and Discussion

The expression for $\bar{\mathcal{G}}(\xi,\alpha,\beta,\varepsilon,\mathcal{E}_1,\mathcal{E}_2,\mathcal{E}_3,k)$ has been obtained and end results are presented through graphs using the software MATHEMATICA. The pertinent constraints present in this argument are amplitude ratio (ε), the homogeneous response rate (α), the permeability constraint (k), the heterogeneous response rate (β), the rigidity $(\mathcal{E}_1)$, the stiffness $(\mathcal{E}_2)$, and the viscous damping force $(\mathcal{E}_3)$. We may ensure that $\mathcal{E}_1,\mathcal{E}_2$ and $\mathcal{E}_3$ cannot be zero all together.

Consider the Figs. 3.2, 3.3, 3.4 for the impact of the rigidness constraint $(\mathcal{E}_1)$ of the elastic wall on the mean effective dispersion coefficient $(\bar{\mathcal{G}})$. Dispersion enhances with increase in wall rigidness $(\mathcal{E}_1)$ for the cases of (a) no stiffness in the wall $(\mathcal{E}_2{=}0)$ and perfectly elastic channel wall $(\mathcal{E}_3{=}0)$ (Fig. 3.2); (b) without stiffness in the wall $(\mathcal{E}_2{=}0)$ and dissipative wall $(\mathcal{E}_3{\neq}0)$ (Fig. 3.3); (c) stiffness in the wall $(\mathcal{E}_2{\neq}0)$ and fully elastic wall $(\mathcal{E}_3{=}0)$ (Fig. 3.4). It is observed that $\bar{\mathcal{G}}$ increases with the stiffness $(\mathcal{E}_2)$. It is true for the cases of (a) perfectly flexible wall $(\mathcal{E}_3{=}0)$ (Fig. 3.5) and (b) dissipative wall $(\mathcal{E}_3{\neq}0)$ (Figs. 3.6, 3.7). Moreover, it is seen that boost in viscous damping force $(\mathcal{E}_3)$ rises $\bar{\mathcal{G}}$ in the case of stiffness in the wall $(\mathcal{E}_2{\neq}0)$ (Figs. 3.8, 3.9, 3.10). It is revealed that $\bar{\mathcal{G}}$ ascends monotonically with an increase in $\mathcal{E}_1,\mathcal{E}_2$ and $\mathcal{E}_3$. This result agreement with the result of Ravikiran and Radhakrishnamacharya [122], Hayat et al. [45].

Figures 3.11 - 3.13 indicates that $\bar{\mathcal{G}}$ enhances with an increase in the permeability constraint (k). These are true for the cases of (i) no stiffness in the wall $(\mathcal{E}_2{=}0)$ and dissipative nature of channel wall ($\mathcal{E}_3 \neq 0$) (Fig. 3.11); (ii) stiffness in the wall ($\mathcal{E}_2 \neq 0$) and dissipative wall ($\mathcal{E}_3 \neq 0$) (Fig. 3.12 and 3.13). This is a direct result of the way that the growing porosity in a channel which thusly generate the fluid speed and cause to ascend the dispersion. Furthermore, $\bar{\mathcal{G}}$ ascends with an increment in the amplitude ratio (ε) (Figs. 3.4, 3.7, 3.10, and 3.13). As already known, the increment in the amplitude ratio is the expansion in the amplitude of the wave across the channel and this cause to increase the fluid velocity within the channel and consequently dispersion may enhance. This outcome concurs with that of Sobh [142], Ravikiran and Radhakrisnamacharya [122].

Dispersion reduces with a homogeneous compound response rate (α) (Figs. 3.3, 3.6, 3.9 and 3.12) and heterogeneous substance response rate (β) (Figs. 3.2, 3.5, 3.8 and 3.11). This result is consistent with the arguments of Padma and Rao [93], Gupta and Gupta [32], Hayat et al. [45], Ravikiran and Radhakrisnamacharya [122].

3.6 Conclusion

This study explores the effect of wall characteristics and chemical responses on an incompressible viscous fluid with peristalsis. It is observed from the previous section that, the concentration profile ($\bar{\mathcal{G}}$) amplifies with a rise in amplitude ratio (ε), permeability constraint (k) and wall characteristics ($\mathcal{E}_1, \mathcal{E}_2$ and $\mathcal{E}_3$). Furthermore, opposite behaviors of homogeneous response rate (α) and heterogeneous response rate (β) constraints are observed on $\bar{\mathcal{G}}$. Finally, it concludes that amplitude ratio, permeability and wall constraints favor the scattering and peristaltic flow increases the dispersion.

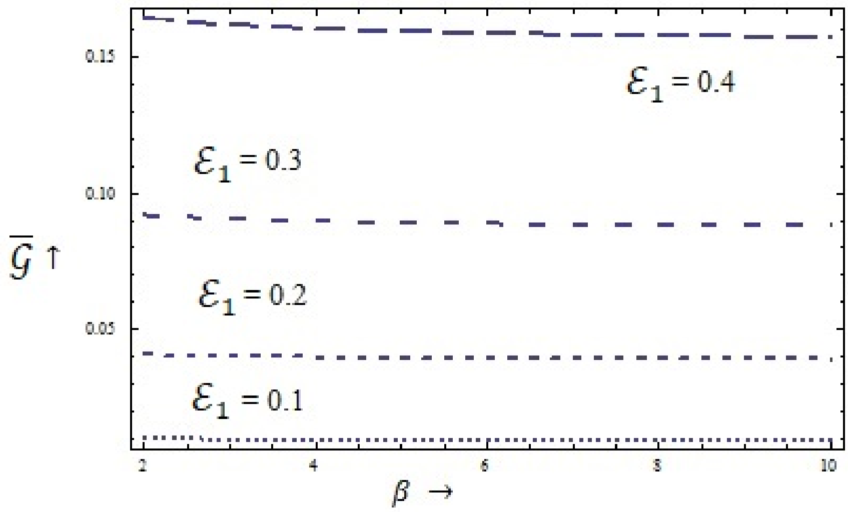

Figure 3.2: Illustration of rigidity ($\mathcal{E}_1$) with scattering coefficient ($\bar{\mathcal{G}}$) when $\mathcal{E}_2 = 0.0$, $\mathcal{E}_3 = 0.00$, $\varepsilon = 0.2$, $\alpha = 1.0$, $k = 0.9$.

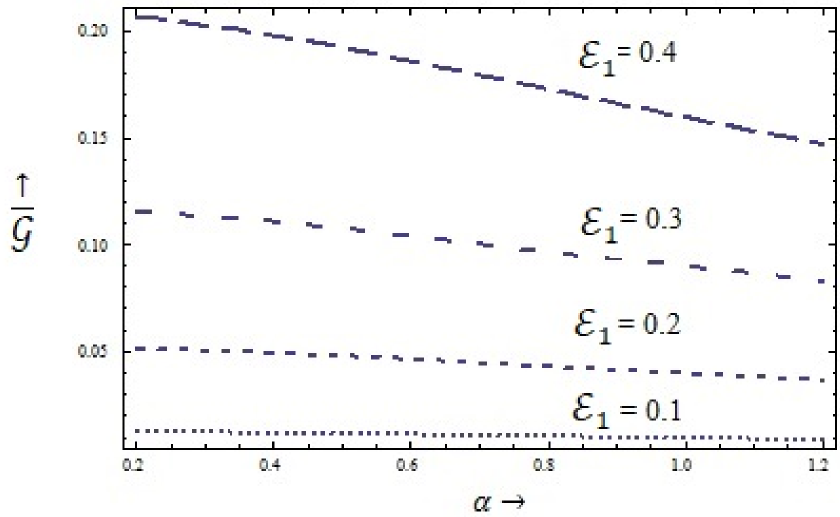

Figure 3.3: Illustration of rigidity ($\mathcal{E}_1$) with scattering coefficient ($\bar{\mathcal{G}}$) when $\mathcal{E}_2 = 0.0$, $\mathcal{E}_3 = 0.06$, $\varepsilon = 0.2$, $\beta = 5.0$, $k = 0.9$.

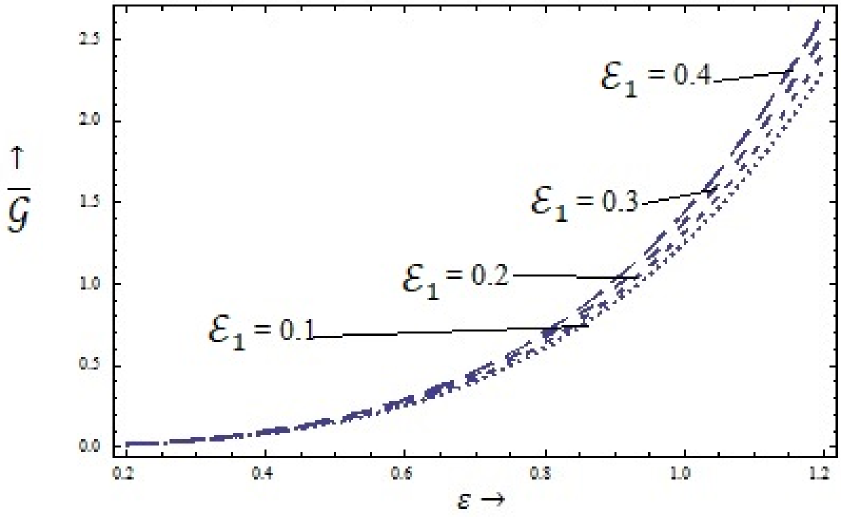

Figure 3.4: Illustration of rigidity ($\mathcal{E}_1$) with scattering coefficient ($\bar{\mathcal{G}}$) when $\mathcal{E}_2 = 4.0$, $\mathcal{E}_3 = 0.00$, $\alpha = 1.0$, $\beta = 5.0$, $k = 0.9$.

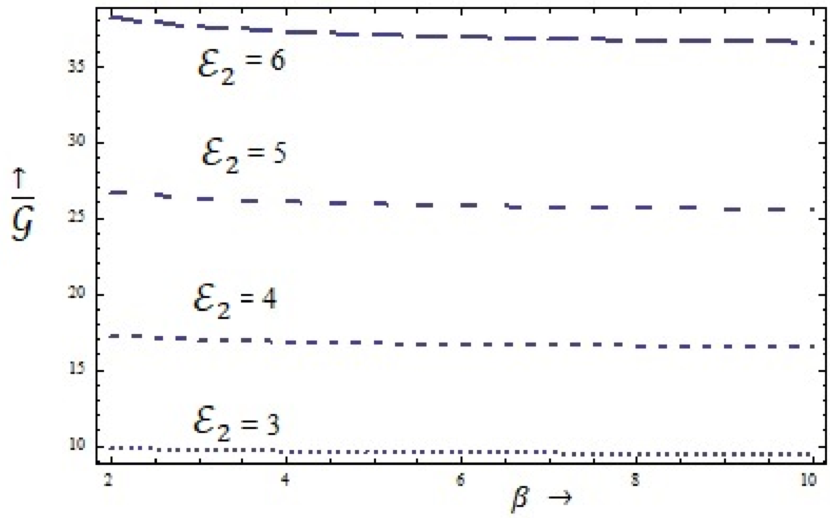

Figure 3.5: Illustration of stiffness ($\mathcal{E}_2$) with scattering coefficient ($\bar{\mathcal{G}}$) when $\mathcal{E}_1 = 0.1$, $\mathcal{E}_3 = 0.00$, $\varepsilon = 0.2$, $\alpha = 1.0$, $k = 0.9$.

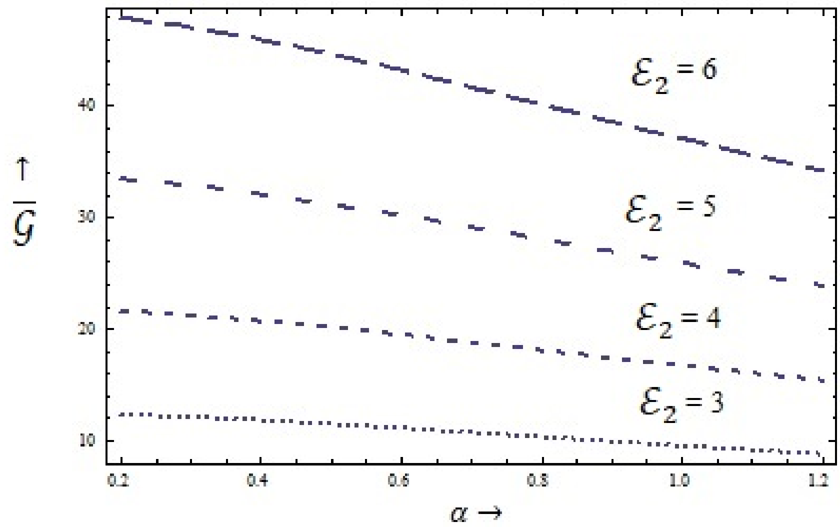

Figure 3.6: Illustration of stiffness ($\mathcal{E}_2$) with scattering coefficient ($\bar{\mathcal{G}}$) when $\mathcal{E}_1 = 0.1$, $\mathcal{E}_3 = 0.06$, $\varepsilon = 0.2$, $\beta = 5.0$, $k = 0.9$.

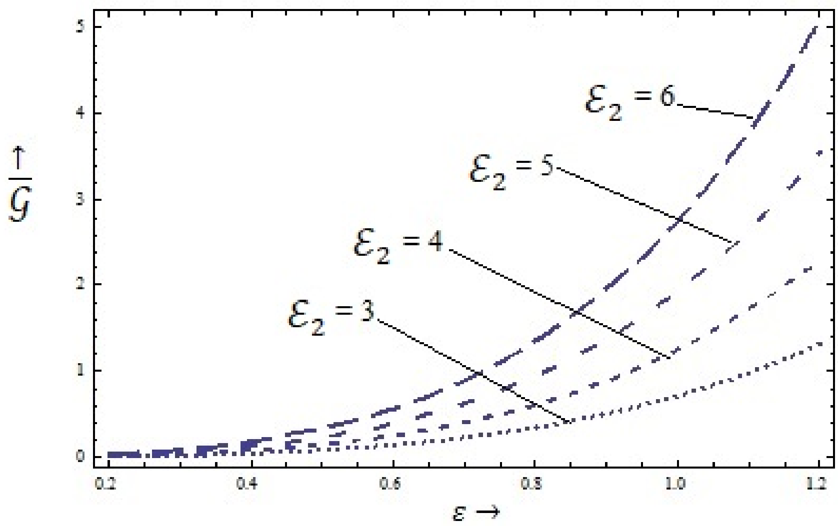

Figure 3.7: Illustration of stiffness ($\mathcal{E}_2$) with scattering coefficient ($\bar{\mathcal{G}}$) when $\mathcal{E}_1 = 0.1$, $\mathcal{E}_3 = 0.06$, $\alpha = 1.0$, $\beta = 5.0$, $k = 0.9$.

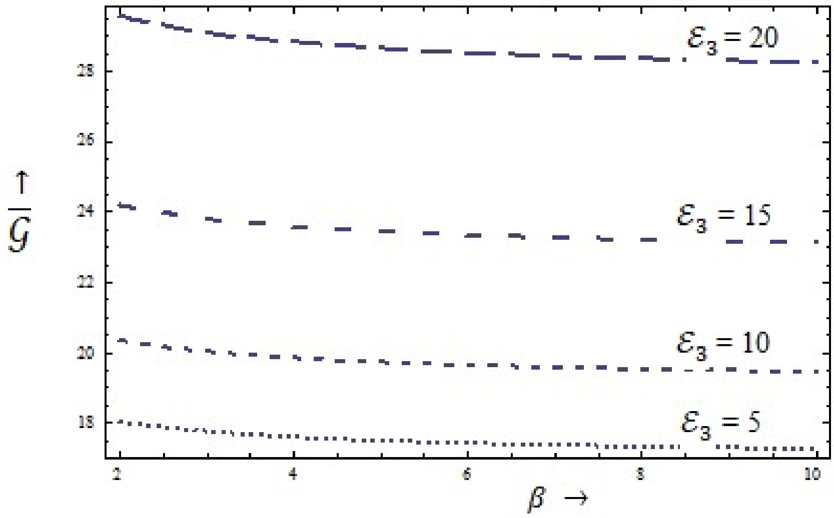

Figure 3.8: Illustration of damping force ($\mathcal{E}_3$) with scattering coefficient ($\bar{\mathcal{G}}$) when $\mathcal{E}_1 = 0.1$, $\mathcal{E}_2 = 4.0$, $\varepsilon = 0.2$, $\alpha = 1.0$, $k = 0.9$.

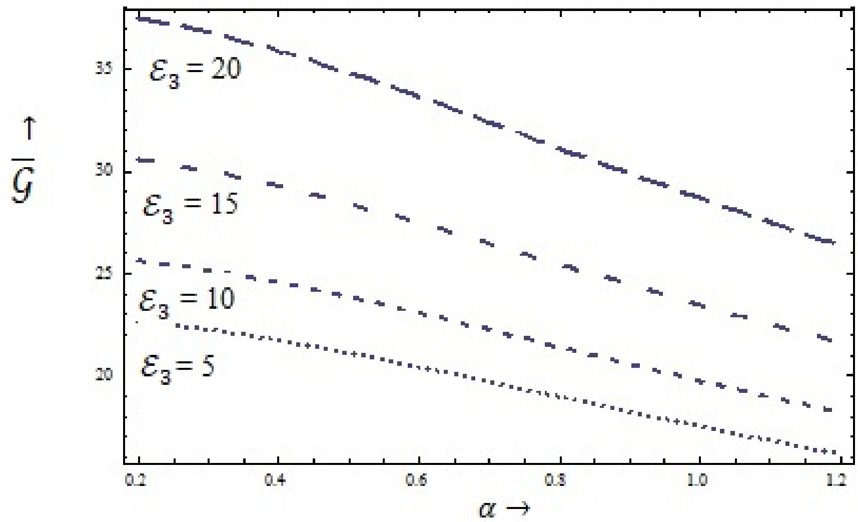

Figure 3.9: Illustration of damping force ($\mathcal{E}_3$) with scattering coefficient ($\bar{\mathcal{G}}$) when $\mathcal{E}_1 = 0.1$, $\mathcal{E}_2 = 4.0$, $\varepsilon = 0.2$, $\beta = 5.0$, $k = 0.9$.

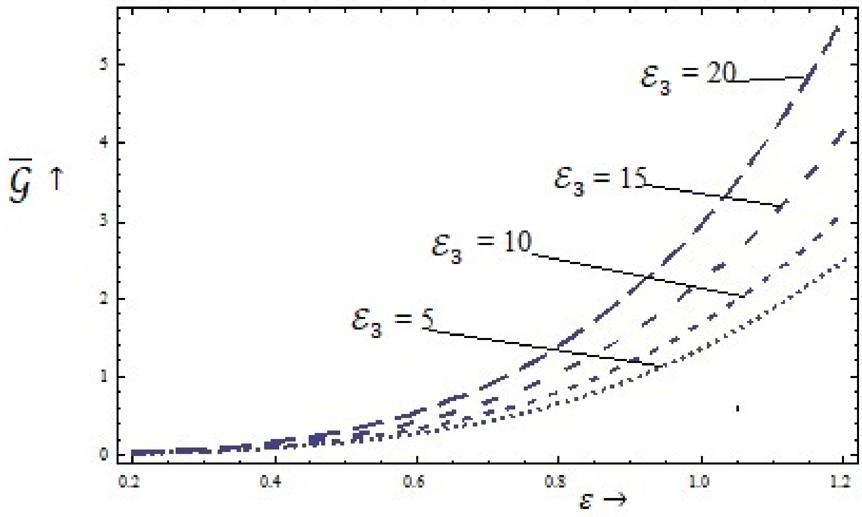

Figure 3.10: Illustration of damping force ($\mathcal{E}_3$) with scattering coefficient ($\bar{\mathcal{G}}$) when $\mathcal{E}_1 = 0.1$, $\mathcal{E}_2 = 4.0$, $\alpha = 1.0$, $\beta = 5.0$, $k = 0.9$.

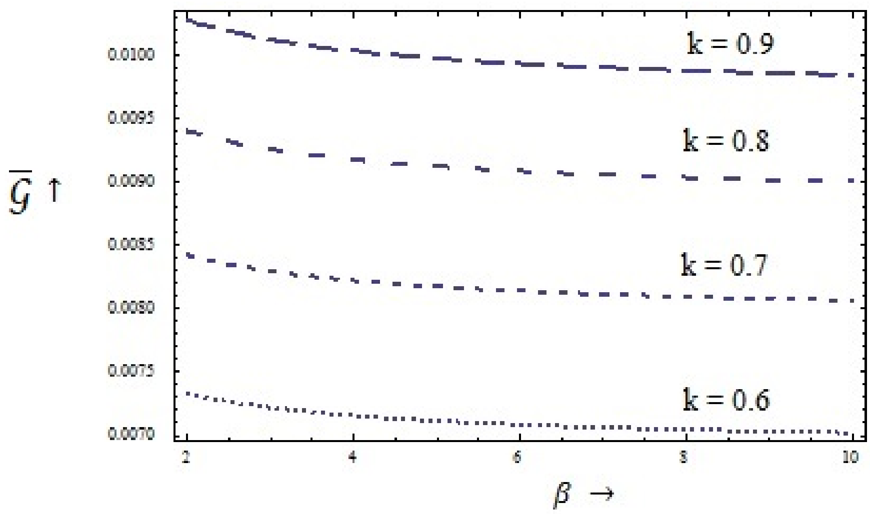

Figure 3.11: Illustration of permeability constraint (k) with scattering coefficient ($\bar{\mathcal{G}}$) when $\mathcal{E}_1 = 0.1$, $\mathcal{E}_2 = 0.0$, $\mathcal{E}_3 = 0.06$, $\varepsilon = 0.2$, $\alpha = 1.0$, $\beta = 5.0$.

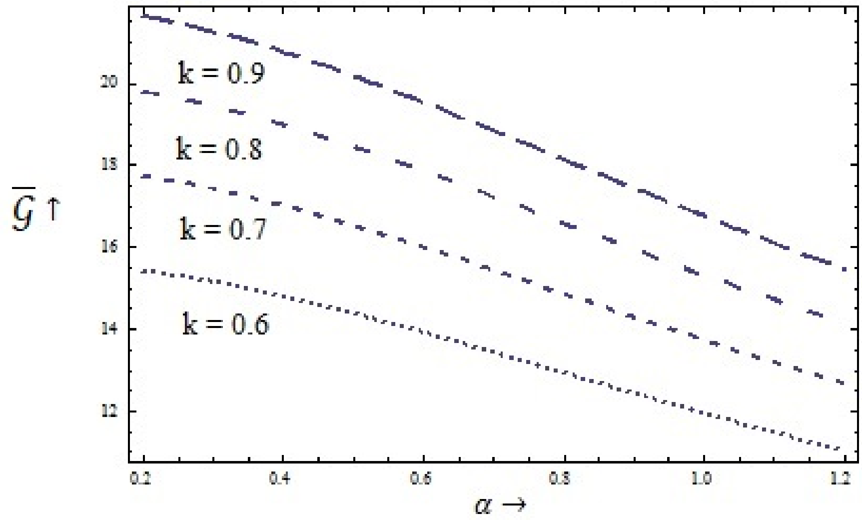

Figure 3.12: Illustration of permeability constraint (k) with scattering coefficient ($\bar{\mathcal{G}}$) when $\mathcal{E}_1 = 0.1$, $\mathcal{E}_2 = 4.0$, $\mathcal{E}_3 = 0.06$, $\varepsilon = 0.2$, $\beta = 5.0$, $\alpha = 1.0$.

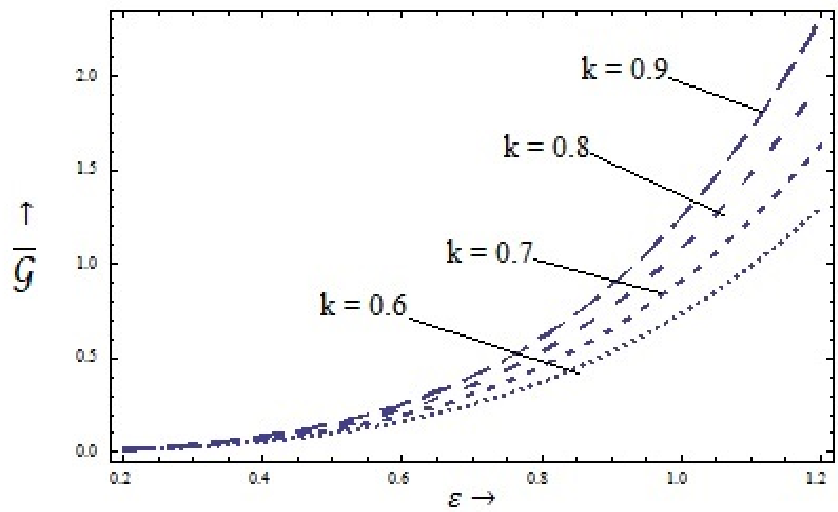

Figure 3.13: Illustration of permeability constraint (k) with scattering coefficient ($\bar{\mathcal{G}}$) when $\mathcal{E}_1 = 0.1$, $\mathcal{E}_2 = 4.0$, $\mathcal{E}_3 = 0.00$, $\alpha = 1.0$, $\beta = 5.0$.

Chapter 4

Effect of Compliant Walls on Magneto-Hydrodynamic Peristaltic Pumping of an Incompressible Viscous Fluid With Chemical Reactions

4.1 Introduction

In the previous chapter, we have studied scattering of a solute in peristaltic pumping of an incompressible viscous liquid through a permeable medium with wall characteristics. In this chapter, the influence of magnetic field on the diffusion of a solute in peristaltic pumping of a viscous fluid with compliant wall is inspected.

Magnetohydrodynamics (MHD) deals with the study of electrically conducting fluids under the influence of electromagnetic field. Research has revealed that numerous physiological liquids have electrically conducting properties in Bioengineering systems. MHD of peristaltic stream is being studied due to its significance in blood pump machines, behavioral modification in cells and tissues, problems about urinary tract and treatment of gastrointestinal mobility related disorders. Currently, studies on interaction of peristalsis with magnetohydrodynamic (MHD) flows of physiological liquids have turned out to be a subject of budding interest for scholars. Such studies are useful mostly for receiving appropriate understanding of the working on different machines utilized by clinicians for driving physiological liquids (Misra et al. [78]). Hence, Mekheimer and Elmabounf [78], Mekheimer [75, 76], Ratishkumar et al. [119], Pandey and Chaube [97], Ramana Kumari and Radhakrishnamacharya [115], Sobh [141, 142] have deliberated the impact of magnetic field with peristalsis in varied circumstances.

Keeping this in view, in this chapter, the influence of magnetic field on dispersion of a solute material in peristaltic pumping of a viscous fluid with compliant wall is explored in the occurrence of simultaneous heterogeneous and homogeneous irreversible chemical responses.

4.2 Formulation of the problem

Figure 4.1 shows the geometry of the magneto-hydrodynamic peristaltic stream of an incompressible viscous fluid in a 2 - dimensional channel with compliant walls and Cartesian coordinates.

The equation of wave shape is deliberated same as in chapter 2 (Eqn. 2.1).

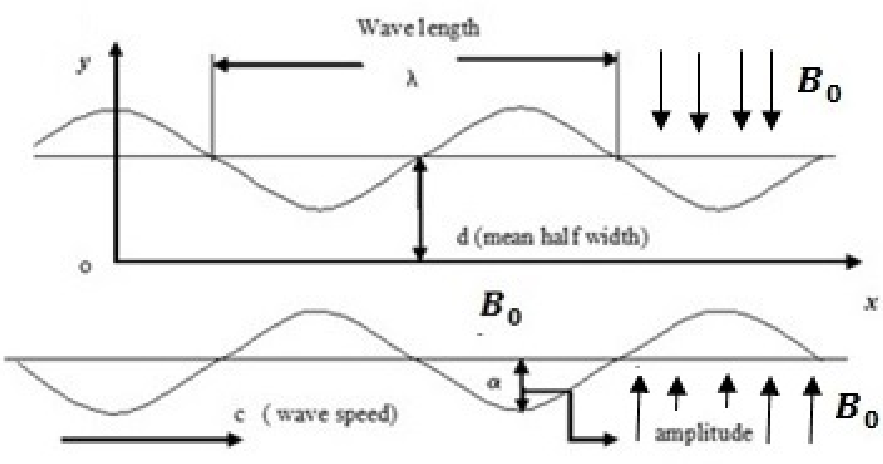

Figure 4.1: Geometry of the problem.

Utilizing the Maxwell's equations, the assumptions regarding magnetic field as specified in chapter 1 (section 1.6), the equations of the viscous fluid as given in chapter 1 (section 1.8.1), and the equivalent flow equations (Gupta and Seshadri [31]) of the present problem are as follows:

$$\frac{\partial \mathcal{U}}{\partial \mathcal{X}}+\frac{\partial \mathcal{V}}{\partial \mathcal{Y}}=0, \tag{4.1}$$

$$-\frac{\partial p}{\partial \mathcal{X}}+\mu\left(\frac{\partial^2}{\partial \mathcal{X}^2}+\frac{\partial^2}{\partial \mathcal{Y}^2}\right)\mathcal{U}-\sigma B_0^2\mathcal{U}=\rho\left[\frac{\partial}{\partial t}+\mathcal{U}\frac{\partial}{\partial \mathcal{X}}+\mathcal{V}\frac{\partial}{\partial \mathcal{Y}}\right]\mathcal{U}, \tag{4.2}$$

$$-\frac{\partial p}{\partial \mathcal{Y}}+\mu\left(\frac{\partial^2}{\partial \mathcal{X}^2}+\frac{\partial^2}{\partial \mathcal{Y}^2}\right)\mathcal{V}=\rho\left[\frac{\partial}{\partial t}+\mathcal{U}\frac{\partial}{\partial \mathcal{X}}+\mathcal{V}\frac{\partial}{\partial \mathcal{Y}}\right]\mathcal{V}, \tag{4.3}$$

where density is ρ, pressure is p, viscosity coefficient is μ, velocity component in the $\mathcal{X}$, $\mathcal{Y}$ direction are $\mathcal{U}$, $\mathcal{V}$ respectively and magnetic field is B_0.

Condition of the elastic wall movement (Mittra and Prasad [86]) is specified as:

$$\mathcal{L}(h)=p-p_0, \tag{4.4}$$

where, the movement of the stretched membrane by the damping force is $\mathcal{L}$ and is intended by the subsequent equation:

$$\mathcal{L} = -\mathcal{T}\frac{\partial^2}{\partial \mathcal{X}^2} + m\frac{\partial^2}{\partial t^2} + \mathsf{C}\frac{\partial}{\partial t}. \tag{4.5}$$

Here, the coefficient of sticky damping force is C, the mass per/area is m, and the membrane tension is $\mathcal{T}$.

4.3 Method of solution

After solving the equations (4.1) to (4.3) under long - wavelength hypothesis, we get

$$\frac{\partial \mathcal{U}}{\partial \mathcal{X}} + \frac{\partial \mathcal{V}}{\partial \mathcal{Y}} = 0, \tag{4.6}$$

$$-\frac{\partial p}{\partial \mathcal{X}} + \mu\frac{\partial^2 \mathcal{U}}{\partial \mathcal{Y}^2} - \sigma B_0^2 \mathcal{U} = 0, \tag{4.7}$$

$$\frac{\partial p}{\partial \mathcal{Y}} = 0. \tag{4.8}$$

The allied border conditions are given as:

$$\mathcal{U} = 0 \text{ at } \quad \mathcal{Y} = \pm h. \tag{4.9}$$

From equation (4.4), (4.5) and (4.7), active periphery conditions at the stretchy walls (Mittra and Prasas [86]) are specified as:

$$\frac{\partial}{\partial x}\mathcal{L}(h) = \mu\frac{\partial^2 \mathcal{U}}{\partial \mathcal{Y}^2} - \sigma B_0^2 \mathcal{U} \quad \text{at} \quad \mathcal{Y} = \pm h, \tag{4.10}$$

where

$$\frac{\partial}{\partial x}\mathcal{L}(h) = \frac{\partial p}{\partial \mathcal{X}} = -\mathcal{T}\frac{\partial^3 h}{\partial \mathcal{X}^3} + m\frac{\partial^3 h}{\partial \mathcal{X}\partial t^2} + \mathsf{C}\frac{\partial^2 h}{\partial \mathcal{X}\partial t} = \mathcal{P}'. \tag{4.11}$$

After solving the equations (4.7) to (4.8) with conditions (4.9) and (4.10), we get

$$\mathcal{U}(\mathcal{Y})=\frac{1}{\mu m_1^2}\frac{\partial p}{\partial \mathcal{X}}\left[\frac{\cosh(m_1\mathcal{Y})}{\cosh(m_1 h)}-1\right]. \tag{4.12}$$

The mean speed is given as:

$$\bar{\mathcal{U}}(\mathcal{Y})=\frac{1}{2h}\int_{-h}^{h}\mathcal{U}(\mathcal{Y})d\mathcal{Y}. \tag{4.13}$$

From equation (4.12) and (4.13), we obtain

$$\bar{\mathcal{U}}=\frac{1}{\mu m_1^2}\frac{\partial p}{\partial \mathcal{X}}\left[\frac{\sinh(m_1 h)}{m_1 h\sinh(m_1 h)}-1\right]. \tag{4.14}$$

Utilizing Alemayehu and Radhakrishnamacharya [9], the liquid speed is specified as:

$$\mathcal{U}_{\mathcal{X}}=\mathcal{U}-\bar{\mathcal{U}}. \tag{4.15}$$

From equations (4.12), (4.14) and (4.15), we attain as:

$$\mathcal{U}_{\mathcal{X}}=\frac{1}{\mu m_1^2}\frac{\partial p}{\partial \mathcal{X}}\left[\frac{m_1\cosh(m_1\mathcal{Y})-\sinh(m_1 h)}{m_1 h\cosh(m_1 h)}\right], \tag{4.16}$$

where

$$\frac{\partial p}{\partial \mathcal{X}}=m\frac{\partial^3 h}{\partial \mathcal{X}\partial t^2}+c\frac{\partial^2 h}{\partial \mathcal{X}\partial t}-\mathcal{T}\frac{\partial^3 h}{\partial \mathcal{X}^3},\quad m_1=\sqrt{\frac{\sigma B_0^2}{\mu}}.$$

4.4 Simultaneous homogeneous and heterogeneous chemical reactions with diffusion

Utilizing $\frac{\partial^2 C}{\partial x^2}\leq\frac{\partial^2 C}{\partial y^2}$ of Taylor [156] and referring Gupta and Gupta [32], the diffusion equation for the concentration C of the substance for the present issue under isothermal conditions is written as:

$$\mathcal{D}\frac{\partial^2 C}{\partial \mathcal{Y}^2} - k_1 C = \mathcal{U}\frac{\partial C}{\partial \mathcal{X}} + \frac{\partial C}{\partial t}. \tag{4.17}$$

Here, the rate constant of first order chemical response is k_1, the molecular diffusion coefficient is $\mathcal{D}$ and liquid concentration is C.

The dimensionless quantities are specified as:

$$\theta = \frac{t}{\bar{t}}, \bar{t} = \frac{\lambda}{\bar{\mathcal{U}}}, \eta = \frac{\mathcal{Y}}{d}, \xi = \frac{(\mathcal{X} - \bar{\mathcal{U}}t)}{\lambda}, \mathcal{H} = \frac{h}{d}, \mathcal{P} = \frac{d^2}{\mu c}\mathcal{P}', \mathcal{M} = \sqrt{\frac{\sigma B_0^2}{\mu}}d. \tag{4.18}$$

For the regular estimations of physiologically essential parameters of this issue, it is normal that $\bar{\mathcal{U}} \approx C$ (Alemayehu and Radhakrishnamacharya [10]).

To proceed further, we use $\bar{\mathcal{U}} \approx C$ in (4.17), equations (4.11), (4.16) and (4.17) are nondimensionalized as:

$$\mathcal{P} = -\varepsilon\left[(\mathcal{E}_1 + \mathcal{E}_2)(2\pi)^3\cos(2\pi\xi) - \mathcal{E}_3(2\pi)^2\sin(2\pi\xi)\right], \tag{4.19}$$

$$\mathcal{U}_{\mathcal{X}} = \frac{d^2}{\mu m^2}\mathcal{P}\left[A_1\cosh(m\eta) - A_2\right], \tag{4.20}$$

$$\frac{\partial^2 C}{\partial \eta^2} - \frac{k_1 d^2}{\mathcal{D}}C = \frac{d^2}{\lambda \mathcal{D}}\mathcal{U}_{\mathcal{X}}\frac{\partial C}{\partial \xi}, \tag{4.21}$$

where
the amplitude ratio is $\varepsilon\left(=\frac{a}{d}\right)$, the rigidity is $\mathcal{E}_1\left(=-\frac{\mathcal{T}d^3}{\lambda^3\mu\mathbf{c}}\right)$, the stiffness is $\mathcal{E}_2 = \left(\frac{m\mathbf{c}d^3}{\lambda^3\mu}\right)$, the viscous damping force in the wall is $\mathcal{E}_3 = \left(\frac{\mathbf{c}d^3}{\mu\lambda^2}\right)$.

The dispersion with first- order irreversible chemical response occur in the mass of the liquid and at the channel walls.

Referring Philp and Chandra [19], the wall conditions are specified as:

$$0 = \mathcal{F}C + \frac{\partial C}{\partial \mathcal{Y}} \quad \text{at} \quad \mathcal{Y} = [a\sin\frac{2\pi}{\lambda}(\mathcal{X} - \bar{\mathcal{U}}t) + d] = h, \tag{4.22}$$

$$0 = -\mathcal{F}C + \frac{\partial C}{\partial \mathcal{Y}} \quad \text{at} \quad \mathcal{Y} = -[a\sin\frac{2\pi}{\lambda}(\mathcal{X} - \bar{\mathcal{U}}t) + d] = -h. \tag{4.23}$$

From equations (4.18), (4.22) and (4.23), we get

$$0 = \beta C + \frac{\partial C}{\partial \eta} \quad \text{at} \quad \eta = [\varepsilon\sin(2\pi\xi) + 1] = \mathcal{H}, \tag{4.24}$$

$$0 = -\beta C + \frac{\partial C}{\partial \eta} \quad \text{at} \quad \eta = -[\varepsilon\sin(2\pi\xi) + 1] = -\mathcal{H}, \tag{4.25}$$

where the heterogeneous response rate constraint is $\beta = \mathcal{F}d$, relating to catalytic response at the dividers.

From equations (4.24), (4.25) the primitive of equation (4.21) as follows:

$$C(\eta) = \left[\frac{d^4}{\lambda\mu\mathcal{D}m^2}\frac{\partial C}{\partial \xi}\right]\mathcal{P}\Big[A_4\cosh(m\eta) - A_5\cosh(\alpha\eta) + A_6 - A_7\cosh(\alpha\eta)\Big], \tag{4.26}$$

and $\alpha = \sqrt{\frac{k_1}{\mathcal{D}}d^2}$, $m = m_1 d = \sqrt{\frac{\sigma}{\mu}}B_0 d = \mathcal{M}$.

As discussed in chapter 2, the volumetric flow rate $\mathcal{Q}$ is defined as:

$$\mathcal{Q} = \int_{-\mathcal{H}}^{\mathcal{H}} C\,\mathcal{U}_{\mathcal{X}} d\eta. \tag{4.27}$$

Using equations (4.20) and (4.26) in equation (4.27), we get

$$\mathcal{Q} = -2\frac{d^6}{\lambda\mu^2\mathcal{D}}\frac{\partial C}{\partial \xi}\mathcal{G}(\xi, \alpha, \beta, \varepsilon, \mathcal{E}_1, \mathcal{E}_2, \mathcal{E}_3, \mathcal{M}). \tag{4.28}$$

where

$$\mathcal{G}(\xi,\alpha,\beta,\varepsilon,\mathcal{E}_1,\mathcal{E}_2,\mathcal{E}_3,\mathcal{M}) = \\ -\frac{\mathcal{P}^2}{\mathcal{M}^4}\Big[\frac{A_1A_4}{2}B_1-(A_1A_5+A_1A_7)B_2+(A_1A_6-A_2A_4)B_3+ \\ (A_2A_5+A_2A_7)B_4-A_2A_6\mathcal{H}\Big], \quad (4.29)$$

$$A_1=\frac{1}{\cosh\mathcal{MH}}, A_2=\frac{\sinh\mathcal{MH}}{\mathcal{MH}\cosh\mathcal{MH}}, A_3=\frac{\sinh\mathcal{MH}}{\alpha\sinh\alpha\mathcal{H}},$$
$$A_4=\frac{1}{(\mathcal{M}^2-\alpha^2)\cosh\mathcal{MH}}, A_6=\frac{\sinh\mathcal{MH}}{\mathcal{MH}\alpha^2\cosh\mathcal{MH}}, \alpha=\sqrt{\frac{k_1}{\mathcal{D}}}d,$$
$$A_5=\frac{\mathcal{M}\sinh\mathcal{MH}+\beta\cosh\mathcal{MH}}{(\mathcal{M}^2-\alpha^2)\cosh\mathcal{MH}(\alpha\sinh\alpha\mathcal{H}+\beta\cosh\alpha\mathcal{H})}, B_3=\frac{\sinh\mathcal{MH}}{\mathcal{M}},$$
$$A_7=\frac{\beta\sinh\mathcal{MH}}{\mathcal{MH}\alpha^2\cosh\mathcal{MH}(\alpha\sinh\alpha\mathcal{H}+\beta\cosh\alpha\mathcal{H})},$$
$$B_1=\frac{2\mathcal{MH}+\sinh 2\mathcal{MH}}{2\mathcal{M}},$$
$$B_2=\frac{\mathcal{M}\sinh\mathcal{MH}\cosh\alpha\mathcal{H}-\alpha\cosh\mathcal{MH}\sinh\alpha\mathcal{H}}{(\mathcal{M}^2-\alpha^2)}, B_4=\frac{\sinh\alpha\mathcal{H}}{\alpha}.$$

Glancing at equation (4.28) with Fick's bylaw of dispersion, the scattering coefficient $\mathcal{D}^*$ was intended such that the solute disperses near to the plane moving with the typical speed of the flow and is specified as:

$$\mathcal{D}^* = 2\frac{d^6}{\mu^2\mathcal{D}}\mathcal{G}(\xi,\alpha,\beta,\varepsilon,\mathcal{E}_1,\mathcal{E}_2,\mathcal{E}_3,\mathcal{M}). \quad (4.30)$$

The mean of $\mathcal{G}$ is $\bar{\mathcal{G}}$ and is attained as:

$$\bar{\mathcal{G}} = \int_0^1 \mathcal{G}(\xi,\alpha,\beta,\varepsilon,\mathcal{E}_1,\mathcal{E}_2,\mathcal{E}_3,\mathcal{M})d\xi, \quad (4.31)$$

4.5 Outcomes and Discussion

The impacts of various constraints on the mean effective scattering coefficient can be observed through the expression $\bar{\mathcal{G}}$. Using MATHEMATICA software the graphs are plotted for equation (4.31).

The effects of the rigidity constraint $(\mathcal{E}_1)$, stiffness $(\mathcal{E}_2)$ and viscous damping force $(\mathcal{E}_3)$ on the dispersion coefficient $(\bar{\mathcal{G}})$ are depicted in Figs. (4.2) - (4.10). Figures 4.2, 4.3 and 4.4 shows the influence of the rigidness $(\mathcal{E}_1)$ of the stretchy wall on the dispersion coefficient $(\bar{\mathcal{G}})$. Dispersion enhances with increase in wall rigidness $(\mathcal{E}_1)$ for an instant of (a) no stiffness in the channel wall ($\mathcal{E}_2$=0) and perfectly elastic wall ($\mathcal{E}_3$=0) (Fig. 4.2); (b) stiffness in the wall ($\mathcal{E}_2 \neq 0$) and dissipative wall ($\mathcal{E}_3 \neq 0$) (Figs. 4.3, 4.4). It is witnessed that $\bar{\mathcal{G}}$ increases with the stiffness $(\mathcal{E}_2)$ for both the cases of (a) dissipative wall ($\mathcal{E}_3 \neq 0$) (Figs. 4.5, 4.6) and (b) perfectly elastic wall ($\mathcal{E}_3$=0) (Fig. 4.7). Furthermore, it is perceived that expansion in viscous damping drive/force $(\mathcal{E}_3)$ ascends $\bar{\mathcal{G}}$ for an illustration $\mathcal{E}_2 \neq 0$ (Figs. 4.8, 4.9, 4.10). This result is in agreement with the results of Hayat et al. [41, 45], Ravikiran and Radhakrisnamacharya [121].

In Figs. (4.11) - (4.13), it is observed that $\bar{\mathcal{G}}$ descends with an increase in magnetic field constraint $(\mathcal{M})$. Furthermore, $\bar{\mathcal{G}}$ ascends with an increment in the amplitude ratio (ε) (Figs. 4.4, 4.7, 4.10, and 4.13). This finding agrees with the conclusion of Sobh [142], Ravikiran and Radhakrisnamacharya [121].

Dispersion reduces with a homogeneous compound response rate (α) (Figs. 4.3, 4.6, and 4.9) and heterogeneous substance response rate (β) (Figs. 4.2,4.5, and 4.8), where as scattering lessening thru β is a lesser amount of important. This result is common since growth in α stimulates an expansion in the sum of moles of solute proficiencies chemical response. This output coincides with the arguments of Padma and Rao [93], Gupta and Gupta [32], Hayat et al. [41, 45], Ravikiran and Radhakrisnamacharya [121].

4.6 Conclusion

In the present study, the effects of magnetic constraint $(\mathcal{M})$, amplitude ratio (ε), homogeneous response rate (α), heterogeneous response rate (β), rigidity $(\mathcal{E}_1)$, stiffness $(\mathcal{E}_2)$ and viscous damping characteristic of the wall ($\mathcal{E}_3$) on dispersion coefficient ($\bar{\mathcal{G}}$) have been inspected for the magneto-hydrodynamic peristaltic pumping of an incompressible viscous fluid in a uniform channel. It is noticed that the concentration profile ($\bar{\mathcal{G}}$) amplifies with a rise in wall features ($\mathcal{E}_1, \mathcal{E}_2, \mathcal{E}_3$), and ε. Furthermore, opposite behaviors of homogeneous response rate (α) and heterogeneous response rate (β) are looked on $\bar{\mathcal{G}}$.

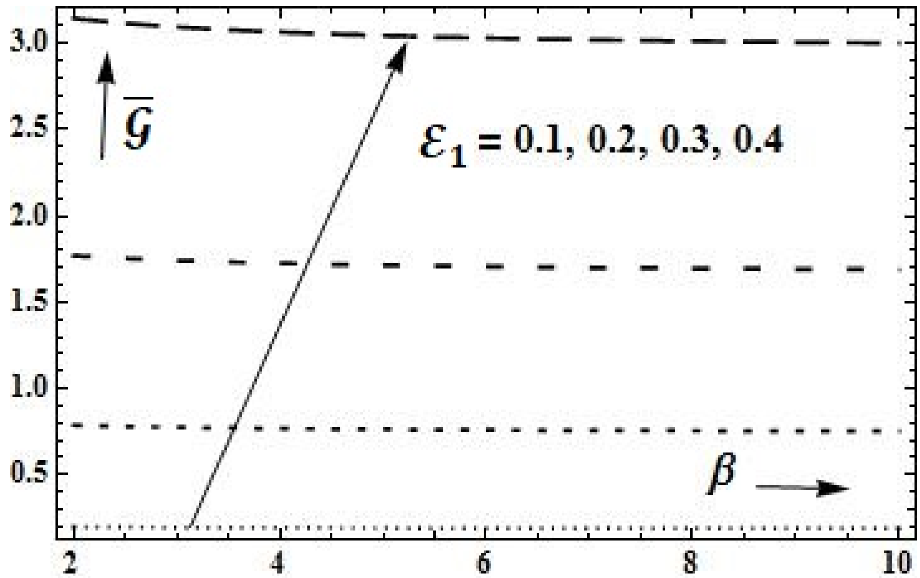

Figure 4.2: Illustration of rigidity ($\mathcal{E}_1$) with scattering coefficient ($\bar{\mathcal{G}}$) when $\mathcal{E}_2 = 0.0$, $\mathcal{E}_3 = 0.00$, $\varepsilon = 0.2$, $\alpha = 1.0$, $\mathcal{M} = 4.0$.

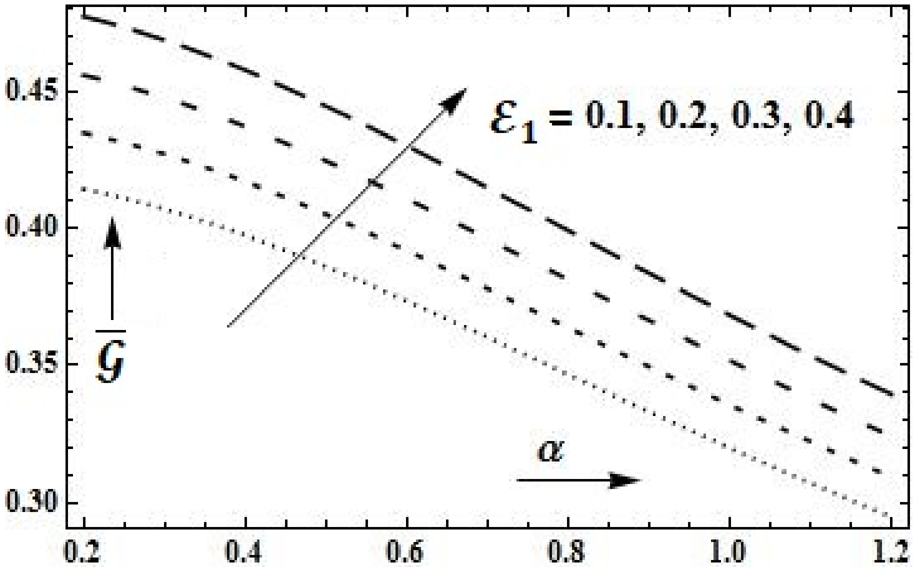

Figure 4.3: Illustration of rigidity ($\mathcal{E}_1$) with scattering coefficient ($\bar{\mathcal{G}}$) when $\mathcal{E}_2 = 4.0$, $\mathcal{E}_3 = 0.06$, $\varepsilon = 0.2$, $\beta = 5.0$, $\mathcal{M} = 4.0$.

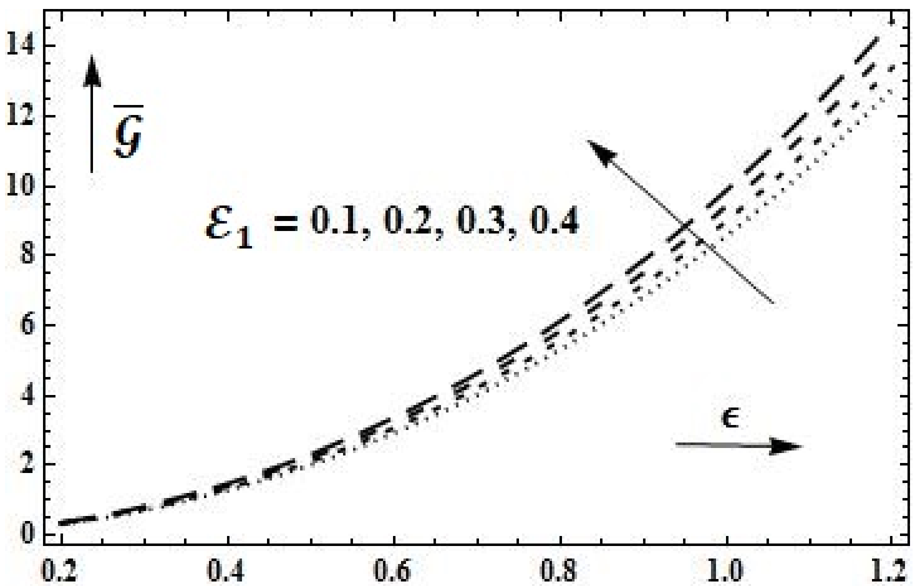

Figure 4.4: Illustration of rigidity ($\mathcal{E}_1$) with scattering coefficient ($\bar{\mathcal{G}}$) when $\mathcal{E}_2 = 4.0$, $\mathcal{E}_3 = 0.06$, $\alpha = 1.0$, $\beta = 5.0$, $\mathcal{M} = 4.0$.

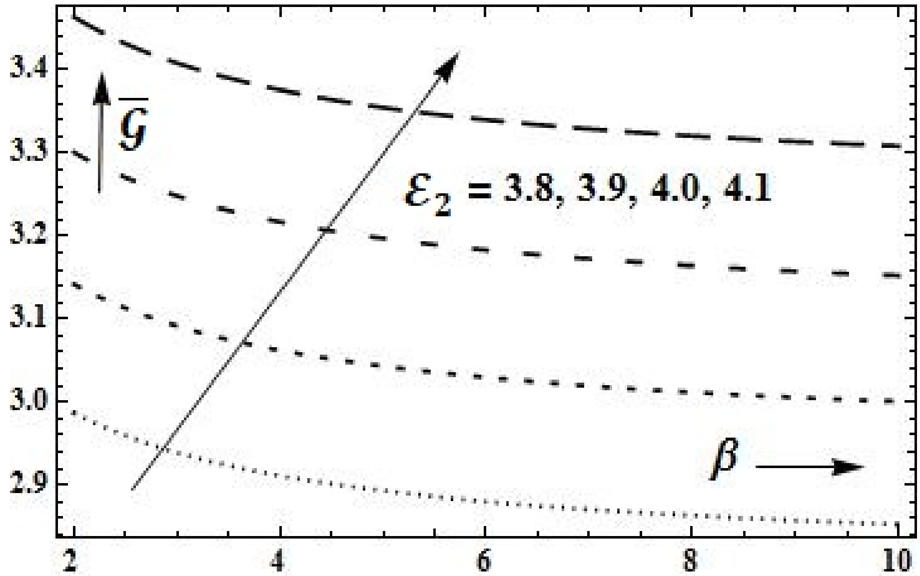

Figure 4.5: Illustration of stiffness ($\mathcal{E}_2$) with scattering coefficient ($\bar{\mathcal{G}}$) when $\mathcal{E}_1 = 0.1$, $\mathcal{E}_3 = 0.06$, $\varepsilon = 0.2$, $\alpha = 1.0$, $\mathcal{M} = 4.0$.

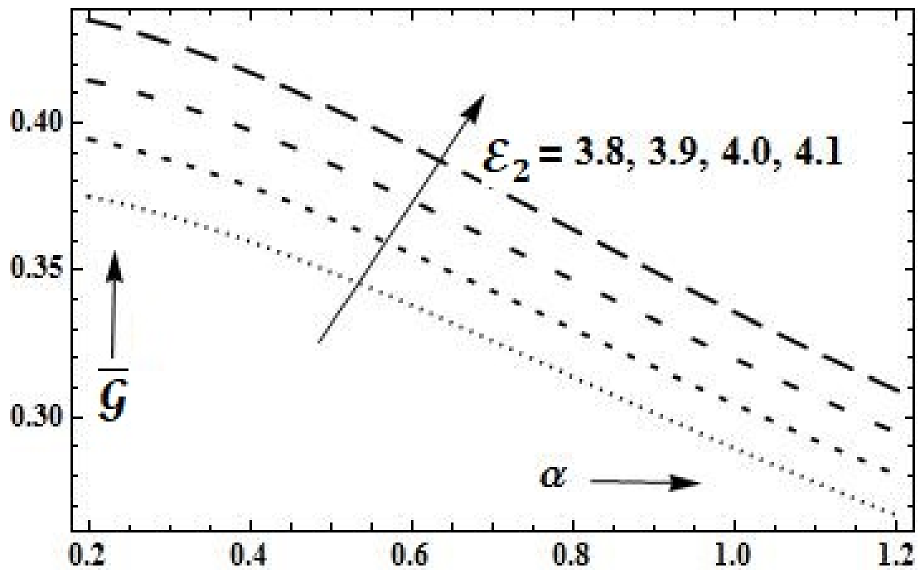

Figure 4.6: Illustration of stiffness ($\mathcal{E}_2$) with scattering coefficient ($\bar{\mathcal{G}}$) when $\mathcal{E}_1 = 0.1$, $\mathcal{E}_3 = 0.06$, $\varepsilon = 0.2$, $\beta = 5.0$, $\mathcal{M} = 4.0$.

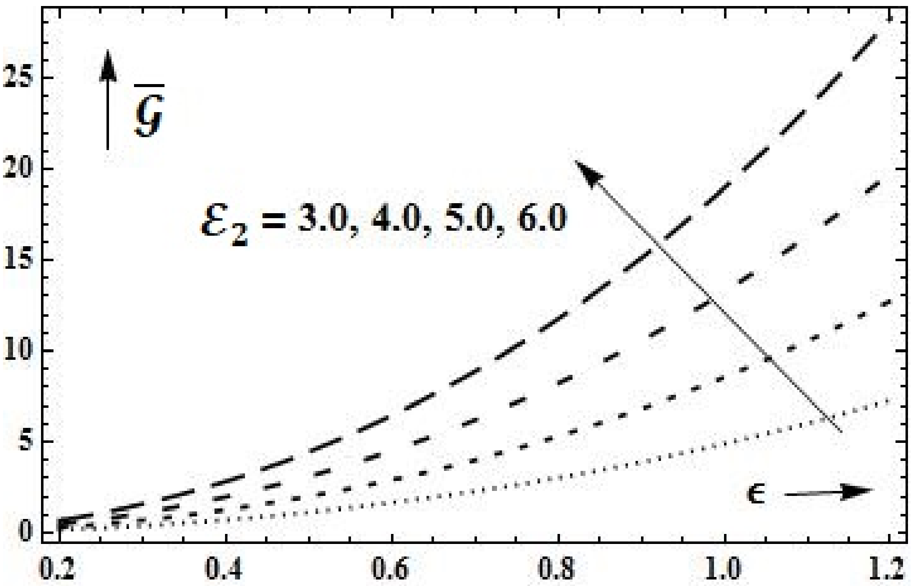

Figure 4.7: Illustration of stiffness ($\mathcal{E}_2$) with scattering coefficient ($\bar{\mathcal{G}}$) when $\mathcal{E}_1 = 0.1$, $\mathcal{E}_3 = 0.00$, $\alpha = 1.0$, $\beta = 5.0$, $\mathcal{M} = 4.0$.

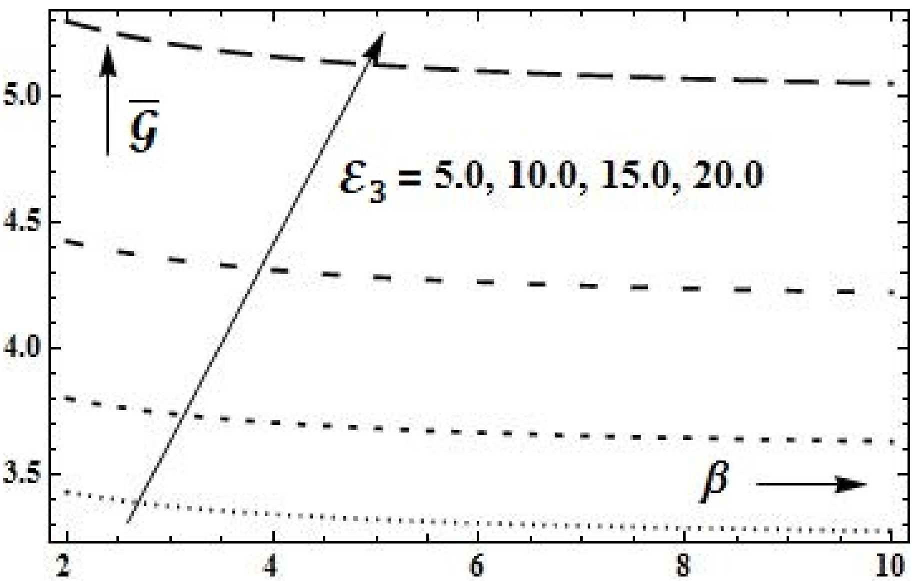

Figure 4.8: Illustration of damping force ($\mathcal{E}_3$) with scattering coefficient ($\bar{\mathcal{G}}$) when $\mathcal{E}_1 = 0.1$, $\mathcal{E}_2 = 4.0$, $\varepsilon = 0.2$, $\alpha = 1.0$, $\mathcal{M} = 4.0$.

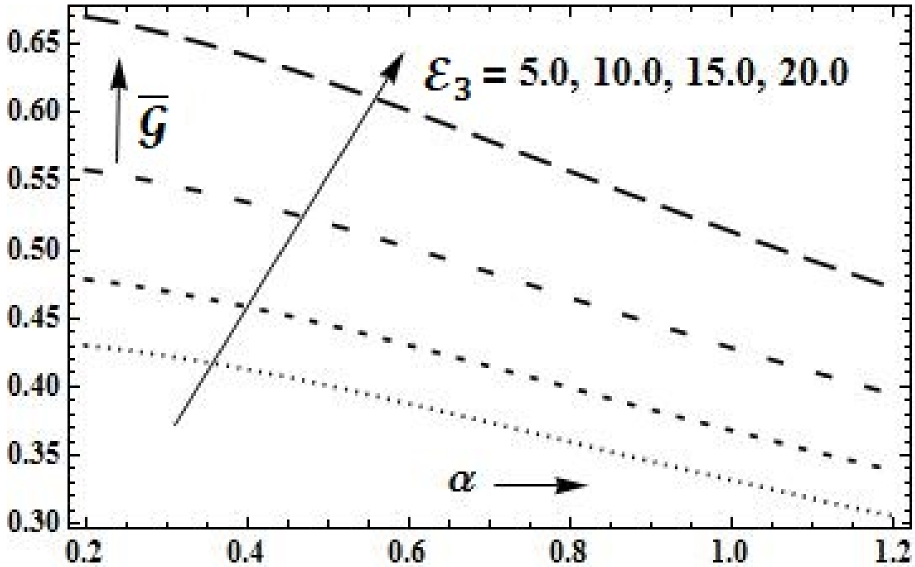

Figure 4.9: Illustration of damping force ($\mathcal{E}_3$) with scattering coefficient ($\bar{\mathcal{G}}$) when $\mathcal{E}_1 = 0.1$, $\mathcal{E}_2 = 4.0$, $\varepsilon = 0.2$, $\beta = 5.0$, $\mathcal{M} = 4.0$.

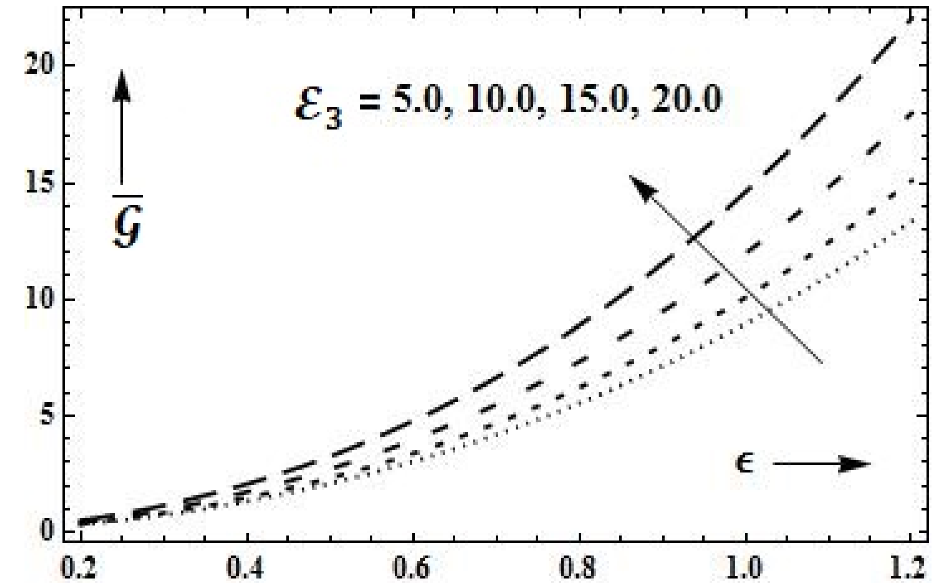

Figure 4.10: Illustration of damping force ($\mathcal{E}_3$) with scattering coefficient ($\bar{\mathcal{G}}$) when $\mathcal{E}_1 = 0.1$, $\mathcal{E}_2 = 4.0$, $\alpha = 1.0$, $\beta = 5.0$, $\mathcal{M} = 4.0$.

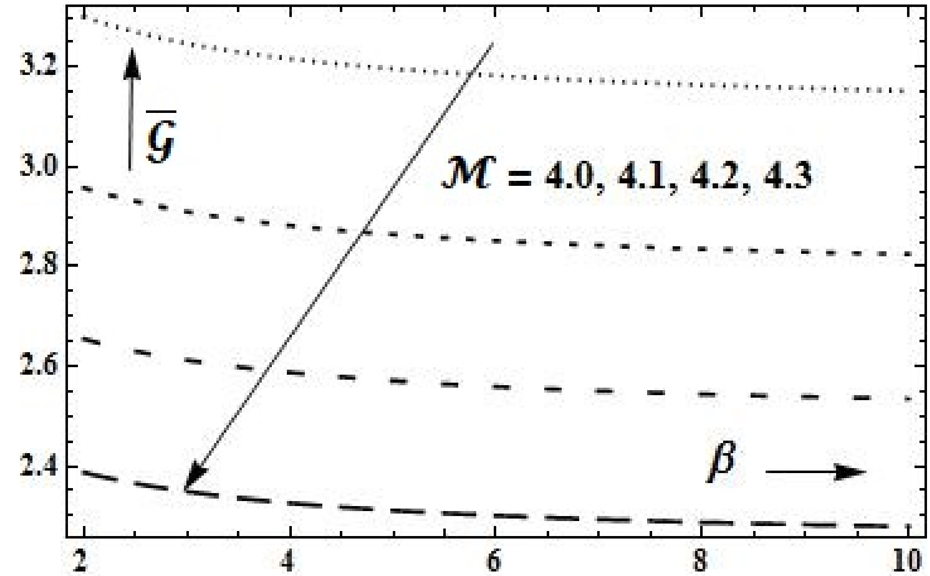

Figure 4.11: Illustration of magnetic constraint ($\mathcal{M}$) with scattering coefficient ($\bar{\mathcal{G}}$) when $\mathcal{E}_1 = 0.1$, $\mathcal{E}_2 = 4.0$, $\mathcal{E}_3 = 0.06$, $\varepsilon = 0.2$, $\alpha = 1.0$.

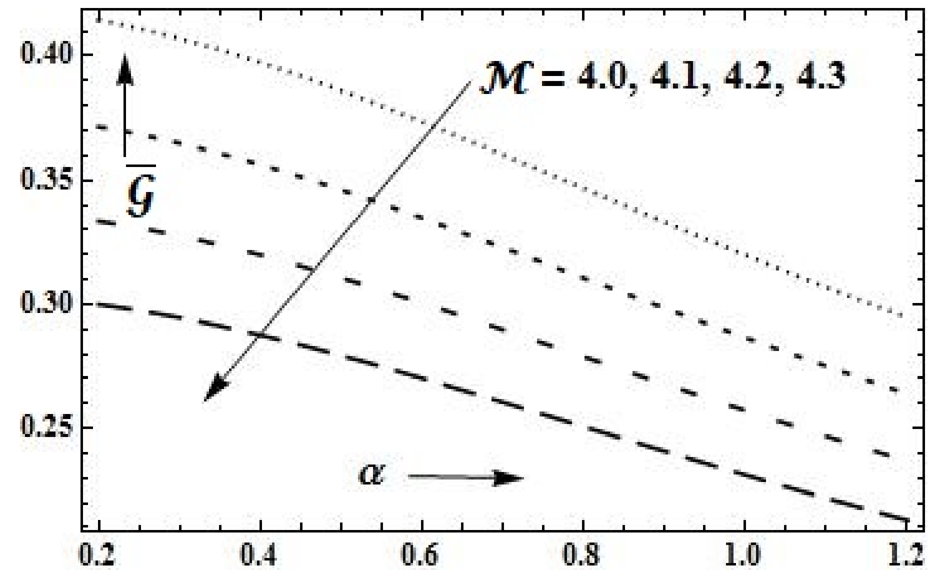

Figure 4.12: Illustration of magnetic constraint ($\mathcal{M}$) with scattering coefficient ($\bar{\mathcal{G}}$) when $\mathcal{E}_1 = 0.1$, $\mathcal{E}_2 = 4.0$, $\mathcal{E}_3 = 0.06$, $\varepsilon = 0.2$, $\beta = 5.0$, $\alpha = 1.0$.

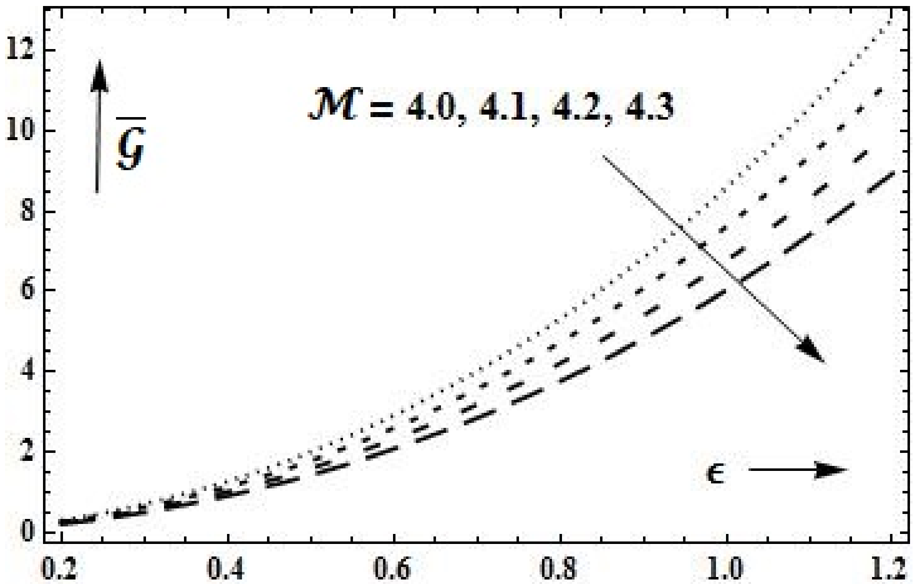

Figure 4.13: Illustration of magnetic constraint ($\mathcal{M}$) with scattering coefficient ($\bar{\mathcal{G}}$) when $\mathcal{E}_1 = 0.1$, $\mathcal{E}_2 = 4.0$, $\mathcal{E}_3 = 0.00$, $\varepsilon = 0.2$, $\alpha = 1.0$, $\beta = 5.0$.

Part - II

Peristalsis and Dispersion of a Solute in Couple Stress Fluid with Chemical Reactions and Wall Effects

Chapter 5

Influence of Creeping Sinusoidal Flow on Dispersion in a Couple Stress Fluid with Chemical Reactions and Wall Properties

5.1 Introduction

The problem of dispersion in the presence of heterogeneous and homogeneous chemical reactions is of importance in several contexts, for example, in nuclear physics, gas absorption in agitated tank, biological systems and the flow of nuclear fuel where heat is generated in the bulk (Mehta and Tiwari [73]). Hence, dispersion of a solute has been extensively studied under dissimilar conditions by many scholars (Bandyopadhyay and Mazumder [13], Hazra et al. [46], Sarkar and Jayaraman [131, 132], MacKenzie and Roberts [69], Nagarani et al. [90], Koo and Song [57], Paul [101, 102] and Kumar and Jayaraman [64]).

Peristaltic flows have been widely studied in the recent decades. Interest in such flows is inspired because of their occurrence in physiological, mechanical and industrial situations. Motivated by this, Haroun [36], Wang et al. [168], Vajravelu et al. [166], Medhavi [72], Radhakrishnamacharya and Murthy [110], Nadeem et al. [88], and Sankad and Radhakrishnamacharya [130] studied peristaltic transport of Newtonian or non-Newtonian fluids under different conditions.

In view of the role played by peristalsis and scattering in engineering and physiological systems, we have investigated, in the last three chapters that the effect of dispersion on peristaltic driving of an incompressible viscous fluid with wall features by including characteristics like: permeable media and magnetic field in the uniform cross section.

In a non-Newtonian fluid models, one fluid model that received considerable attention in the latest past, is the couple stress fluid, which seems to be a suitable model to explain some industrial and physiological fluids. It is seen that couple stress fluid behaviors are exceptionally useful in understanding dissimilar physiological and mechanical procedures. The couple stress model introduced by Stokes [151] has distinct features. The key feature of couple stresses is to introduce a size dependent effect. This fluid is able to describe blood, suspension fluids, and various types of lubricants. Such studies clarify the behavior of rheological complex liquids. Some studies on the peristaltic transport of couple stress fluid have been reported in the introduction chapter. After these studies, few investigators have explored the wall effects on different fluids with peristalsis (Sankad and Radhakrishnamacharya [129], Shit and Roy [137], Ellahi et al. [25], Hayat et al. [44], and Hina et al. [47]).

Existing information on the topic witnessed that an analytical treatment of the creeping sinusoidal flow and dispersion of a couple stress fluid with the chemical reaction and wall features have been never reported. Motivated from the reported literature, in this chapter, we have investigated the wall and chemical effects on the creeping sinusoidal stream and dispersion of a couple stress fluid with combined heterogeneous and homogeneous irreversible chemical reactions. The analytical expression for the mean effective dispersion coefficient has been derived by utilizing Taylor's limiting condition and long wavelength hypothesis. The principle outcomes are presented through graphs.

5.2 Formulation of the problem

Consider the flow of couple stress liquid with peristalsis in a channel. Figure 5.1 depicts the wave shape.

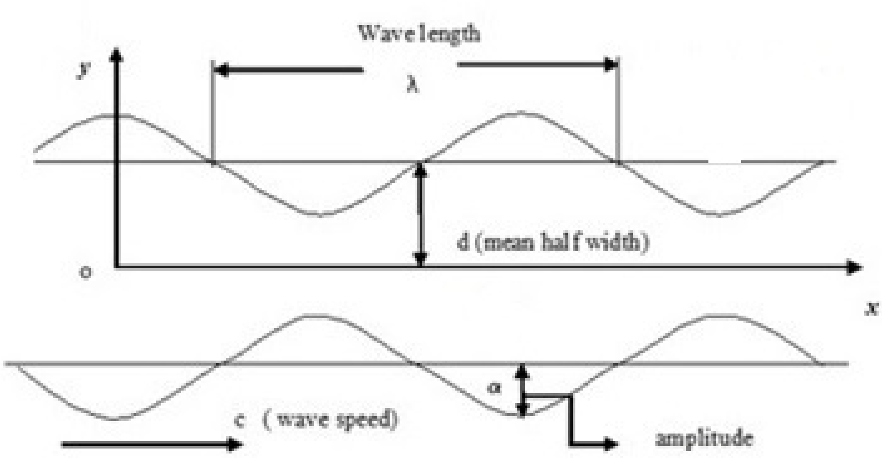

Figure 5.1: Geometry of the problem.

The equation of wave shape is considered same as in previous chapter 2 (Eqn. 2.1).

The relating flow conditions (Mekheimer [74]) of the present issue are:

$$\frac{\partial \mathcal{U}}{\partial \mathcal{X}}+\frac{\partial \mathcal{V}}{\partial \mathcal{Y}}=0, \tag{5.1}$$

$$-\frac{\partial p}{\partial \mathcal{X}}+\mu\nabla^2\mathcal{U}-\eta^{'}\nabla^4\mathcal{U}=\rho\left[\frac{\partial}{\partial t}+\mathcal{V}\frac{\partial}{\partial \mathcal{Y}}+\mathcal{U}\frac{\partial}{\partial \mathcal{X}}\right]\mathcal{U}, \tag{5.2}$$

$$-\frac{\partial p}{\partial \mathcal{Y}}+\mu\nabla^2\mathcal{V}-\eta^{'}\nabla^4\mathcal{V}=\rho\left[\frac{\partial}{\partial t}+\mathcal{V}\frac{\partial}{\partial \mathcal{Y}}+\mathcal{U}\frac{\partial}{\partial \mathcal{X}}\right]\mathcal{V}, \tag{5.3}$$

where $\frac{\partial^2}{\partial \mathcal{X}^2}+\frac{\partial^2}{\partial \mathcal{Y}^2}=\nabla^2$, $\nabla^2\nabla^2=\nabla^4$, the constant associated with couple stress fluid is η', the fluid density is ρ, the viscosity coefficient is μ, the velocity components in the $\mathcal{X}$, $\mathcal{Y}$ direction is $\mathcal{U}$, $\mathcal{V}$ respectively and the pressure is p.

Referring Mittra and Prasad [86], the condition of the flexible wall movement is specified as:

$$\mathcal{L}(h)=p-p_0, \tag{5.4}$$

where, the movement of the stretched membrane by the damping force is $\mathcal{L}$ and is intended by the subsequent equation:

$$\mathcal{L}=-\mathcal{T}\frac{\partial^2}{\partial \mathcal{X}^2}+m\frac{\partial^2}{\partial t^2}+\mathsf{C}\frac{\partial}{\partial t}. \tag{5.5}$$

Here, the coefficient of sticky damping force is C, the mass per/area is m, and the membrane tension is $\mathcal{T}$.

5.3 Method of Solution

Neglecting the body couples and body strengthens, under long wavelength hypothesis (Alemayehu and Radhakrishnamacharya [10]), equations (5.1) to (5.3) yield as:

$$\frac{\partial \mathcal{U}}{\partial \mathcal{X}}+\frac{\partial \mathcal{V}}{\partial \mathcal{Y}}=0, \tag{5.6}$$

$$-\frac{\partial p}{\partial \mathcal{X}}+\mu\frac{\partial^2\mathcal{U}}{\partial \mathcal{Y}^2}-\eta'\frac{\partial^4\mathcal{U}}{\partial \mathcal{Y}^4}=0, \tag{5.7}$$

$$-\frac{\partial p}{\partial \mathcal{Y}} = 0. \tag{5.8}$$

The allied border conditions are specified as:

$$\mathcal{U} = 0 \ , \frac{\partial^2 \mathcal{U}}{\partial \mathcal{Y}^2} = 0 \ , \text{at} \quad \mathcal{Y} = \pm h. \tag{5.9}$$

From equation (5.4), (5.5) and (5.7), active periphery conditions at the stretchy walls (Mittra and Prasas [86]) are specified as:

$$\frac{\partial}{\partial \mathcal{X}} \mathcal{L}(h) = \mu \frac{\partial^2 \mathcal{U}}{\partial \mathcal{Y}^2} - \eta' \frac{\partial^4 \mathcal{U}}{\partial \mathcal{Y}^4} = 0 \quad \text{at} \quad \mathcal{Y} = \pm h, \tag{5.10}$$

where

$$-\mathcal{T} \frac{\partial^3 h}{\partial \mathcal{X}^3} + m \frac{\partial^3 h}{\partial \mathcal{X} \partial t^2} + \mathsf{C} \frac{\partial^2 h}{\partial \mathcal{X} \partial t} = \frac{\partial}{\partial \mathcal{X}} \mathcal{L}(h) = \frac{\partial p}{\partial \mathcal{X}}. \tag{5.11}$$

Solving the equations (5.7) and (5.8) with (5.9) and (5.10) we obtain

$$\mathcal{U}(\mathcal{Y}) = -\frac{1}{\mu} \left(\frac{\partial p}{\partial \mathcal{X}} \right) \left[A_1' \cosh(m' \mathcal{Y}) + A_2' \mathcal{Y}^2 + A_3' \right]. \tag{5.12}$$

The mean speed is specified as:

$$\bar{\mathcal{U}}(\mathcal{Y}) = \frac{1}{2h} \int_{-h}^{h} \mathcal{U}(\mathcal{Y}) d\mathcal{Y}. \tag{5.13}$$

Equations (5.12) and (5.13) yield as:

$$\bar{\mathcal{U}}(\mathcal{Y}) = -\frac{1}{\mu} \left(\frac{\partial p}{\partial \mathcal{X}} \right) \left[A_1' \frac{\cosh(m' \mathcal{Y})}{m' h} + A_2' \frac{h^2}{3} + A_3' \right]. \tag{5.14}$$

Utilizing Alemayehu and Radhakrishnamacharya [10], the liquid speed is given as:

$$\mathcal{U}_{\mathcal{X}} = \mathcal{U} - \bar{\mathcal{U}}. \tag{5.15}$$

Equations (5.12), (5.14) and (5.15) yield as:

$$\mathcal{U}_{\mathcal{X}} = -\frac{1}{\mu}\left(\frac{\partial p}{\partial \mathcal{X}}\right)\left[A_1' \cosh(m'\mathcal{Y}) + A_2'\mathcal{Y}^2 + A_4'\right], \tag{5.16}$$

where

$$\mathcal{A}_1' = \frac{1}{m'^2 \cosh(m'h)}, \quad \mathcal{A}_2' = -\frac{1}{2}, \quad \mathcal{A}_3' = \frac{h^2}{2} - \frac{1}{m'^2},$$
$$\mathcal{A}_4' = -\frac{\mathcal{A}_1' \sinh(m'h)}{m'h} - \frac{\mathcal{A}_2' h^2}{3}.$$

5.4 Simultaneous homogeneous and heterogeneous chemical reactions with diffusion

As discussed in earlier chapter 2, the diffusion equation for the concentration C of the substance for the present issue under isothermal conditions:

$$\mathcal{D}\frac{\partial^2 C}{\partial \mathcal{Y}^2} - k_1 C = \mathcal{U}\frac{\partial C}{\partial \mathcal{X}} + \frac{\partial C}{\partial t}. \tag{5.17}$$

Here, the rate constant of first order chemical response is k_1, the molecular diffusion coefficient is $\mathcal{D}$ and liquid concentration is C.

The dimensionless quantities are specified as:

$$\eta = \frac{\mathcal{Y}}{d},\ m = d\sqrt{\frac{\mu}{\eta'}},\ \theta = \frac{t}{\bar{t}},\ \bar{t} = \frac{\lambda}{\bar{\mathcal{U}}},\ \mathcal{H} = \frac{h}{d},\ P = \frac{d^2}{\mu c \lambda}P',\ \xi = \frac{(\mathcal{X} - \bar{\mathcal{U}}t)}{\lambda}. \tag{5.18}$$

For the regular estimations of physiologically essential parameters of this issue, it is normal that $\bar{\mathcal{U}} \approx C$ ([10]).

To proceed further, we use $\bar{\mathcal{U}} \approx C$ in (5.17) and the conditions (5.11), (5.16), (5.17) are non-dimensionalized as:

$$\mathcal{P} = -\varepsilon\left[-\mathcal{E}_3(2\pi)^2\sin(2\pi\xi) + (\mathcal{E}_1+\mathcal{E}_2)(2\pi)^3\cos(2\pi\xi)\right], \tag{5.19}$$

$$\mathcal{U}_{\mathcal{X}} = -\frac{d^2}{\mu}\frac{\partial p}{\partial \mathcal{X}}\left[A_1\cosh(m\eta) + A_2\eta^2 + A_3\right], \tag{5.20}$$

$$\frac{\partial^2 C}{\partial \eta^2} - \frac{k_1 d^2}{\mathcal{D}}C = \frac{d^2}{\lambda\mathcal{D}}\mathcal{U}_{\mathcal{X}}\frac{\partial C}{\partial \xi}, \tag{5.21}$$

where
the amplitude ratio is $\varepsilon\left(=\frac{a}{d}\right)$, the rigidity is $\mathcal{E}_1\left(=-\frac{\mathcal{T}d^3}{\lambda^3\mu\mathbf{c}}\right)$, the stiffness is $\mathcal{E}_2 = \left(\frac{m\mathbf{c}d^3}{\lambda^3\mu}\right)$, the viscous damping force in the wall is $\mathcal{E}_3 = \left(\frac{\mathbf{c}d^3}{\mu\lambda^2}\right)$, and the couple stress constraint is $\gamma\left(=d\sqrt{\frac{\mu}{\eta'}}\right)$.

The dispersion with first- order irreversible chemical response occur in the mass of the liquid and at the channel walls.

Referring Philip and Chandra [19], the wall conditions are specified as:

$$0 = \mathcal{F}C + \frac{\partial C}{\partial \mathcal{Y}} \quad \text{at} \quad \mathcal{Y} = [a\sin\frac{2\pi}{\lambda}(\mathcal{X} - \bar{\mathcal{U}}t) + d] = h, \tag{5.22}$$

$$0 = -\mathcal{F}C + \frac{\partial C}{\partial \mathcal{Y}} \quad \text{at} \quad \mathcal{Y} = -[a\sin\frac{2\pi}{\lambda}(\mathcal{X} - \bar{\mathcal{U}}t) + d] = -h. \tag{5.23}$$

Equations (5.18), (5.22) and (5.23) yields as:

$$0 = \beta C + \frac{\partial C}{\partial \eta} \quad \text{at} \quad \eta = [\varepsilon\sin(2\pi\xi) + 1] = \mathcal{H}, \tag{5.24}$$

$$0 = -\beta C + \frac{\partial C}{\partial \eta} \quad \text{at} \quad \eta = -[\varepsilon\sin(2\pi\xi) + 1] = -\mathcal{H}, \tag{5.25}$$

where the heterogeneous response rate constraint is $\beta = \mathcal{F}d$, relating to catalytic response at the dividers.

Utilizing equations (5.24) and (5.25), the primitive of (5.21) is obtained as:

$$C(\eta) = -\frac{d^4}{\lambda\mu\mathcal{D}}\frac{\partial C}{\partial\xi}\mathcal{P}\Big[A_4\cosh(m\eta)+A_5\cosh(\alpha\eta)+A_6\eta^2+A_7\Big]. \tag{5.26}$$

The volumetric flow rate $\mathcal{Q}$ stated as in chapter 2 is specified as:

$$\mathcal{Q} = \int_{-\mathcal{H}}^{\mathcal{H}} C\,\mathcal{U}_{\mathcal{X}} d\eta. \tag{5.27}$$

Using (5.20) and (5.26) in (5.27), we obtain

$$\mathcal{Q} = -2\frac{d^6}{\lambda\mu^2\mathcal{D}}\frac{\partial C}{\partial\xi}\mathcal{G}(\xi,\alpha,\beta,\varepsilon,\mathcal{E}_1,\mathcal{E}_2,\mathcal{E}_3,\gamma), \tag{5.28}$$

where,

$$\begin{aligned}\mathcal{G}(\xi,\alpha,\beta,\varepsilon,\mathcal{E}_1,\mathcal{E}_2,\mathcal{E}_3,\gamma) = \Big\{ -\mathcal{P}^2\Big[&\frac{A_1A_4}{2}B_1+A_1A_5B_2 \\ &+(A_1A_6+A_2A_4)B_3+A_2A_5B_4+(A_1A_7+A_3A_4)B_5+A_3A_5B_6 \\ &+A_2A_6\frac{\mathcal{H}^5}{5}+(A_2A_7+A_3A_6)\frac{H^3}{3}+A_3A_7\mathcal{H}\Big]\Big\},\end{aligned} \tag{5.29}$$

$$
\begin{gathered}
A_1 = \frac{1}{m^2\cosh(m\mathcal{H})},\ A_2 = -\frac{1}{2},\ A_3 = -\frac{\sinh(m\mathcal{H})}{m^3\mathcal{H}\cosh(m\mathcal{H})} + \frac{\mathcal{H}^2}{6}, \\
A_4 = \frac{A_1}{m^2-\alpha^2},\ A_5 = -\frac{A_1}{(m^2-\alpha^2)}\frac{\mathcal{L}_2}{\mathcal{L}_1} + \frac{2A_2\mathcal{H}}{\alpha^2\mathcal{L}_1} - \frac{A_2\beta}{\alpha^2\mathcal{L}_1}\left(\mathcal{H}^2 + \frac{2}{\alpha^2}\right) + \frac{A_3\beta}{\alpha^2\mathcal{L}_1}, \\
A_6 = -\frac{A_2}{\alpha^2},\ A_7 = -\frac{2A_2}{\alpha^4} - \frac{A_3}{\alpha^2},\ \mathcal{L}_1 = \alpha\sinh(\alpha\mathcal{H}) + \beta\cosh(\alpha\mathcal{H}), \\
\mathcal{L}_2 = m\sinh(m\mathcal{H}) + \beta\cosh(m\mathcal{H}),\ B_1 = \frac{\sinh(2m\mathcal{H}) + 2m\mathcal{H}}{2m}, \\
B_2 = \frac{m\sinh(m\mathcal{H})\cosh(\alpha\mathcal{H}) - \alpha\cosh(m\mathcal{H})\sinh(\alpha\mathcal{H})}{m^2-\alpha^2}, \\
B_3 = \frac{\mathcal{H}^2\sinh(m\mathcal{H})}{m} - \frac{2\mathcal{H}\cosh(m\mathcal{H})}{m^2} + \frac{2\sinh(m\mathcal{H})}{m^3},\ B_5 = \frac{\sinh(m\mathcal{H})}{m}, \\
B_4 = \frac{\mathcal{H}^2\sinh(\alpha\mathcal{H})}{\alpha} - \frac{2\mathcal{H}\cosh(\alpha\mathcal{H})}{\alpha^2} + \frac{2\sinh(\alpha\mathcal{H})}{\alpha^3},\ B_6 = \frac{\sinh(\alpha\mathcal{H})}{\alpha}.
\end{gathered}
$$

Looking at equation (5.28) with Fick's law of scattering, the dispersing coefficient $\mathcal{D}^*$ was computed to such an extent that the solute disperses near to the plane moving with the typical speed of the flow and is specified as:

$$
\mathcal{D}^* = 2\frac{d^6}{\mu^2\mathcal{D}}\mathcal{G}(\xi,\alpha,\beta,\varepsilon,\mathcal{E}_1,\mathcal{E}_2,\mathcal{E}_3,\gamma). \tag{5.30}
$$

The mean of $\mathcal{G}$ is $\bar{\mathcal{G}}$ and is attained as:

$$
\bar{\mathcal{G}} = \int_0^1 \mathcal{G}(\xi,\alpha,\beta,\varepsilon,\mathcal{E}_1,\mathcal{E}_2,\mathcal{E}_3,\gamma)d\xi. \tag{5.31}
$$

5.5 Outcomes and Discussion

This part is composed to discuss the influence of various constraints on the concentration profile. The mean effective scattering coefficient is seen through the function $\bar{\mathcal{G}}$ for simultaneous heterogeneous-homogeneous responses given by equation (5.31). $\bar{\mathcal{G}}$ was computed by the software MATHEMATICA and end results are presented graphically. It might be assured that rigidity ($\mathcal{E}_1$), stiffness ($\mathcal{E}_2$) and damping force ($\mathcal{E}_3$) of the wall can't be zero all together.

The impacts of the rigidity ($\mathcal{E}_1$), stiffness ($\mathcal{E}_2$) and damping force ($\mathcal{E}_3$) on the dissipating coefficient ($\bar{\mathcal{G}}$) are represented in Figs. 5.2 - 5.10. As discussed in previous chapters, it is experiential that $\bar{\mathcal{G}}$ rises as growth in rigidity ($\mathcal{E}_1$) for the following cases of (a) toughness in the wall ($\mathcal{E}_2 \neq 0$) and dissipative wall ($\mathcal{E}_3 \neq 0$) (Fig. 5.2); (b) without toughness in the wall ($\mathcal{E}_2 = 0$) and dissipative wall ($\mathcal{E}_3 \neq 0$) (Fig. 5.3, 5.4). It is observed that $\bar{\mathcal{G}}$ increases with the toughness of the wall ($\mathcal{E}_2$) for the case of dissipative wall ($\mathcal{E}_3 \neq 0$) (Figs. 5.5, 5.6, 5.7). Additionally, it is seen that boost in viscous damping characterstics of the wall ($\mathcal{E}_3$) amplifies $\bar{\mathcal{G}}$ for both the cases of (a) toughness in the wall ($\mathcal{E}_2 \neq 0$) (Figs. 5.8, 5.10) and (b) without toughness in the wall ($\mathcal{E}_2 = 0$) (Fig. 5.9).

This understanding might be real because, increments in the elasticity of the conduit walls help the stream moment which causes to enhance the diffusion. Furthermore, $\bar{\mathcal{G}}$ rises with an augmentation in the amplitude ratio (ε) (Figs. 5.4, 5.7, 5.10, and 5.13). As definitely known, an increment in the amplitude ratio is the expansion in the amplitude of the wave across the channel and this cause to increase the fluid velocity within the channel and consequently may enhance dispersion.

The consequences of the couple stress constraint (γ) on the scattering coefficient ($\bar{\mathcal{G}}$) are depicted in Figs. 5.11-5.13. It is experiential that $\bar{\mathcal{G}}$ leads to an increase in couple stress constraint (γ) when there is toughness in the wall ($\mathcal{E}_2 \neq 0$) and dissipative wall ($\mathcal{E}_3 \neq 0$).

Scattering lessens with homogeneous reaction rate (α) (Figs. 5.3, 5.6, 5.9, and 5.12) and heterogeneous reaction rate (β) (Figures 5.2, 5.5, 5.8, and 5.11), where as scattering lessening thru β is a lesser amount of importance. This result is common since growth in α stimulates an expansion in the sum of moles of solute proficiencies chemical response. This outcome is reliable with the contentions of [93] and [45].

5.6 Conclusion

The present study leads us to understand numerically the effects of homogeneous response rate constraint (α), heterogeneous response rate constraint (β), couple stress constraint

(γ), amplitude ratio (ε), rigidity ($\mathcal{E}_1$), stiffness ($\mathcal{E}_2$), and damping force ($\mathcal{E}_3$) of the wall on dispersion coefficient ($\bar{\mathcal{G}}$), which is of great importance for the movement of chyme in the small intestine of the digestive system. It is looked out that the concentration profile ($\bar{\mathcal{G}}$) rises with an amplify in amplitude ratio, couple stress constraint and wall features. It also explored that concentration profile ($\bar{\mathcal{G}}$) descends with a rise in the heterogeneous response rate and homogeneous response rate. Finally, it concludes that amplitude ratio, couple stress constraint and wall properties favor the scattering.

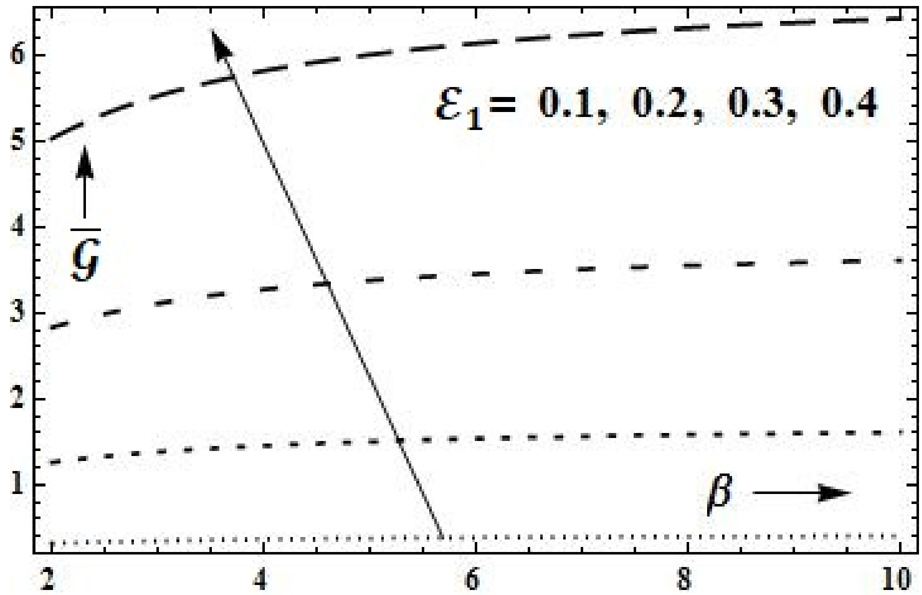

Figure 5.2: Illustration of rigidity ($\mathcal{E}_1$) with scattering coefficient ($\bar{\mathcal{G}}$) when $\mathcal{E}_2 = 4.0$, $\mathcal{E}_3 = 0.06$, $\varepsilon = 0.2$, $\alpha = 1.0$, $\gamma = 2.0$.

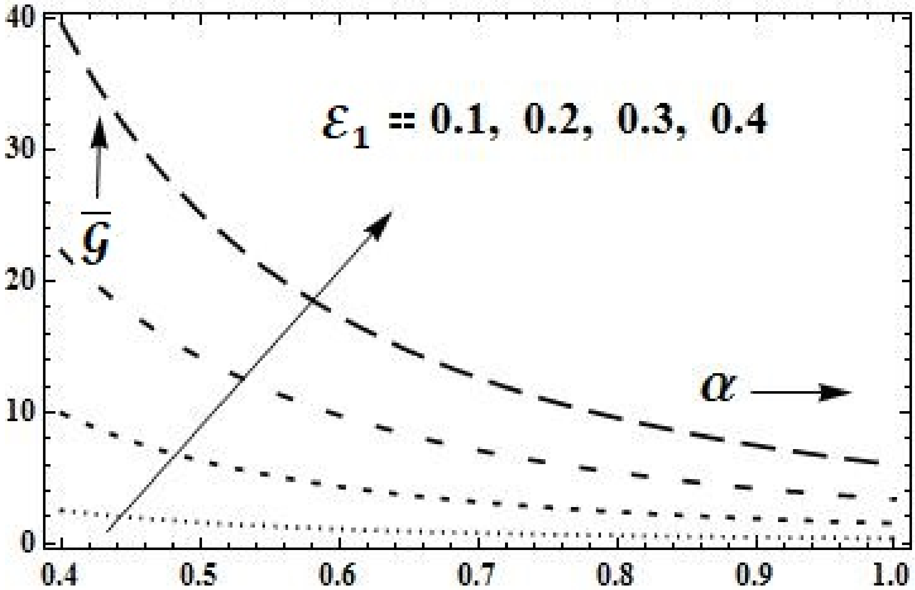

Figure 5.3: Illustration of rigidity ($\mathcal{E}_1$) with scattering coefficient ($\bar{\mathcal{G}}$) when $\mathcal{E}_2 = 0.0$, $\mathcal{E}_3 = 0.06$, $\varepsilon = 0.2$, $\beta = 5.0$, $\gamma = 2.0$.

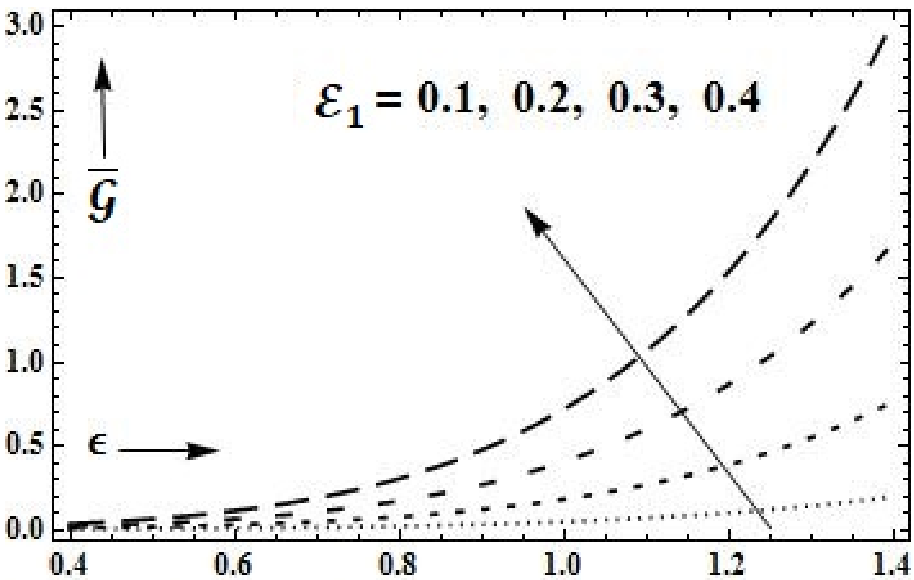

Figure 5.4: Illustration of rigidity ($\mathcal{E}_1$) with scattering coefficient ($\bar{\mathcal{G}}$) when $\mathcal{E}_2 = 0.0$, $\mathcal{E}_3 = 0.06$, $\alpha = 1.0$, $\beta = 5.0$, $\gamma = 2.0$.

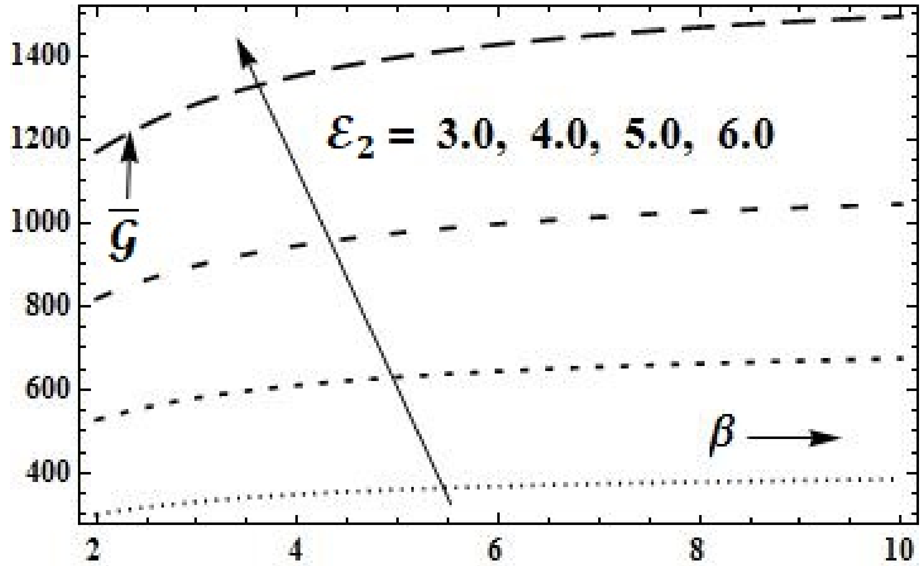

Figure 5.5: Illustration of stiffness ($\mathcal{E}_2$) with scattering coefficient ($\bar{\mathcal{G}}$) when $\mathcal{E}_1 = 0.1$, $\mathcal{E}_3 = 0.06$, $\varepsilon = 0.2$, $\alpha = 1.0$, $\gamma = 2.0$.

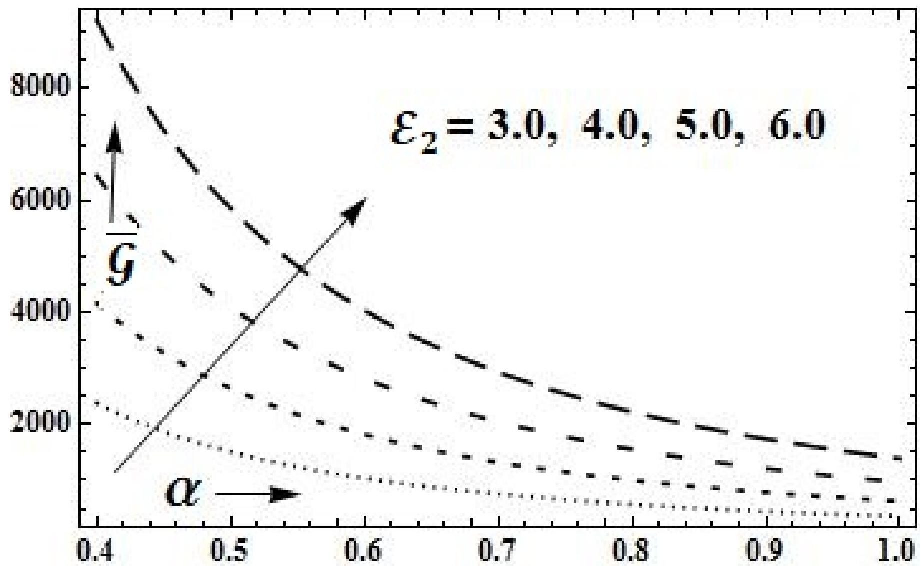

Figure 5.6: Illustration of stiffness ($\mathcal{E}_2$) with scattering coefficient ($\bar{\mathcal{G}}$) when $\mathcal{E}_1 = 0.1$, $\mathcal{E}_3 = 0.06$, $\varepsilon = 0.2$, $\beta = 5.0$, $\gamma = 2.0$.

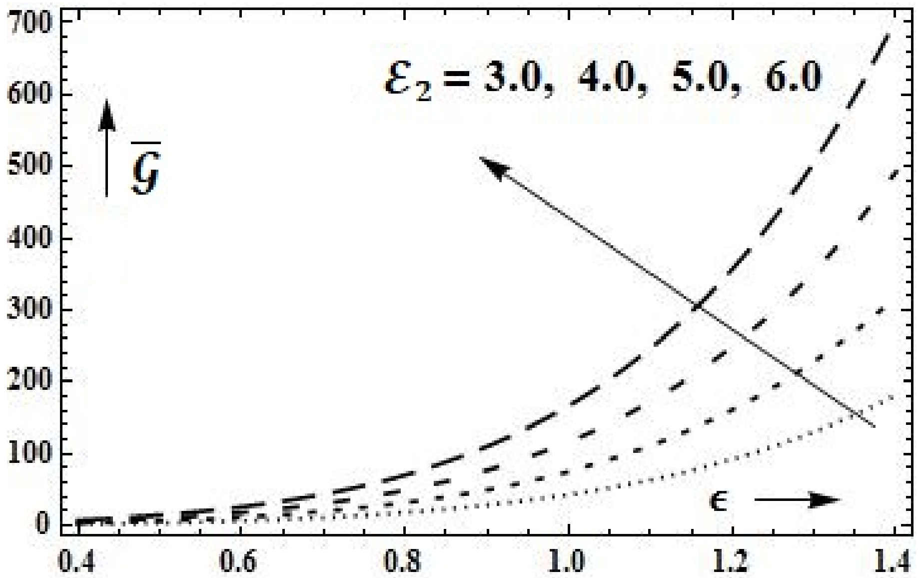

Figure 5.7: Illustration of stiffness ($\mathcal{E}_2$) with scattering coefficient ($\bar{\mathcal{G}}$) when $\mathcal{E}_1 = 0.1$, $\mathcal{E}_3 = 0.06$, $\alpha = 1.0$, $\beta = 5.0$, $\gamma = 2.0$.

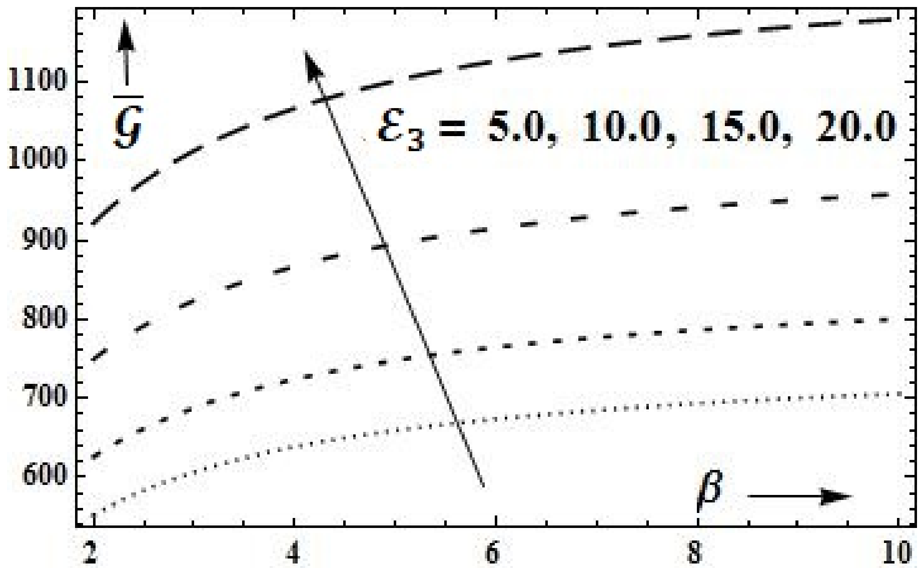

Figure 5.8: Illustration of damping force ($\mathcal{E}_3$) with scattering coefficient ($\bar{\mathcal{G}}$) when $\mathcal{E}_1 = 0.1$, $\mathcal{E}_2 = 4.0$, $\varepsilon = 0.2$, $\alpha = 1.0$, $\gamma = 2.0$.

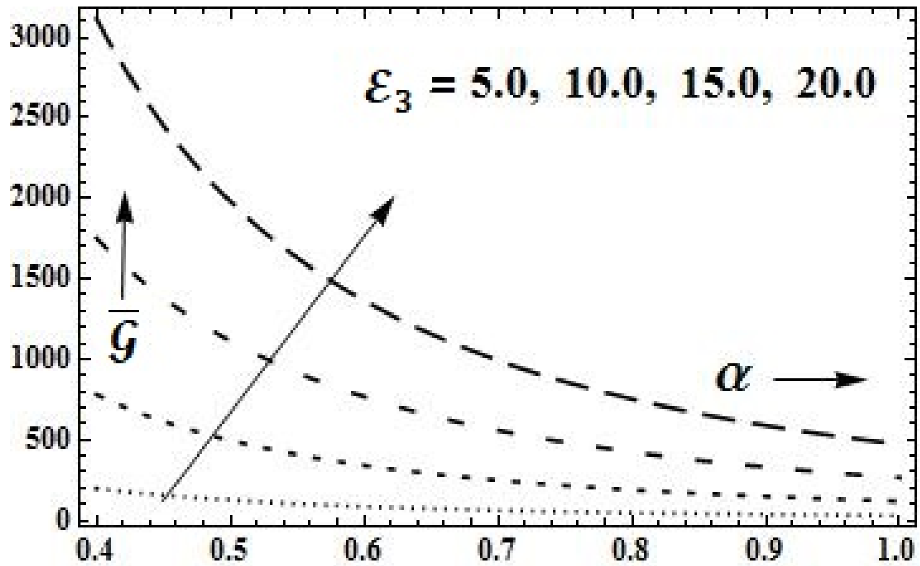

Figure 5.9: Illustration of damping force ($\mathcal{E}_3$) with scattering coefficient ($\bar{\mathcal{G}}$) when $\mathcal{E}_1 = 0.1$, $\mathcal{E}_2 = 0.0$, $\varepsilon = 0.2$, $\beta = 5.0$, $\gamma = 2.0$.

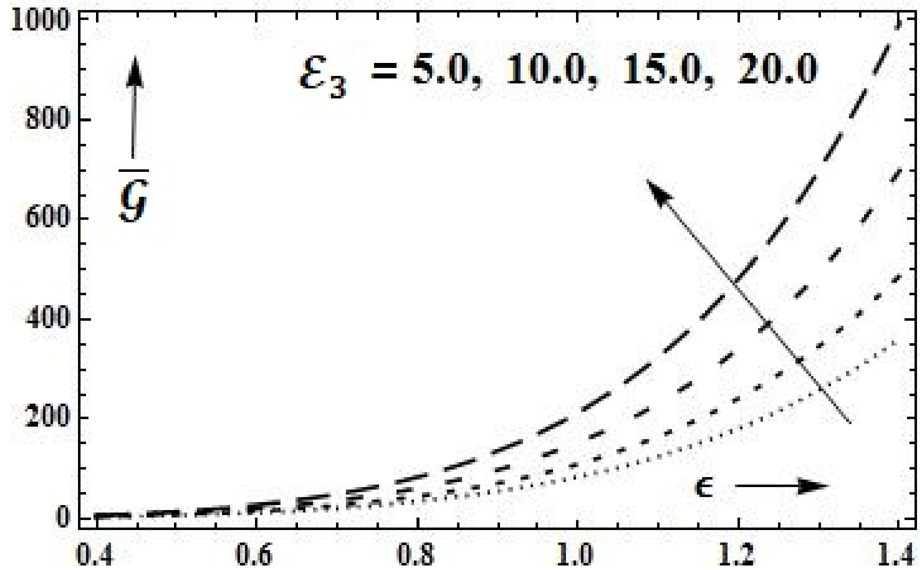

Figure 5.10: Illustration of damping force ($\mathcal{E}_3$) with scattering coefficient ($\bar{\mathcal{G}}$) when $\mathcal{E}_1 = 0.1$, $\mathcal{E}_2 = 4.0$, $\alpha = 1.0$, $\beta = 5.0$, $\gamma = 2.0$.

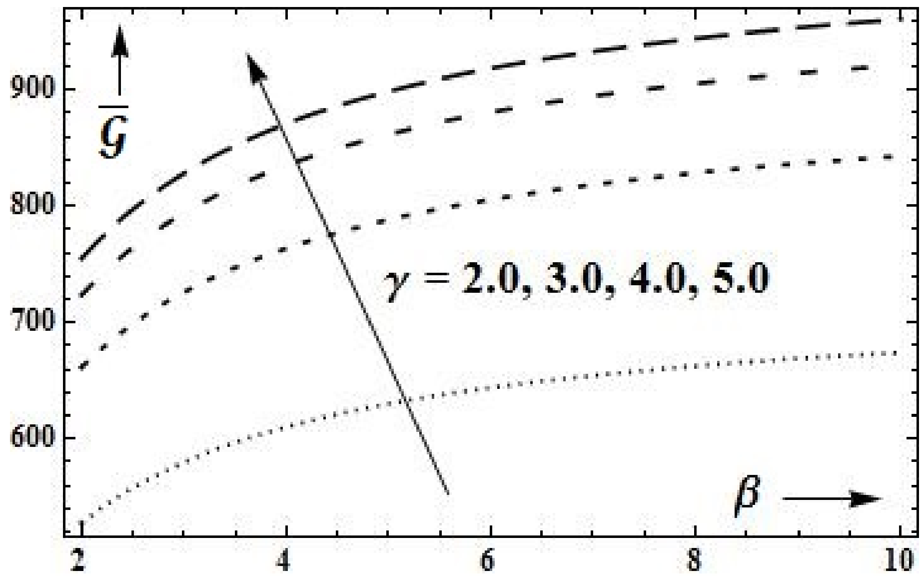

Figure 5.11: Illustration of couple stress constraint (γ) with scattering coefficient ($\bar{\mathcal{G}}$) when $\mathcal{E}_1 = 0.1$, $\mathcal{E}_2 = 4.0$, $\mathcal{E}_3 = 0.06$, $\varepsilon = 0.2$, $\alpha = 1.0$.

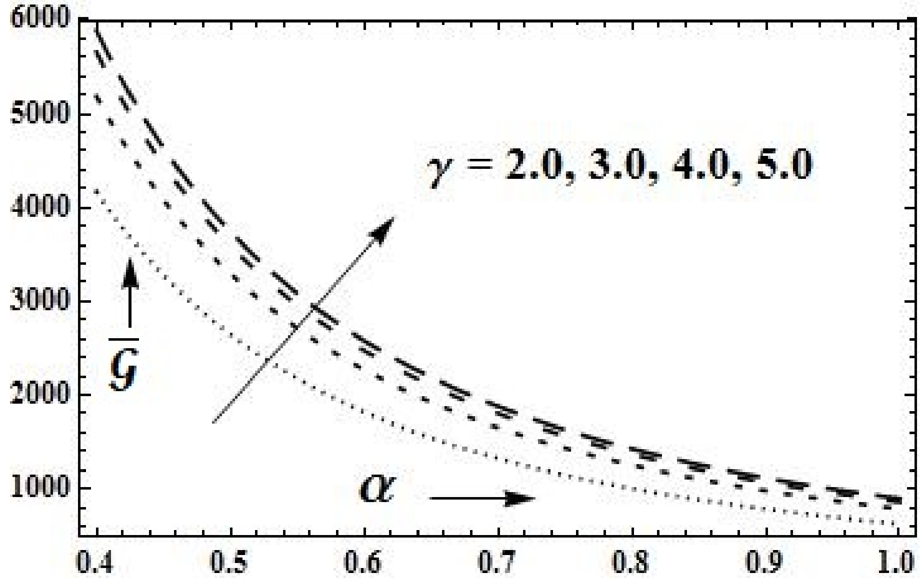

Figure 5.12: Illustration of couple stress constraint (γ) with scattering coefficient ($\bar{\mathcal{G}}$) when $\mathcal{E}_1 = 0.1$, $\mathcal{E}_2 = 4.0$, $\mathcal{E}_3 = 0.06$, $\varepsilon = 0.2$, $\beta = 5.0$.

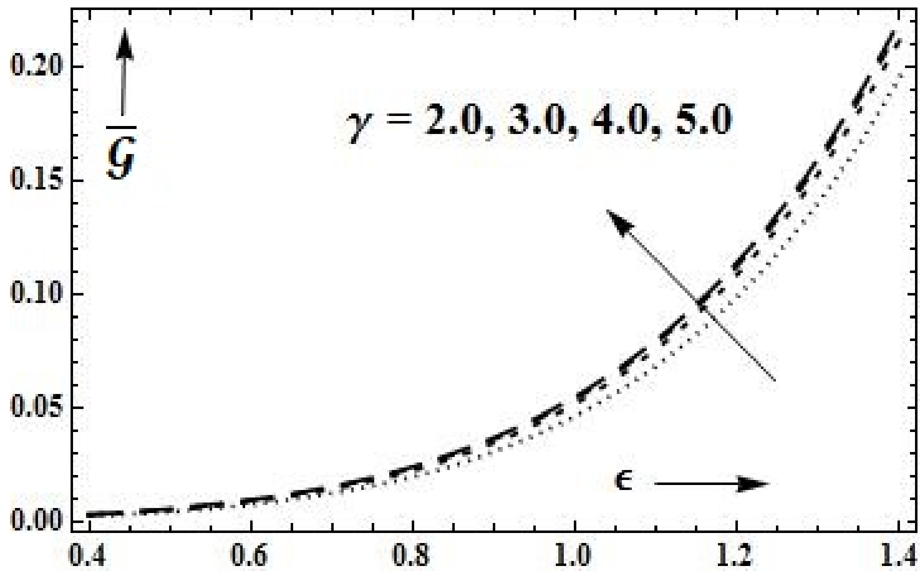

Figure 5.13: Illustration of couple stress constraint (γ) with scattering coefficient ($\bar{\mathcal{G}}$) when $\mathcal{E}_1 = 0.1$, $\mathcal{E}_2 = 4.0$, $\mathcal{E}_3 = 0.06$, $\varepsilon = 0.2$, $\alpha = 1.0$, $\beta = 5.0$.

Chapter 6

Creeping Sinusoidal Flow and Dispersion of a Solute in Couple Stress Fluid through a Porous Medium with Compliant Walls and Chemical Reactions

6.1 Introduction

In the last chapter, we have studied the dispersion of a solute matter in creeping sinusoidal flow of a couple stress fluid with wall features. Here, we have investigated the scattering of a solute in creeping sinusoidal movement of a couple stress fluid through a porous medium with compliant walls. Creeping sinusoidal flow with porous intermediate has attained significance in the current decade because of its practical applications, chiefly in biomechanics and geophysical fluid dynamics. Hence, Srinivas et al. [144], Sobh and Mady [143], Saffman [125], Rathod and Kulkarni [118], Rao and Mishra [116], Quintard et al. [108], Porta [104], Pal [96], Misra et al. [82], Hayat et al. [40] have studied the effect of porosity on different fluids with peristalsis.

The study of interaction of peristalsis with diffusion may lead to a better understanding of the flow situations in physiological systems. Hence, in this chapter, the influences of combined heterogeneous and homogeneous chemical response on the creeping flow of a couple stress fluid through a permeable medium with compliant walls have been investigated. Applying Taylor's approach, hypothesis of long wavelength, periphery limitation of stretchy walls, the closed form solution has been obtained for the scattering coefficient and effects of relevant constraints on it are studied.

6.2 Formulation of the problem

The flow of an incompressible and couple stress fluid through a permeable medium with peristalsis in a uniform channel is considered. Figure 6.1 depicts the wave shape.

The travelling sinusoidal wave equation is carried out as in chapter 2 (Eqn. 2.1) and the basic equations (Mekheimeri [74]) governing the flow of the current problem are as follows:

$$\frac{\partial \mathcal{U}}{\partial \mathcal{X}} + \frac{\partial \mathcal{V}}{\partial \mathcal{Y}} = 0, \tag{6.1}$$

$$-\frac{\partial p}{\partial \mathcal{X}} + \mu \nabla^2 \mathcal{U} - \eta' \nabla^4 \mathcal{U} - \left(\frac{\mu}{\bar{k}}\right) \mathcal{U} = \rho \left[\frac{\partial}{\partial t} + \mathcal{U}\frac{\partial}{\partial \mathcal{X}} + \mathcal{V}\frac{\partial}{\partial \mathcal{Y}}\right] \mathcal{U}, \tag{6.2}$$

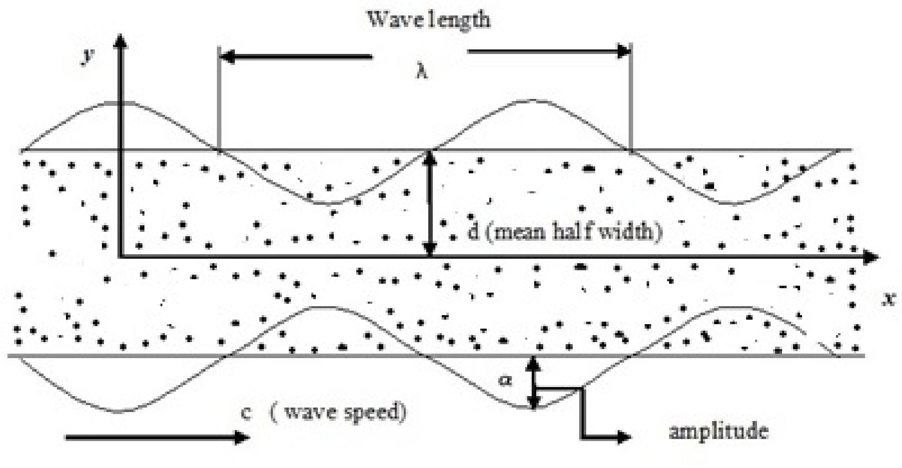

Figure 6.1: Geometry of the problem.

$$-\frac{\partial p}{\partial \mathcal{Y}} + \mu \nabla^2 \mathcal{V} - \eta' \nabla^4 \mathcal{V} - \left(\frac{\mu}{\bar{k}}\right) \mathcal{V} = \rho \left[\frac{\partial}{\partial t} + \mathcal{U}\frac{\partial}{\partial \mathcal{X}} + \mathcal{V}\frac{\partial}{\partial \mathcal{Y}}\right] \mathcal{V}, \tag{6.3}$$

where $\nabla^2 = \frac{\partial^2}{\partial x^2} + \frac{\partial^2}{\partial y^2}$, $\nabla^4 = \nabla^2\nabla^2$, the fluid density is ρ, the pressure is p, the viscosity coefficient is μ, the velocity component in the $\mathcal{X}$, $\mathcal{Y}$ directions are $\mathcal{U}$, $\mathcal{V}$, the constant associated with couple stress fluid is η', the permeability constraint is $\bar{k}$.

Referring Mittra and Prasad [86], the condition of the flexible wall movement is specified as:

$$\mathcal{L}(h) = p - p_0, \tag{6.4}$$

where, the movement of the stretched membrane by the damping force is $\mathcal{L}$ and is intended by the subsequent equation:

$$\mathcal{L} = -\mathcal{T}\frac{\partial^2}{\partial \mathcal{X}^2} + m\frac{\partial^2}{\partial t^2} + \mathbf{C}\frac{\partial}{\partial t}. \tag{6.5}$$

Here, the coefficient of sticky damping force is $\mathbf{C}$, the mass per/area is m, and the membrane tension is $\mathcal{T}$.

6.3 Method of Solution

Neglecting the body couples and body strengthens, under long wavelength hypothesis (Alemayehu and Radhakrishnamacharya [10]), equations (6.1) to (6.3) yield as:

$$\frac{\partial \mathcal{U}}{\partial \mathcal{X}} + \frac{\partial \mathcal{V}}{\partial \mathcal{Y}} = 0, \tag{6.6}$$

$$-\frac{\partial p}{\partial \mathcal{X}} + \mu \frac{\partial^2 \mathcal{U}}{\partial \mathcal{Y}^2} - \eta' \frac{\partial^4 \mathcal{U}}{\partial \mathcal{Y}^4} - \frac{\mu}{\bar{k}} \mathcal{U} = 0, \tag{6.7}$$

$$-\frac{\partial p}{\partial \mathcal{Y}} = 0. \tag{6.8}$$

The related periphery conditions are as stated:

$$\mathcal{U} = 0 \ , \frac{\partial^2 \mathcal{U}}{\partial \mathcal{Y}^2} = 0 \ , \text{at} \quad \mathcal{Y} = \pm h. \tag{6.9}$$

From equation (6.4), (6.5) and (6.7), active periphery conditions at the stretchy walls (Mittra and Prasas [86]) are specified as:

$$\frac{\partial}{\partial \mathcal{X}} \mathcal{L}(h) = \mu \frac{\partial^2 \mathcal{U}}{\partial \mathcal{Y}^2} - \eta' \frac{\partial^4 \mathcal{U}}{\partial \mathcal{Y}^4} - \frac{\mu}{\bar{k}} \mathcal{U} = 0 \quad \text{at} \quad \mathcal{Y} = \pm h, \tag{6.10}$$

where

$$\frac{\partial}{\partial \mathcal{X}} \mathcal{L}(h) = \frac{\partial p}{\partial \mathcal{X}} = -\mathcal{T} \frac{\partial^3 h}{\partial \mathcal{X}^3} + m \frac{\partial^3 h}{\partial \mathcal{X} \partial t^2} + \mathsf{C} \frac{\partial^2 h}{\partial \mathcal{X} \partial t}. \tag{6.11}$$

After solving the equations (6.7) and (6.8) with conditions (6.9) and (6.10), we get

$$\mathcal{U}(\mathcal{Y}) = -\frac{\bar{k}}{\mu} \left(\frac{\partial p}{\partial \mathcal{X}} \right) \left[A_1' \cosh(m_1' \mathcal{Y}) + A_2' \cosh(m_2' \mathcal{Y}) + 1 \right], \tag{6.12}$$

where

$$m_1' = \sqrt{\tfrac{\mu}{2\eta'}\left(1+\sqrt{1-\tfrac{4\eta'}{\mu\bar{k}}}\right)},\ m_2' = \sqrt{\tfrac{\mu}{2\eta'}\left(1-\sqrt{1-\tfrac{4\eta'}{\mu\bar{k}}}\right)}.$$

The mean speed is specified as:

$$\bar{\mathcal{U}} = \frac{1}{2h}\int_{-h}^{h}\mathcal{U}(\mathcal{Y})d\mathcal{Y}. \tag{6.13}$$

From equation (6.12) and (6.13), we get

$$\bar{\mathcal{U}} = -\frac{\bar{k}}{\mu}\left(\frac{\partial p}{\partial \mathcal{X}}\right)\left[\frac{A_1'}{m_1'h}\sinh(m_1'h)+\frac{A_2'}{m_2'h}\sinh(m_2'h)+1\right]. \tag{6.14}$$

Employing Ravikiran and Radhakrishnamacharya [122], the fluid velocity is given by the equation as:

$$\mathcal{U}_{\mathcal{X}} = \mathcal{U}-\bar{\mathcal{U}}. \tag{6.15}$$

From equations (6.12), (6.14) and (6.15), we obtain

$$\mathcal{U}_{\mathcal{X}} = -\frac{\bar{k}}{\mu}\left(\frac{\partial p}{\partial \mathcal{X}}\right)\left[A_1'\cosh(m_1'\mathcal{Y})+A_2'\cosh(m_2'\mathcal{Y})-\frac{A_1'}{m_1'h}\sinh(m_1'h)-\frac{A_2'}{m_2'h}\sinh(m_2'h)\right], \tag{6.16}$$

where
$A_1' = \frac{(m_2')^2}{\left[(m_1')^2-(m_2')^2\right]\cosh(m_1'h)},\ A_2' = \frac{-(m_1')^2}{\left[(m_1')^2-(m_2')^2\right]\cosh(m_2'h)},$

$\mathcal{P}' = -\mathcal{T}\frac{\partial^3 h}{\partial \mathcal{X}^3}+m\frac{\partial^3 h}{\partial \mathcal{X}\partial t^2}+\mathsf{C}\frac{\partial^2 h}{\partial \mathcal{X}\partial t}.$

6.4 Simultaneous homogeneous and heterogeneous chemical reactions with diffusion

The dispersion equation for the concentration C of the substance of the current issue under isothermal conditions as discussed in earlier chapters i.e.

$$\mathcal{D}\frac{\partial^2 C}{\partial \mathcal{Y}^2} - k_1 C = \mathcal{U}\frac{\partial C}{\partial \mathcal{X}} + \frac{\partial C}{\partial t}. \tag{6.17}$$

Here, the rate constant of first order chemical response is k_1, the molecular diffusion coefficient is $\mathcal{D}$ and the liquid concentration is C.

The dimensionless quantities are specified as:

$$\theta = \frac{t}{\bar{t}}, \quad \bar{t} = \frac{\lambda}{\bar{\mathcal{U}}}, \quad \eta = \frac{\mathcal{Y}}{d}, \quad \xi = \frac{(\mathcal{X} - \bar{\mathcal{U}}t)}{\lambda}, \quad \mathcal{H} = \frac{h}{d}, \quad \mathcal{P} = \frac{d^2}{\mu c \lambda}\mathcal{P}', \quad k = \frac{\bar{k}}{d^2}. \tag{6.18}$$

For the regular estimations of physiologically essential parameters of this issue, it is normal that $\bar{\mathcal{U}} \approx C$ ([10]).

To proceed further, we use $\bar{\mathcal{U}} \approx C$ in (6.17) and the equations (6.11), (6.16), (6.17) are non-dimensionalized as:

$$\mathcal{P} = -\varepsilon\left[(\mathcal{E}_1 + \mathcal{E}_2)(2\pi)^3\cos(2\pi\xi) - \mathcal{E}_3(2\pi)^2\sin(2\pi\xi)\right], \tag{6.19}$$

$$\mathcal{U}_{\mathcal{X}} = -k\frac{d^2}{\mu}\frac{\partial p}{\partial \mathcal{X}}\left[A_1\cosh(m_1\eta) + A_2\cosh(m_2\eta) + A_3\right], \tag{6.20}$$

$$\frac{\partial^2 C}{\partial \eta^2} - \frac{k_1 d^2}{\mathcal{D}}C = \frac{d^2}{\lambda\mathcal{D}}\mathcal{U}_{\mathcal{X}}\frac{\partial C}{\partial \xi}, \tag{6.21}$$

where

$m_1 = m_1' d = \sqrt{\frac{\gamma^2}{2}\left(1 + \sqrt{1 - \frac{4}{\gamma^2 k}}\right)}, \;\; m_2 = m_2' d = \sqrt{\frac{\gamma^2}{2}\left(1 - \sqrt{1 - \frac{4}{\gamma^2 k}}\right)},$

the amplitude ratio is $\varepsilon\left(=\frac{a}{d}\right)$, the rigidity is $\mathcal{E}_1\left(=-\frac{\mathcal{T}d^3}{\lambda^3\mu\mathbf{c}}\right)$, the stiffness is $\mathcal{E}_2=\left(\frac{m\mathbf{c}d^3}{\lambda^3\mu}\right)$, the viscous damping force in the wall is $\mathcal{E}_3=\left(\frac{\mathbf{c}d^3}{\mu\lambda^2}\right)$, the couple stress constraint is $\gamma\left(=d\sqrt{\frac{\mu}{\eta'}}\right)$, and the permeability constraint is $k\left(=\frac{\bar{k}}{d^2}\right)$.

The dispersion with first- order irreversible chemical response occur in the mass of the liquid and at the channel walls.

Referring Philip and Chandra [19], the wall conditions are specified as:

$$0=\mathcal{F}C+\frac{\partial C}{\partial \mathcal{Y}} \quad \text{at} \quad \mathcal{Y}=[a\sin\frac{2\pi}{\lambda}(\mathcal{X}-\bar{\mathcal{U}}t)+d]=h, \tag{6.22}$$

$$0=-\mathcal{F}C+\frac{\partial C}{\partial \mathcal{Y}} \quad \text{at} \quad \mathcal{Y}=-[a\sin\frac{2\pi}{\lambda}(\mathcal{X}-\bar{\mathcal{U}}t)+d]=-h. \tag{6.23}$$

From equations (6.18), (6.22) and (6.23), we get

$$0=\beta C+\frac{\partial C}{\partial \eta} \quad \text{at} \quad \eta=[\varepsilon\sin(2\pi\xi)+1]=\mathcal{H}, \tag{6.24}$$

$$0=-\beta C+\frac{\partial C}{\partial \eta} \quad \text{at} \quad \eta=-[\varepsilon\sin(2\pi\xi)+1]=-\mathcal{H}, \tag{6.25}$$

where the heterogeneous response rate parameter corresponding to the catalytic response at the walls is $\beta=\mathcal{F}d$.

From equations (6.24) and (6.25), we obtain the primitive of equation (6.21) as follows:

$$C(\eta)=-\frac{kd^4}{\lambda\mu\mathcal{D}}\frac{\partial C}{\partial \xi}\mathcal{P}\Big[A_4\cosh(m_1\eta)+A_5\cosh(m_2\eta)+A_6\cosh(\alpha\eta)+A_7\Big]. \tag{6.26}$$

The volumetric rate $\mathcal{Q}$ stated as in chapter 2 is considered as:

$$\mathcal{Q} = \int_{-\mathcal{H}}^{\mathcal{H}} C\,\mathcal{U}_{\mathcal{X}} d\eta. \tag{6.27}$$

Using equations (6.20) and (6.26) in equation (6.27), we obtain

$$\mathcal{Q} = -2\frac{d^6}{\lambda\mu^2\mathcal{D}}\frac{\partial C}{\partial \xi}G(\xi,\alpha,\beta,\varepsilon,\mathcal{E}_1,\mathcal{E}_2,\mathcal{E}_3,k,\gamma), \tag{6.28}$$

where

$$\begin{aligned}\mathcal{G}(\xi,\alpha,\beta,\varepsilon,\mathcal{E}_1,\mathcal{E}_2,\mathcal{E}_3,k,\gamma) = \\ -k^2\mathcal{P}^2\Big[\frac{A_1A_4}{2}B_1 + \frac{A_2A_5}{2}B_2 + (A_1A_5+A_2A_4)B_3 + A_1A_6B_4 + A_2A_6B_5 \\ + (A_1A_7+A_3A_4)B_6 + (A_2A_7+A_3A_5)B_7 + A_3A_6B_8 + A_3A_7\mathcal{H}\Big].\end{aligned} \tag{6.29}$$

Glancing at equation (6.28) with Fick's bylaw of dispersion, the scattering coefficient $\mathcal{D}^*$ was intended such that the solute disperses near to the plane moving with the typical speed of the flow and is specified as:

$$\mathcal{D}^* = 2\frac{d^6}{\mu^2\mathcal{D}}\mathcal{G}(\xi,\alpha,\beta,\varepsilon,\mathcal{E}_1,\mathcal{E}_2,\mathcal{E}_3,k,\gamma). \tag{6.30}$$

and

$$A_1 = \frac{(m_2)^2}{[(m_1)^2-(m_2)^2]\cosh(m_1\mathcal{H})},\ A_2 = \frac{-(m_1)^2}{[(m_1)^2-(m_2)^2]\cosh(m_2\mathcal{H})},$$
$$A_3 = \frac{-(m_2)^2\sinh(m_1\mathcal{H})}{m_1\mathcal{H}\,[(m_1)^2-(m_2)^2]\cosh(m_1\mathcal{H})} + \frac{(m_1)^2\sinh(m_2\mathcal{H})}{m_2\mathcal{H}\,[(m_1)^2-(m_2)^2]\cosh(m_2\mathcal{H})},$$
$$A_4 = \frac{(m_2)^2}{[(m_1)^2-(\alpha)^2]\,[(m_1)^2-(m_2)^2]\cosh(m_1\mathcal{H})},\ A_6 = A_3L_1 - A_4L_2 - A_5L_3,$$
$$A_5 = \frac{-(m_1)^2}{[(m_2)^2-(\alpha)^2]\,[(m_1)^2-(m_2)^2]\cosh(m_2\mathcal{H})}, \qquad A_7 = -\frac{A_3}{\alpha^2},$$
$$L_1 = \frac{\beta}{\alpha^2(\alpha\sinh(\alpha\mathcal{H})+\beta\cosh(\alpha\mathcal{H}))}, \qquad L_2 = \frac{(m_1\sinh m_1\mathcal{H}+\beta\cosh m_1\mathcal{H})}{(\alpha\sinh\alpha\mathcal{H}+\beta\cosh\alpha\mathcal{H})},$$
$$L_3 = \frac{(m_2\sinh m_2\mathcal{H}+\beta\cosh m_2\mathcal{H})}{(\alpha\sinh\alpha\mathcal{H}+\beta\cosh\alpha\mathcal{H})}, \qquad B_1 = \frac{2m_1\mathcal{H}+\sinh 2m_1\mathcal{H}}{2m_1},$$
$$B_2 = \frac{2m_2\mathcal{H}+\sinh 2m_2\mathcal{H}}{2m_2},\ B_6 = \frac{\sinh m_1\mathcal{H}}{m_1},\ B_7 = \frac{\sinh m_2\mathcal{H}}{m_2},\ B_8 = \frac{\sinh\alpha\mathcal{H}}{\alpha},$$
$$B_3 = \frac{m_1\sinh m_1\mathcal{H}\cosh m_2\mathcal{H} - m_2\cosh m_1\mathcal{H}\sinh m_2\mathcal{H}}{[(m_1)^2-(m_2)^2]},$$
$$B_4 = \frac{m_1\sinh m_1\mathcal{H}\cosh\alpha\mathcal{H} - \alpha\cosh m_1\mathcal{H}\sinh\alpha\mathcal{H}}{[(m_1)^2-(\alpha)^2]},$$
$$B_5 = \frac{m_2\sinh m_2\mathcal{H}\cosh\alpha\mathcal{H} - \alpha\cosh m_2\mathcal{H}\sinh\alpha\mathcal{H}}{[(m_2)^2-(\alpha)^2]}, \qquad \alpha = \sqrt{\frac{k_1}{\mathcal{D}}}d.$$

The mean of $\mathcal{G}$ is $\bar{\mathcal{G}}$ and is attained as:

$$\bar{\mathcal{G}} = \int_0^1 \mathcal{G}(\xi,\alpha,\beta,\varepsilon,\mathcal{E}_1,\mathcal{E}_2,\mathcal{E}_3,k,\gamma)d\xi. \tag{6.31}$$

6.5 Outcomes and Discussion

The equation (6.31) gives the diffusion coefficient $\mathcal{D}^*$ through the expression $\bar{\mathcal{G}}$, which has been found by numerical integration using the software MATHEMATICA and end results are presented through graphs.

The effects of the rigidness ($\mathcal{E}_1$), stiffness ($\mathcal{E}_2$) and viscous damping characteristic of the wall ($\mathcal{E}_3$) on the scattering coefficient ($\bar{\mathcal{G}}$) are depicted in Figs. 6.2 - 6.10. It is revealed that $\bar{\mathcal{G}}$ rises as growth in rigidity $(\mathcal{E}_1)$ for an instant of (a) no stiffness in the wall ($\mathcal{E}_2$=0) and perfectly elastic channel wall ($\mathcal{E}_3$=0) (Fig. 6.2); (b) no stiffness in the wall ($\mathcal{E}_2$=0) and dissipative wall ($\mathcal{E}_3 \neq 0$) (Fig. 6.3); (c) stiffness in the wall ($\mathcal{E}_2 \neq 0$) and fully elastic wall ($\mathcal{E}_3$=0) (Fig. 6.4). It is observed that $\bar{\mathcal{G}}$ increases with the toughness of the wall $(\mathcal{E}_2)$ for both the cases of (a) wall is perfectly elastic in nature ($\mathcal{E}_3$=0) (Fig. 6.5) and (b) wall is dissipative in nature ($\mathcal{E}_3 \neq 0$) (Figs. 6.6, 5.7). It is also seen that boost in viscous damping characteristics of the wall $(\mathcal{E}_3)$ amplifies $\bar{\mathcal{G}}$ if there is stiffness in the wall ($\mathcal{E}_2 \neq 0$) (Figs. 6.8, 6.9, 6.10). It is witnessed that $\bar{\mathcal{G}}$ rises monotonically with upswing in $\mathcal{E}_1, \mathcal{E}_2$ and $\mathcal{E}_3$. The increments in the flexibility of the channel walls help the stream moment, which causes to enhance the scattering.

Figures 6.11 - 6.13 shows that $\bar{\mathcal{G}}$ enhances with an amply in the permeability constraint k. The growing porosity in a channel, generates the fluid speed and cause to ascend the dispersion. Furthermore, $\bar{\mathcal{G}}$ ascends with an increment in the amplitude ratio (ε) (Figs. 6.4, 6.7, 6.10, 6.13, and 6.16). Also, it is understood that the increment in the amplitude ratio is the expansion in the amplitude of the wave across the channel and this cause to increase the fluid velocity within the channel and consequently dispersion may enhance. In Figs. 6.14 - 6.16 it is observed that $\bar{\mathcal{G}}$ descends with an ascend in couple stress constraint (γ).

Dispersion reduces with homogeneous compound response rate constraint (α) (Figs. 6.3, 6.6, 6.9, 6.12, and 6.15) and heterogeneous substance response rate constraint (β) (Figs. 6.2, 6.5, 6.8, 6.11, and 6.14). These results are consistent with the arguments of [93], [122].

6.6 Conclusion

This work analyzes the effect of compliant walls and chemical reactions on the creeping sinusoidal flow of a couple stress liquid through a permeable medium. It is observed from the previous section that, the concentration profile $(\bar{\mathcal{G}})$ amplifies with a rise in amplitude ratio, permeable constraint and wall constraints. Further, opposite behaviors of couple stress constraint, homogeneous response rate constraint and heterogeneous response rate constraint noticed on concentration profile $(\bar{\mathcal{G}})$.

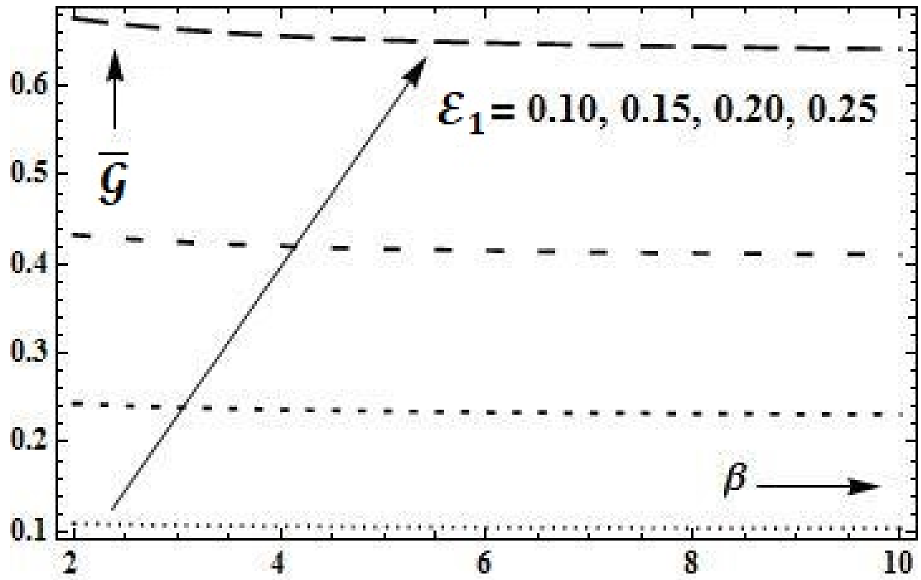

Figure 6.2: Illustration of $\bar{\mathcal{G}}$ for $\mathcal{E}_1$ with $\varepsilon = 0.2$, $\alpha = 1.0$, $k = 0.002$, $\gamma = 2.0$, $\mathcal{E}_2 = 0.0$, $\mathcal{E}_3 = 0.0$

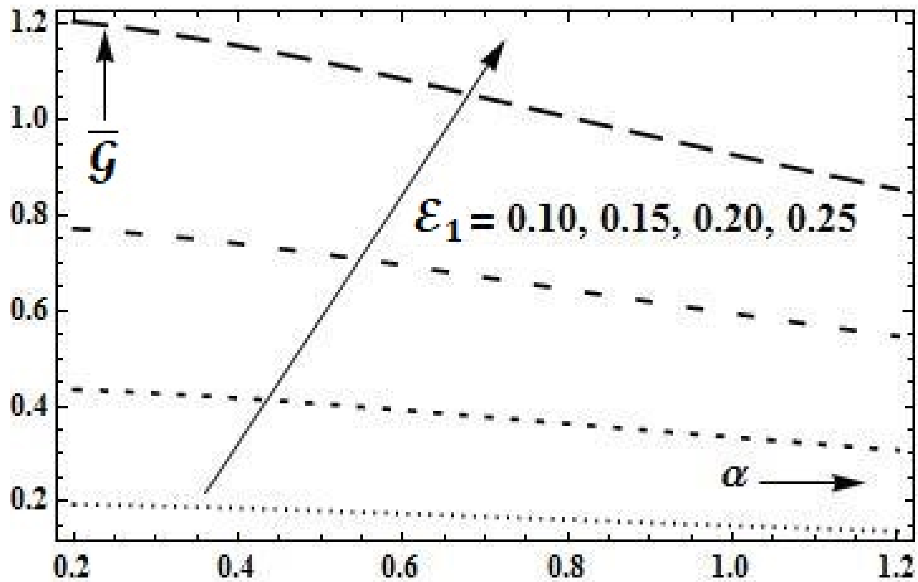

Figure 6.3: Illustration of $\bar{\mathcal{G}}$ for $\mathcal{E}_1$ with $\varepsilon = 0.2$, $\beta = 5.0$, $k = 0.002$, $\gamma = 2$, $\mathcal{E}_2 = 0.0$, $\mathcal{E}_3 = 0.06$

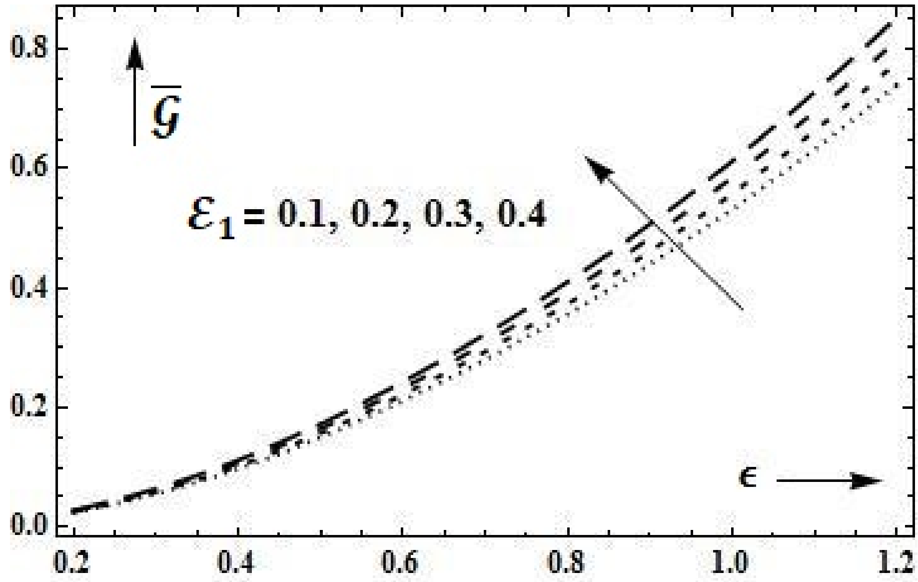

Figure 6.4: Illustration of $\bar{\mathcal{G}}$ for $\mathcal{E}_1$ with $\alpha = 1.0$, $\beta = 5.0$, $k = 0.002$, $\gamma = 2.0$, $\mathcal{E}_2 = 4.0$, $\mathcal{E}_3 = 0.00$

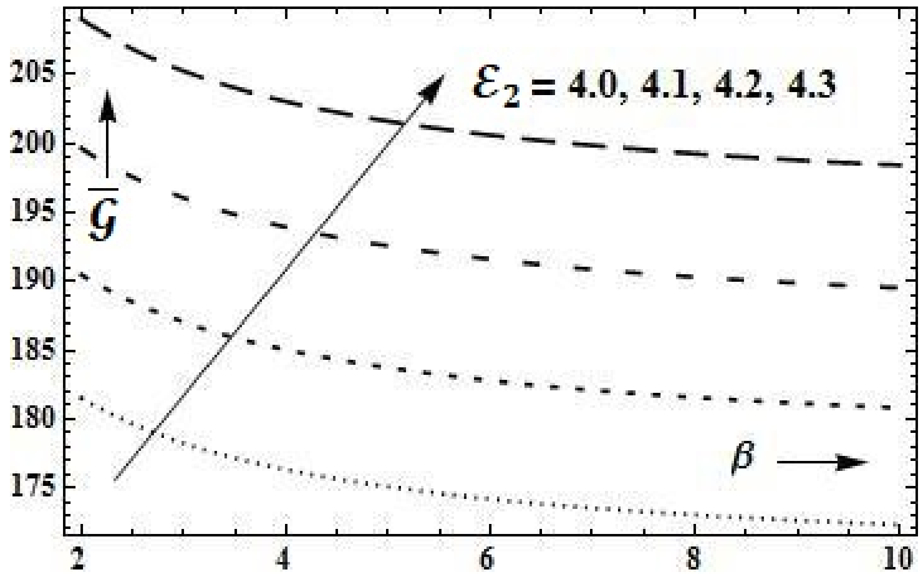

Figure 6.5: Illustration of $\bar{\mathcal{G}}$ for $\mathcal{E}_2$ with $\varepsilon = 0.2$, $\alpha = 1.0$, $k = 0.002$, $\gamma = 2.0$, $\mathcal{E}_1 = 0.1$, $\mathcal{E}_3 = 0.00$

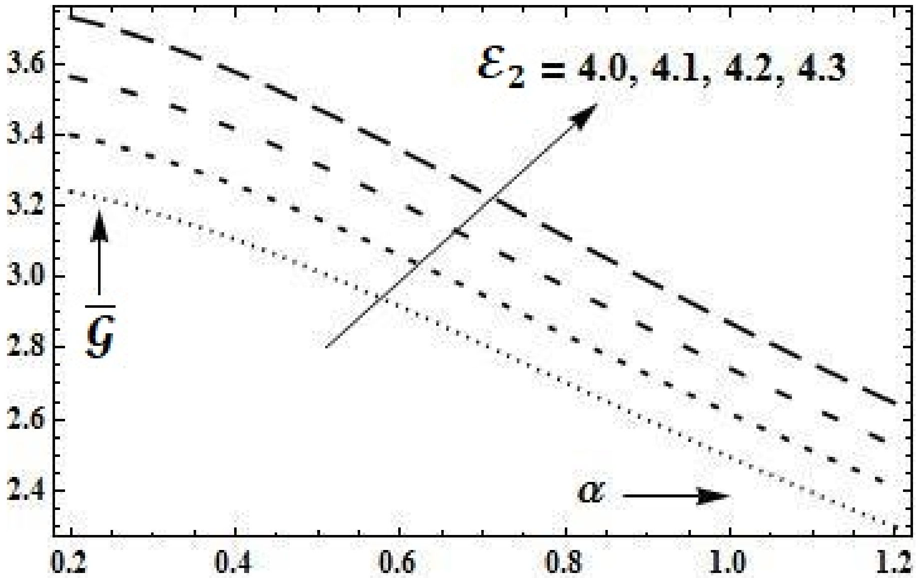

Figure 6.6: Illustration of $\bar{\mathcal{G}}$ for $\mathcal{E}_2$ with $\varepsilon = 0.2$, $\beta = 5.0$, $k = 0.002$, $\gamma = 2.0$, $\mathcal{E}_1 = 0.1$, $\mathcal{E}_3 = 0.06$

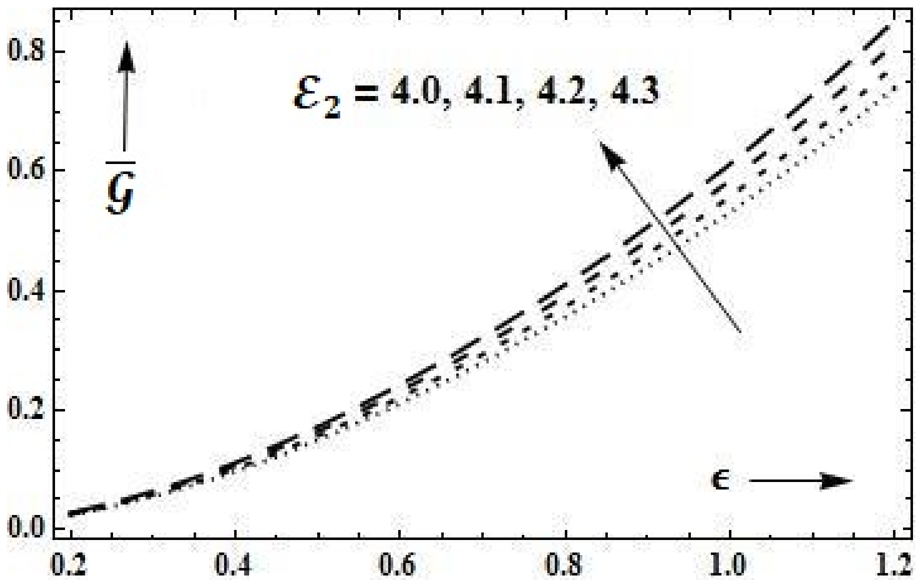

Figure 6.7: Illustration of $\bar{\mathcal{G}}$ for $\mathcal{E}_2$ with $\alpha = 1.0$, $\beta = 5.0$, $k = 0.002$, $\gamma = 2.0$, $\mathcal{E}_1 = 0.1$, $\mathcal{E}_3 = 0.06$

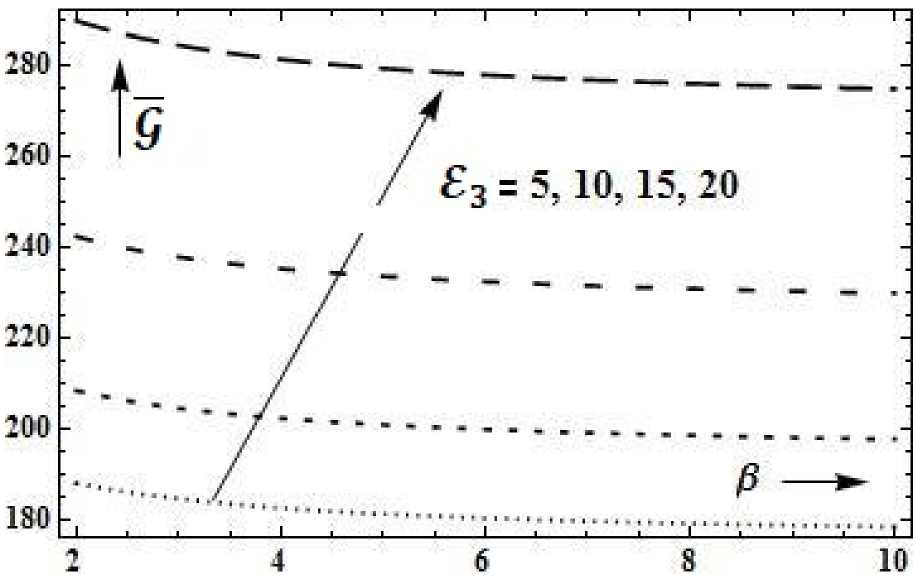

Figure 6.8: Illustration of $\bar{\mathcal{G}}$ for $\mathcal{E}_3$ with $\varepsilon = 0.2$, $\alpha = 1.0$, $k = 0.002$, $\gamma = 2.0$, $\mathcal{E}_1 = 0.1$, $\mathcal{E}_2 = 4.0$

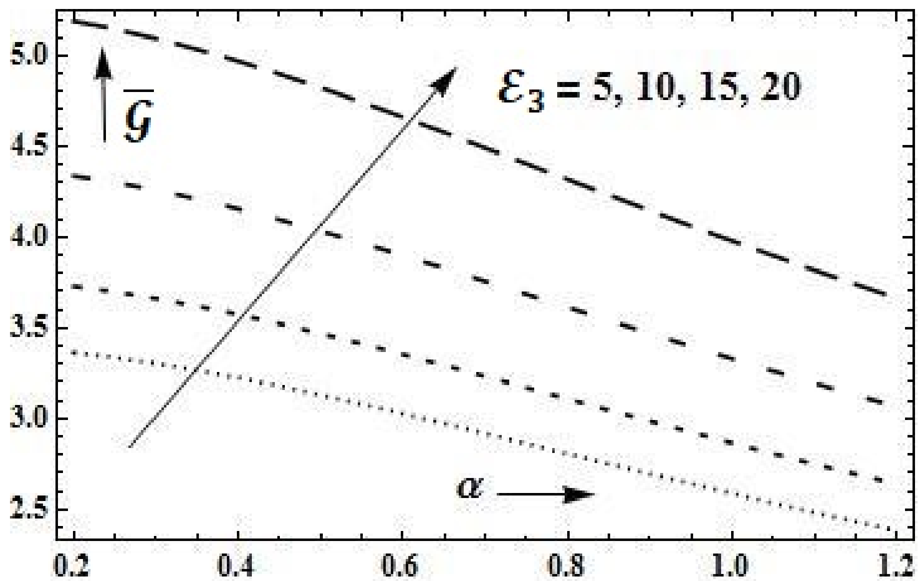

Figure 6.9: Illustration of $\bar{\mathcal{G}}$ for $\mathcal{E}_3$ with $\varepsilon = 0.2$, $\beta = 5.0$, $k = 0.002$, $\gamma = 2.0$, $\mathcal{E}_1 = 0.1$, $\mathcal{E}_2 = 4.0$

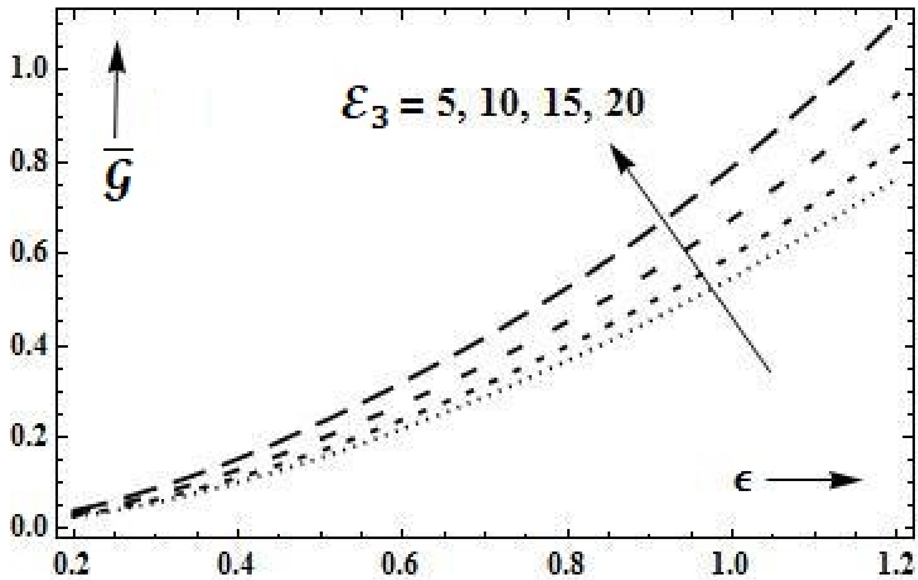

Figure 6.10: Illustration of $\bar{\mathcal{G}}$ for $\mathcal{E}_3$ with $\alpha = 1.0$, $\beta = 5.0$, $k = 0.002$, $\gamma = 2.0$, $\mathcal{E}_1 = 0.1$, $\mathcal{E}_2 = 4.0$

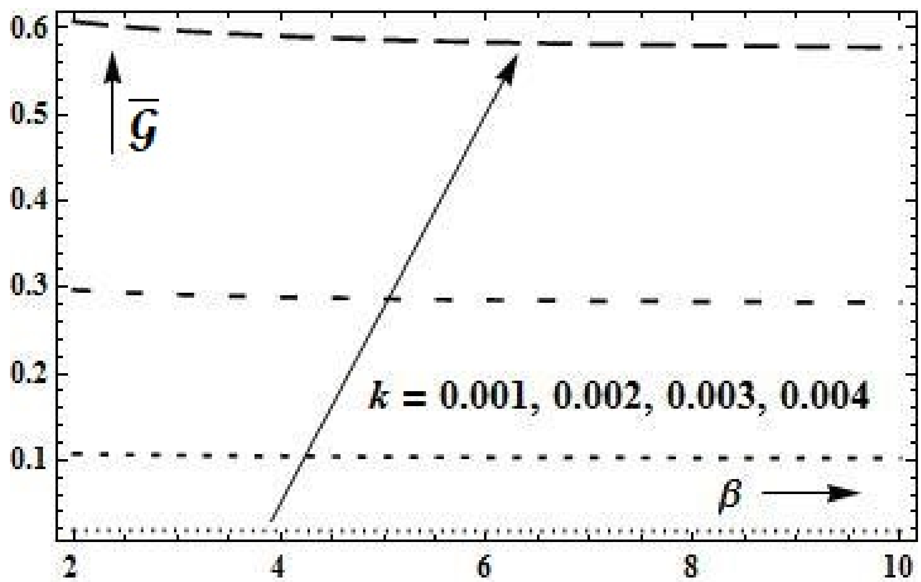

Figure 6.11: Illustration of $\bar{\mathcal{G}}$ for k with $\varepsilon = 0.2$, $\alpha = 1.0$, $\gamma = 2.0$, $\mathcal{E}_1 = 0.1$, $\mathcal{E}_2 = 0.0$, $\mathcal{E}_3 = 0.06$

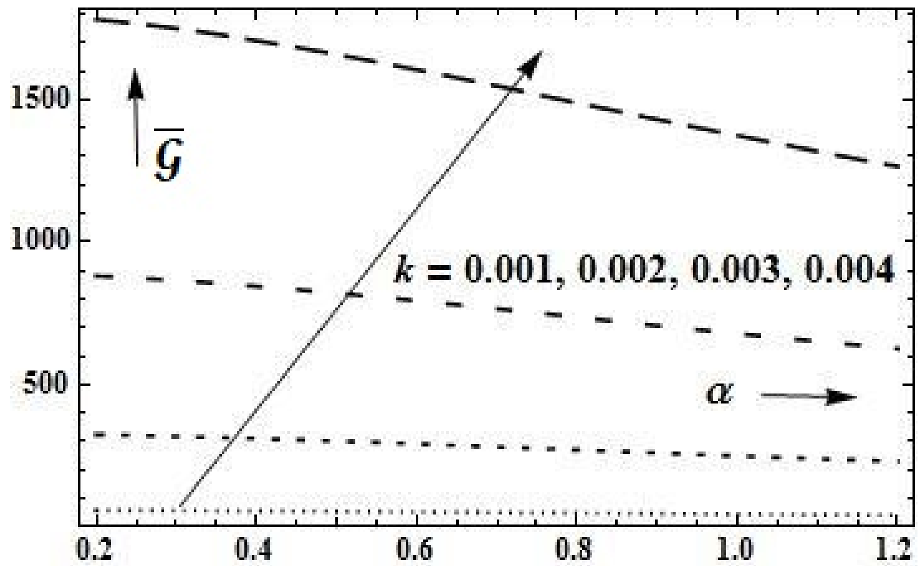

Figure 6.12: Illustration of $\bar{\mathcal{G}}$ for k with $\varepsilon = 0.2$, $\beta = 5.0$, $\gamma = 2.0$, $\mathcal{E}_1 = 0.1$, $\mathcal{E}_2 = 4.0$, $\mathcal{E}_3 = 0.06$

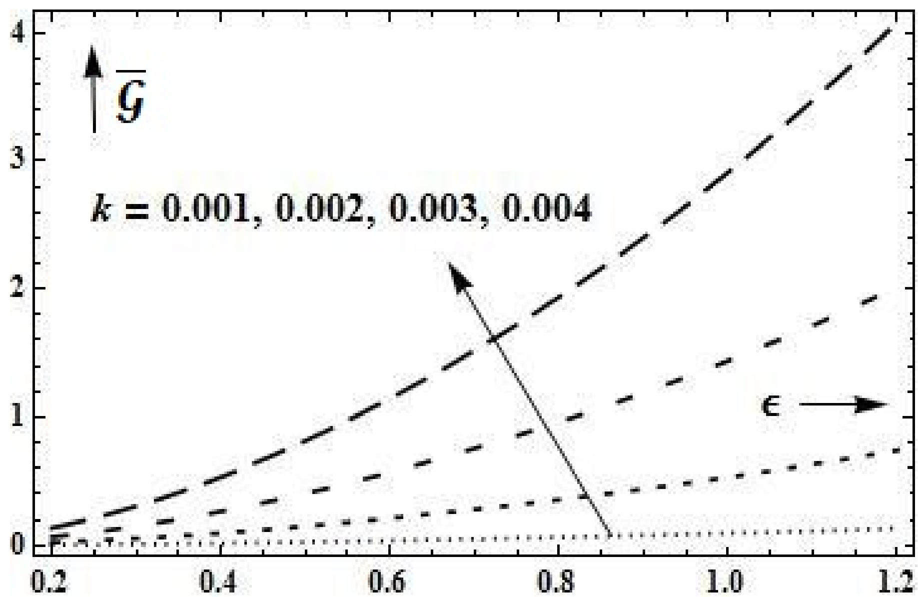

Figure 6.13: Illustration of $\bar{\mathcal{G}}$ for k with $\alpha = 1.0$, $\beta = 5.0$, $\gamma = 2.0$, $\mathcal{E}_1 = 0.1$, $\mathcal{E}_2 = 4.0$, $\mathcal{E}_3 = 0.00$

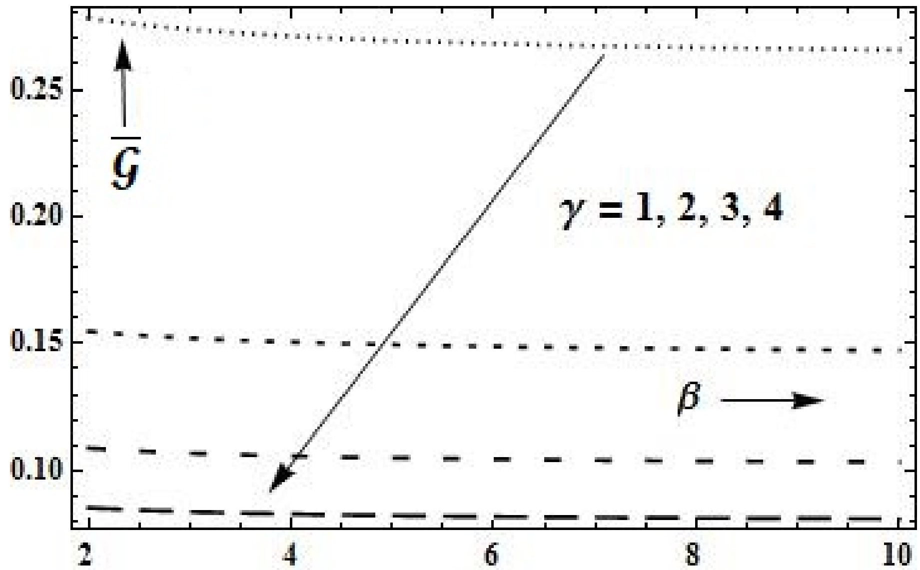

Figure 6.14: Illustration of $\bar{\mathcal{G}}$ for γ with $\varepsilon = 0.2$, $\alpha = 1.0$, $k = 0.002$, $\mathcal{E}_1 = 0.1$, $\mathcal{E}_2 = 0.0$, $\mathcal{E}_3 = 0.06$

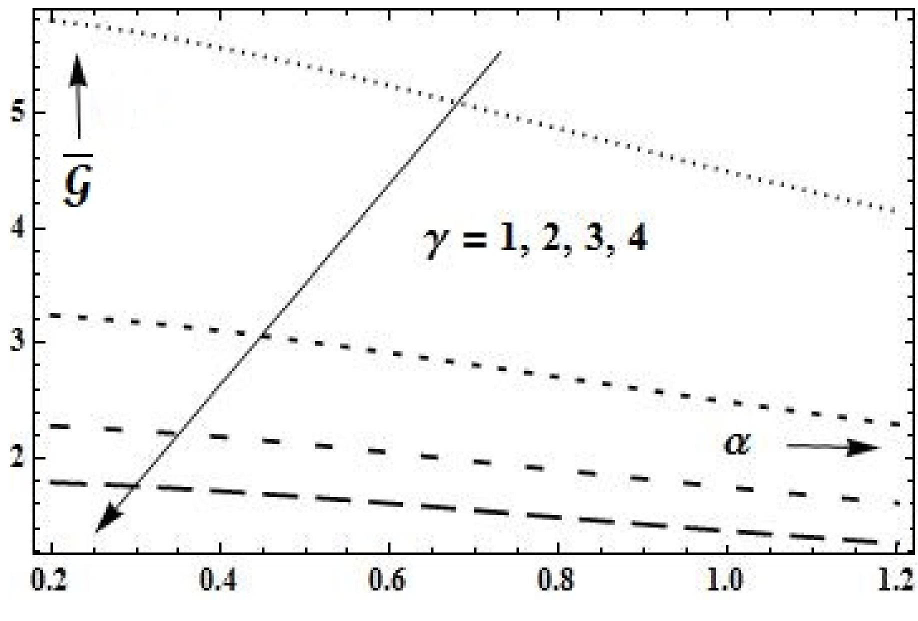

Figure 6.15: Illustration of $\bar{\mathcal{G}}$ for γ with $\varepsilon = 0.2$, $\beta = 5.0$, $k = 0.002$, $\mathcal{E}_1 = 0.1$, $\mathcal{E}_2 = 4.0$, $\mathcal{E}_3 = 0.06$

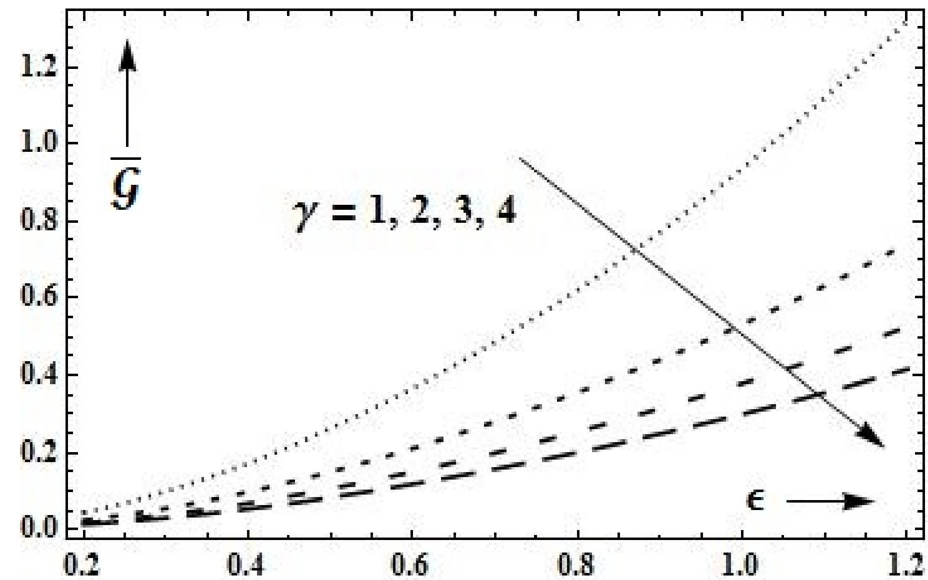

Figure 6.16: Illustration of $\bar{\mathcal{G}}$ for γ with $\alpha = 1.0$, $\beta = 5.0$, $\mathcal{E}_1 = 0.1$,$\mathcal{E}_2 = 4.0$, $\mathcal{E}_3 = 0.00$

Chapter 7

Interaction of Peristaltic Pumping on Dispersion in a MHD Couple Stress Fluid with Chemical Reactions and Wall Properties

7.1 Introduction

In chapter six, we presented dispersion of a matter in creeping sinusoidal flow of a couple stress fluid through a permeable medium with wall properties. In this chapter, we have explored the wall and chemical effects on the creeping sinusoidal stream and dispersion of a solute material in the MHD couple stress fluid. Magnetohydrodynamic (MHD) peristaltic flow nature of liquid is especially imperative in physiological and mechanical procedures. In the existence of magnetic field, many fluids possess an electrically conducting nature, which is an important aspect of the physical situation in the flow problems of magnetohydrodynamics. It is useful for tumor treatment, MRI (Magnetic Resonance Imaging) scanning, blood pumping, reduction of bleeding during surgeries, targeted transportation of drugs, and so on. Magneto-therapy is an essential application to the human body. This heals the diseases like ulceration, inflammations and diseases of the uterus. Some researchers (Hayat et al [42], Kim [56], Kothandapani and Srinivas [60], Tripathi and Beg [163]) have explored the magneto-hydrodynamic characteristics of non-Newtonian liquids through different circumstances.

The objective of this chapter is to study the effects of simultaneous heterogeneous and homogeneous chemical responses on scattering of a solute in MHD peristaltic pumping of a couple stress fluid with wall properties. The closed form solution has been obtained for the effective scattering coefficient by applying long wavelength hypothesis and condition of Taylor's limit. The effects of different values of penetrating constraints are discussed in detail through graphs.

7.2 Formulation of the Problem

Consider the magneto-hydrodynamic couple stress fluid with peristalsis in the 2- dimensional channel. Figure 7.1 depicts the wave shape.

Referring the Maxwell's equations, the presumptions regarding magnetic field as specified in chapter 1 (section 1.6), the equations of the couple stress fluid as mentioned in chapter

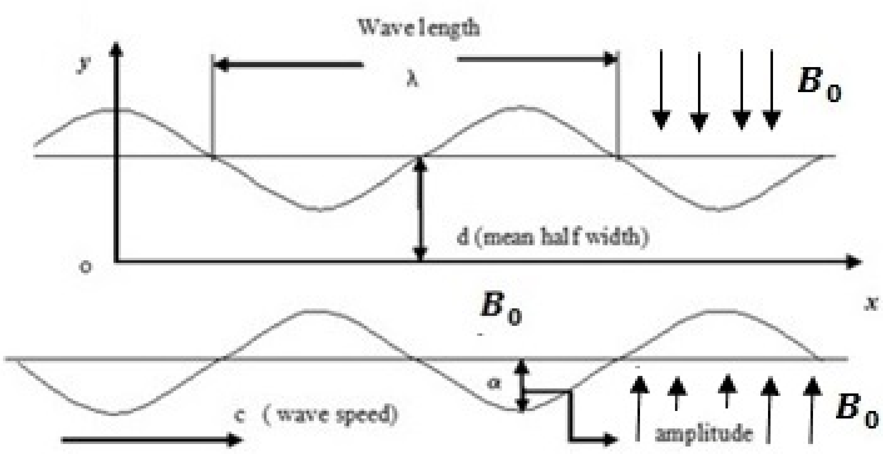

Figure 7.1: Geometry of the problem.

1 (section 1.8.2), and The relating flow conditions ([74]) of the current issue are:

$$\frac{\partial \mathcal{U}}{\partial \mathcal{X}}+\frac{\partial \mathcal{V}}{\partial \mathcal{Y}}=0, \tag{7.1}$$

$$-\frac{\partial p}{\partial \mathcal{X}}+\mu\nabla^2\mathcal{U}-\eta^{'}\nabla^4\mathcal{U}-\sigma B_0^2\mathcal{U}=\rho\left[\frac{\partial}{\partial t}+\mathcal{U}\frac{\partial}{\partial \mathcal{X}}+\mathcal{V}\frac{\partial}{\partial \mathcal{Y}}\right]\mathcal{U}, \tag{7.2}$$

$$-\frac{\partial p}{\partial \mathcal{Y}}+\mu\nabla^2\mathcal{V}-\eta^{'}\nabla^4\mathcal{V}=\rho\left[\frac{\partial}{\partial t}+\mathcal{U}\frac{\partial}{\partial \mathcal{X}}+\mathcal{V}\frac{\partial}{\partial \mathcal{Y}}\right]\mathcal{V}, \tag{7.3}$$

where $\frac{\partial^2}{\partial \mathcal{X}^2}+\frac{\partial^2}{\partial \mathcal{Y}^2}=\nabla^2$, $\nabla^2\nabla^2=\nabla^4$, the constant associated with couple stress fluid is η', the fluid density is ρ, the viscosity coefficient is μ, the velocity components in the $\mathcal{X}$, $\mathcal{Y}$ direction is $\mathcal{U}$, $\mathcal{V}$, the pressure is p and the magnetic field is B_0.

Referring Mittra and Prasad [86], the condition of the flexible wall movement is specified as:

$$\mathcal{L}(h)=p-p_0, \tag{7.4}$$

where, the movement of the stretched membrane by the damping force is $\mathcal{L}$ and is intended by the subsequent equation as:

$$\mathcal{L} = -\mathcal{T}\frac{\partial^2}{\partial \mathcal{X}^2} + m\frac{\partial^2}{\partial t^2} + \mathsf{C}\frac{\partial}{\partial t}. \tag{7.5}$$

Here, the coefficient of sticky damping force is C, the mass per/area is m, and the membrane tension is $\mathcal{T}$.

7.3 Method of Solution

Neglecting the body couples and body strengthens, under long - wavelength hypothesis ([10]), equation (7.1) to (7.3) yield as:

$$\frac{\partial \mathcal{U}}{\partial \mathcal{X}} + \frac{\partial \mathcal{V}}{\partial \mathcal{Y}} = 0, \tag{7.6}$$

$$-\frac{\partial p}{\partial \mathcal{X}} + \mu\frac{\partial^2 \mathcal{U}}{\partial \mathcal{Y}^2} - \eta'\frac{\partial^4 \mathcal{U}}{\partial \mathcal{Y}^4} - \sigma B_0^2 \mathcal{U} = 0, \tag{7.7}$$

$$-\frac{\partial p}{\partial \mathcal{Y}} = 0. \tag{7.8}$$

The allied border conditions are stated as:

$$\mathcal{U} = 0, \ \ \frac{\partial^2 \mathcal{U}}{\partial \mathcal{Y}^2} = 0, \ \text{at} \quad \mathcal{Y} = \pm h. \tag{7.9}$$

From equation (7.4), (7.5) and (7.7), active periphery conditions at the stretchy walls (Mittra and Prasas [86]) are specified as:

$$\frac{\partial}{\partial \mathcal{X}}\mathcal{L}(h) = \mu\frac{\partial^2 \mathcal{U}}{\partial \mathcal{Y}^2} - \eta'\frac{\partial^4 \mathcal{U}}{\partial \mathcal{Y}^4} - \sigma B_0^2 \mathcal{U} = 0, \quad \text{at} \quad \mathcal{Y} = \pm h, \tag{7.10}$$

where

$$\frac{\partial}{\partial \mathcal{X}}\mathcal{L}(h) = \frac{\partial p}{\partial \mathcal{X}} = \mathcal{P}' = -\mathcal{T}\frac{\partial^3 h}{\partial \mathcal{X}^3} + m\frac{\partial^3 h}{\partial \mathcal{X}\partial t^2} + \mathsf{C}\frac{\partial^2 h}{\partial \mathcal{X}\partial t}. \tag{7.11}$$

Solving the equations (7.7) and (7.8) with (7.9) and (7.10) we obtain

$$\mathcal{U}(\mathcal{Y}) = -\frac{1}{\sigma B_0^2}\left(\frac{\partial p}{\partial \mathcal{X}}\right)\left[A_1'\cosh(m_1'\mathcal{Y}) + A_2'\cosh(m_2'\mathcal{Y}) + 1\right], \tag{7.12}$$

where, $m_1' = \sqrt{\frac{\mu}{2\eta'}\left(1+\sqrt{1-\frac{4\eta'\sigma B_0^2}{\mu^2}}\right)}$, $m_2' = \sqrt{\frac{\mu}{2\eta'}\left(1-\sqrt{1-\frac{4\eta'\sigma B_0^2}{\mu^2}}\right)}$.

The mean speed is specified as:

$$\bar{\mathcal{U}} = \frac{1}{2h}\int_{-h}^{h}\mathcal{U}(\mathcal{Y})d\mathcal{Y}. \tag{7.13}$$

Equations (7.12) and (7.13) yield as:

$$\bar{\mathcal{U}} = -\frac{1}{\sigma B_0^2}\left(\frac{\partial p}{\partial \mathcal{X}}\right)\left[\frac{A_1'}{m_1'h}\sinh(m_1'h) + \frac{A_2'}{m_2'h}\sinh(m_2'h) + 1\right]. \tag{7.14}$$

Utilizing Ravikiran and Radhakrishnamacharya [122], the liquid speed is given by the condition:

$$\mathcal{U}_{\mathcal{X}} = \mathcal{U} - \bar{\mathcal{U}}. \tag{7.15}$$

Equations (7.12), (7.14) and (7.15) yield as:

$$\mathcal{U}_{\mathcal{X}} = -\frac{1}{\sigma B_0^2}\left(\frac{\partial p}{\partial \mathcal{X}}\right)\left[A_1'\cosh(m_1'\mathcal{Y}) + A_2'\cosh(m_2'\mathcal{Y}) - \frac{A_1'}{m_1'h}\sinh(m_1'h) - \frac{A_2'}{m_2'h}\sinh(m_2'h)\right], \tag{7.16}$$

where

$A_1' = \frac{(m_2')^2}{\left[(m_1')^2-(m_2')^2\right]\cosh(m_1'h)}$, $\qquad A_2' = \frac{-(m_1')^2}{\left[(m_1')^2-(m_2')^2\right]\cosh(m_2'h)}$,

$\mathcal{P}' = -\mathcal{T}\frac{\partial^3 h}{\partial \mathcal{X}^3} + m\frac{\partial^3 h}{\partial \mathcal{X}\partial t^2} + \mathsf{C}\frac{\partial^2 h}{\partial \mathcal{X}\partial t}$.

7.4 Simultaneous heterogeneous and homogeneous chemical reactions with diffusion

Alluding Taylor [156] and Gupta and Gupta [32], the diffusion equation for the concentration C of the material for the current issue is

$$\mathcal{D}\frac{\partial^2 C}{\partial \mathcal{Y}^2} - k_1 C = \mathcal{U}\frac{\partial C}{\partial \mathcal{X}} + \frac{\partial C}{\partial t}. \tag{7.17}$$

Here, the rate constant of first order chemical response is k_1, the molecular diffusion coefficient is $\mathcal{D}$ and liquid concentration is C.

The dimensionless quantities are specified as:

$$\eta = \frac{\mathcal{Y}}{d}, \xi = \frac{(\mathcal{X} - \bar{\mathcal{U}}t)}{\lambda}, \mathcal{H} = \frac{h}{d}, \mathcal{P} = \frac{d^2}{\mu c \lambda}\mathcal{P}', \theta = \frac{t}{\bar{t}}, \bar{t} = \frac{\lambda}{\bar{\mathcal{U}}}, \mathcal{M} = \sqrt{\frac{\sigma B_0^2 d^2}{\mu}}. \tag{7.18}$$

For the regular estimations of physiologically essential parameters of this issue, it is normal that $\bar{\mathcal{U}} \approx C$ (Ravikiran and Radhakrishnamacharya [123]).

To proceed further, we use $\bar{\mathcal{U}} \approx C$ in (7.17) and the conditions (7.11), (7.16), (7.17) are non-dimensionalized as:

$$\mathcal{P} = -\varepsilon\left[-\mathcal{E}_3(2\pi)^2\sin(2\pi\xi) + (\mathcal{E}_1 + \mathcal{E}_2)(2\pi)^3\cos(2\pi\xi)\right], \tag{7.19}$$

$$\mathcal{U}_{\mathcal{X}} = -\frac{1}{\sigma B_0^2}\frac{\partial p}{\partial \mathcal{X}}\left[A_1\cosh(m_1\eta) + A_2\cosh(m_2\eta) + A_3\right], \tag{7.20}$$

$$\frac{\partial^2 C}{\partial \eta^2} - \frac{k_1 d^2}{\mathcal{D}}C = \frac{d^2}{\lambda \mathcal{D}}\mathcal{U}_{\mathcal{X}}\frac{\partial C}{\partial \xi}, \tag{7.21}$$

where

$$m_1 = m_1' d = \sqrt{\frac{\gamma^2}{2}\left(1+\sqrt{1-\frac{4\mathcal{M}^2}{\gamma^2}}\right)}, \; m_2 = m_2' d = \sqrt{\frac{\gamma^2}{2}\left(1-\sqrt{1-\frac{4\mathcal{M}^2}{\gamma^2}}\right)},$$

the amplitude ratio is $\varepsilon \left(= \frac{a}{d}\right)$, the rigidity is $\mathcal{E}_1 \left(= -\frac{\mathcal{T}d^3}{\lambda^3 \mu \mathbf{c}}\right)$, the stiffness is $\mathcal{E}_2 = \left(\frac{m\mathbf{c}d^3}{\lambda^3 \mu}\right)$, the viscous damping force in the wall is $\mathcal{E}_3 = \left(\frac{\mathbf{c}d^3}{\mu \lambda^2}\right)$, the couple stress constraint is $\gamma \left(= d\sqrt{\frac{\mu}{\eta'}}\right)$ and the magnitic field constraint is $\mathcal{M}\left(= B_0 d\sqrt{\frac{\sigma}{\mu}}\right)$.

The dispersion with first- order irreversible chemical response occur in the mass of the liquid and at the channel walls.

Referring Chandra and Phlip [19], the wall conditions are specified as:

$$0 = \mathcal{F}C + \frac{\partial C}{\partial \mathcal{Y}} \quad \text{at} \quad \mathcal{Y} = [a \sin \frac{2\pi}{\lambda}(\mathcal{X} - \bar{\mathcal{U}}t) + d] = h, \tag{7.22}$$

$$0 = -\mathcal{F}C + \frac{\partial C}{\partial \mathcal{Y}} \quad \text{at} \quad \mathcal{Y} = -[a \sin \frac{2\pi}{\lambda}(\mathcal{X} - \bar{\mathcal{U}}t) + d] = -h. \tag{7.23}$$

Equation (7.18), (7.22) and (7.23) yields as:

$$0 = \beta C + \frac{\partial C}{\partial \eta} \quad \text{at} \quad \eta = [\varepsilon \sin(2\pi\xi) + 1] = \mathcal{H}, \tag{7.24}$$

$$0 = -\beta C + \frac{\partial C}{\partial \eta} \quad \text{at} \quad \eta = -[\varepsilon \sin(2\pi\xi) + 1] = -\mathcal{H}, \tag{7.25}$$

where the heterogeneous response rate constraint is $\beta = \mathcal{F}d$, relating to catalytic response at the dividers.

Utilizing (7.24) and (7.25), the primitive of (7.21) is obtained as:

$$C(\eta) = -\frac{d^2}{\lambda \mathcal{D}} \frac{1}{\sigma B_0^2} \frac{\partial C}{\partial \xi} \frac{\partial p}{\partial \mathcal{X}} \Big[A_4 \cosh(m_1 \eta) + A_5 \cosh(m_2 \eta) + A_6 \cosh(\alpha \eta) + A_7 \Big]. \quad (7.26)$$

The volumetric rate $\mathcal{Q}$ defined as in chapter 2 is reflected as:

$$\mathcal{Q} = \int_{-\mathcal{H}}^{\mathcal{H}} C \mathcal{U}_{\mathcal{X}} d\eta. \quad (7.27)$$

Using (7.20) and (7.26) in (7.27), we obtain

$$\mathcal{Q} = -2 \frac{d^6}{\lambda \mu^2 \mathcal{D}} \frac{\partial C}{\partial \xi} G(\xi, \varepsilon, \alpha, \beta, \mathcal{E}_1, \mathcal{E}_2, \mathcal{E}_3, \mathcal{M}, \gamma), \quad (7.28)$$

where

$G(\xi, \varepsilon, \alpha, \beta, \mathcal{E}_1, \mathcal{E}_2, \mathcal{E}_3, \mathcal{M}, \gamma) = -\frac{\mathcal{P}^2}{\mathcal{M}^4} \Big[\frac{A_1 A_4}{2} B_1 + \frac{A_2 A_5}{2} B_2 + (A_1 A_5 + A_2 A_4) B_3 + A_1 A_6 B_4$
$+ A_2 A_6 B_5 + (A_1 A_7 + A_3 A_4) B_6 + (A_2 A_7 + A_3 A_5) B_7 + A_3 A_6 B_8 + A_3 A_7 \mathcal{H} \Big],$

$A_1 = \frac{(m_2)^2}{\left[(m_1)^2 - (m_2)^2\right] \cosh(m_1 \mathcal{H})}, \ A_2 = \frac{-(m_1)^2}{\left[(m_1)^2 - (m_2)^2\right] \cosh(m_2 \mathcal{H})},$

$A_3 = \frac{-(m_2)^2 \sinh(m_1 \mathcal{H})}{m_1 \mathcal{H} \left[(m_1)^2 - (m_2)^2\right] \cosh(m_1 \mathcal{H})} + \frac{(m_1)^2 \sinh(m_2 \mathcal{H})}{m_2 \mathcal{H} \left[(m_1)^2 - (m_2)^2\right] \cosh(m_2 \mathcal{H})},$

$A_4 = \frac{(m_2)^2}{\left[(m_1)^2 - (\alpha)^2\right] \left[(m_1)^2 - (m_2)^2\right] \cosh(m_1 \mathcal{H})}, \ A_6 = A_3 L_1 - A_4 L_2 - A_5 L_3,$

$A_5 = \frac{-(m_1)^2}{\left[(m_2)^2 - (\alpha)^2\right] \left[(m_1)^2 - (m_2)^2\right] \cosh(m_2 \mathcal{H})}, \qquad A_7 = -\frac{A_3}{\alpha^2},$

$L_1 = \frac{\beta}{\alpha^2 (\alpha \sinh(\alpha \mathcal{H}) + \beta \cosh(\alpha \mathcal{H}))}, \qquad L_2 = \frac{(m_1 \sinh(m_1 \mathcal{H}) + \beta \cosh(m_1 \mathcal{H}))}{(\alpha \sinh(\alpha \mathcal{H}) + \beta \cosh(\alpha \mathcal{H}))},$

$L_3 = \frac{(m_2 \sinh(m_2 \mathcal{H}) + \beta \cosh(m_2 \mathcal{H}))}{(\alpha \sinh(\alpha \mathcal{H}) + \beta \cosh(\alpha \mathcal{H}))}, \qquad B_1 = \frac{2 m_1 \mathcal{H} + \sinh(2 m_1 \mathcal{H})}{2 m_1},$

$B_2 = \frac{2 m_2 \mathcal{H} + \sinh(2 m_2 \mathcal{H})}{2 m_2}, \ B_6 = \frac{\sinh(m_1 \mathcal{H})}{m_1}, \ B_7 = \frac{\sinh(m_2 \mathcal{H})}{m_2}, \ B_8 = \frac{\sinh(\alpha \mathcal{H})}{\alpha},$

$B_3 = \frac{m_1 \sinh(m_1 \mathcal{H}) \cosh(m_2 \mathcal{H}) - m_2 \cosh(m_1 \mathcal{H}) \sinh(m_2 \mathcal{H})}{\left[(m_1)^2 - (m_2)^2\right]},$

$B_4 = \frac{m_1 \sinh(m_1 \mathcal{H}) \cosh(\alpha \mathcal{H}) - \alpha \cosh(m_1 \mathcal{H}) \sinh(\alpha \mathcal{H})}{\left[(m_1)^2 - (\alpha)^2\right]},$

$B_5 = \frac{m_2 \sinh(m_2 \mathcal{H}) \cosh(\alpha \mathcal{H}) - \alpha \cosh(m_2 \mathcal{H}) \sinh(\alpha \mathcal{H})}{\left[(m_2)^2 - (\alpha)^2\right]}, \quad \alpha = \sqrt{\frac{k_1}{\mathcal{D}}} d.$

Looking at (6.28) with Fick's law of scattering, the dispersing coefficient $\mathcal{D}^*$ was computed to such an extent that the solute disperses near to the plane moving with the typical speed of the flow and is specified as:

$$\mathcal{D}^* = 2\frac{d^6}{\mu^2\mathcal{D}}G(\xi,\varepsilon,\alpha,\beta,E_1,\mathcal{E}_2,\mathcal{E}_3,\mathcal{M},\gamma). \tag{7.29}$$

The mean of $\mathcal{G}$ is $\bar{\mathcal{G}}$ and is attained as

$$\bar{\mathcal{G}} = \int_0^1 \mathcal{G}(\xi,\varepsilon,\alpha,\beta,\mathcal{E}_1,\mathcal{E}_2,\mathcal{E}_3,\mathcal{M},\gamma)d\xi. \tag{7.30}$$

7.5 Outcomes and Discussion

The expression $\bar{\mathcal{G}}(\xi,\varepsilon,\alpha,\beta,\mathcal{E}_1,\mathcal{E}_2,\mathcal{E}_3,\mathcal{M},\gamma)$ as shown in equation (7.30) and is used to observe the domino effects of various constraints on the effective scattering coefficient.

The effects of the couple stress constraint (γ) and magnetic field constraint $(\mathcal{M})$ on the scattering coefficient $(\bar{\mathcal{G}})$ are depicted in Figs. 7.2 - 7.7. It is observed that $\bar{\mathcal{G}}$ descends with an increase in couple stress constraint (γ) (Figs. 7.2 - 7.4). This finding agrees with the conclusion of Alemayehu-Radhakrishnamacharya [10]. Figures 7.5 -7.7 depicts that $\bar{\mathcal{G}}$ descends with an increase in magnetic field constraint $(\mathcal{M})$. This finding agrees with the conclusion of Ravikiran and Radhakrishnamacharya [123].

The impacts of the rigidity constraint $(\mathcal{E}_1)$ of the wall on the dissipating coefficient $(\bar{\mathcal{G}})$ are illustrated in Figs. 7.8 - 7.10. It is experiential that $\bar{\mathcal{G}}$ ascends monotonically with an expansion in $\mathcal{E}_1$ in the following cases of (a) no stiffness in the wall ($\mathcal{E}_2$=0) and perfectly elastic channel wall ($\mathcal{E}_3$=0) (Fig. 7.8); (b) no stiffness in the wall ($\mathcal{E}_2$=0) and dissipative wall ($\mathcal{E}_3 \neq 0$) (Fig.7.9) and (c) stiffness in the wall ($\mathcal{E}_2 \neq 0$) and perfectly elastic wall ($\mathcal{E}_3$=0) (Fig.7.10). It is noticed from the figures 7.11 - 7.13 that the mean effective dispersion coefficient increases with stiffness in the wall for the cases of (a) perfectly elastic wall ($\mathcal{E}_3$=0) (Fig. 7.11) and (b) dissipative wall ($\mathcal{E}_3 \neq 0$) (Figs. 7.12, 7.13). Figures 7.14 - 7.16 shows that dispersion coefficient increases as the viscous damping force increases in the

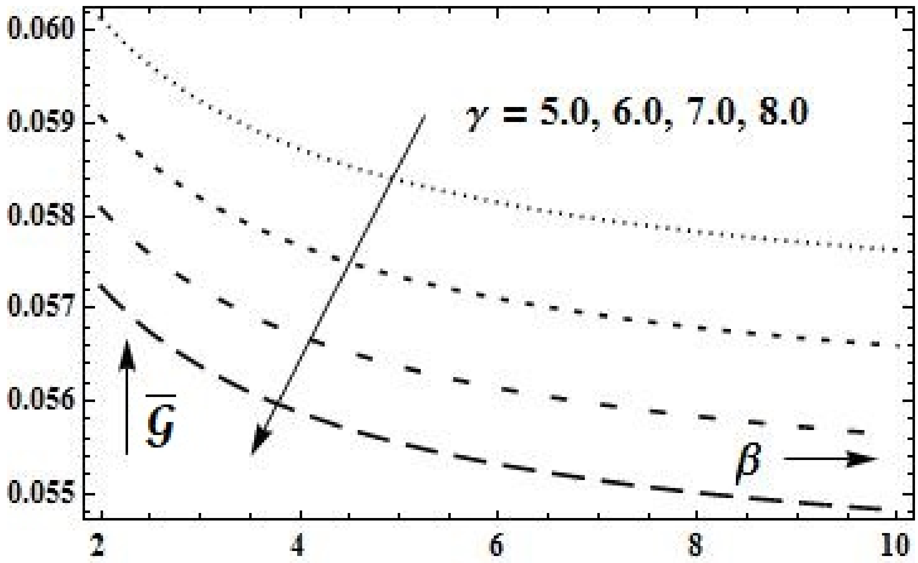

Figure 7.2: Illustration of $\bar{\mathcal{G}}$ for γ when $\varepsilon = 0.2$, $\alpha = 1.0$, $\mathcal{M} = 5.5$, $\mathcal{E}_1 = 0.1$, $\mathcal{E}_2 = 0.0$, $\mathcal{E}_3 = 0.06$

case of stiffness in the wall ($\mathcal{E}_2 \neq 0$) (Figs. 7.14, 7.15, 7.16). Furthermore, $\bar{\mathcal{G}}$ ascends with an increment in the amplitude ratio (ε) (Figs. 7.4, 7.7, 7.10, 7.13 and 7.16). This outcome concurs with that of [142] and [121].

It is seen that $\bar{\mathcal{G}}$ descends with an increase in the homogeneous compound response rate constraint (α) (Figs. 7.3, 7.6, 7.9, 7.12, and 7.15). Also, it is noticed from the figures 7.2, 7.5, 7.8, 7.11, and 7.14 that the scattering diminishes with heterogeneous substance response rate constraint (β), and the decrease in the effective scattering coefficient is sharp in a section near to the wall. This agrees with the chemical point of view because the reactions which affect diffusion happen only at the surface for heterogeneous substance response. This implies that the heterogeneous substance response tends to decrease the scattering of the solute.

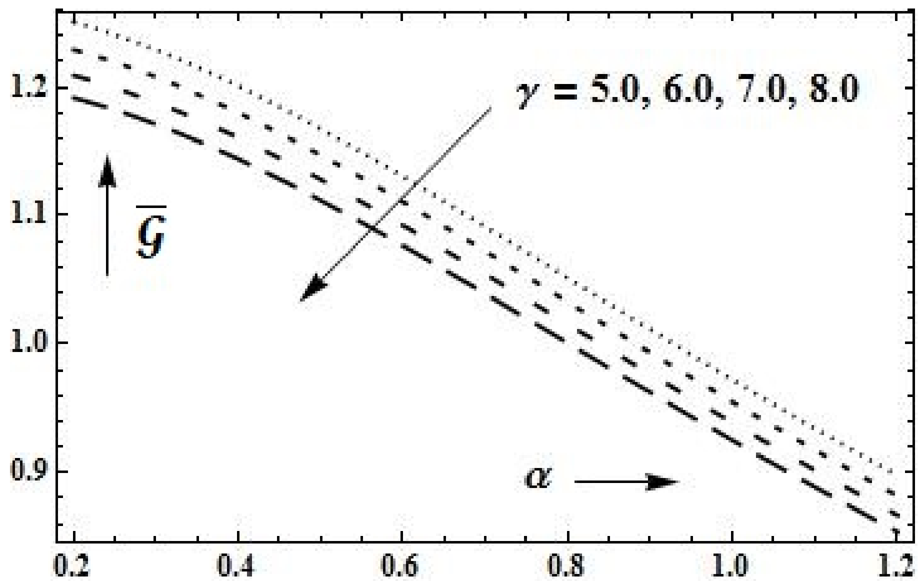

Figure 7.3: Illustration of $\bar{\mathcal{G}}$ for γ when $\varepsilon = 0.2$, $\beta = 5.0$, $\mathcal{M} = 5.5$, $\mathcal{E}_1 = 0.1$, $\mathcal{E}_2 = 4.0$, $\mathcal{E}_3 = 0.06$

7.6 Conclusion

The effects of magnetic constraint ($\mathcal{M}$), couple stress constraint (γ), amplitude ratio (ε), homogeneous response rate (α), heterogeneous response rate (β), rigidity ($\mathcal{E}_1$), stiffness ($\mathcal{E}_2$), damping characteristic ($\mathcal{E}_3$) of the wall on scattering coefficient ($\bar{\mathcal{G}}$) have been inspected for peristaltic pumping of a couple stress fluid. It is seen that the concentration profile ($\bar{\mathcal{G}}$) rises with an amplify in amplitude ratio and wall constraints, but descends with a rise in the heterogeneous response rate, homogeneous response rate, couples stress and magnetic field constraints. Finally, rigidity ($\mathcal{E}_1$), stiffness ($\mathcal{E}_2$), damping force ($\mathcal{E}_3$) of the wall and amplitude ratio (ε) favor the scattering, while couple stress constraint (γ) homogeneous response rate constraint (α) and heterogeneous response rate constraint (β) resist the scattering.

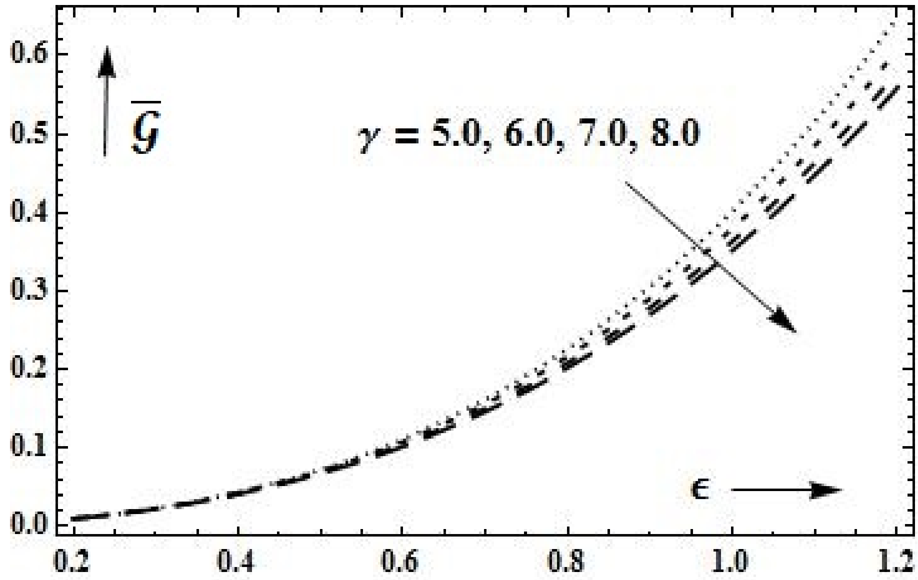

Figure 7.4: Illustration of $\bar{\mathcal{G}}$ for γ when $\alpha = 1.0$, $\beta = 5.0$, $\mathcal{M} = 5.5$, $\mathcal{E}_1 = 0.1$, $\mathcal{E}_2 = 4.0$, $\mathcal{E}_3 = 0.00$

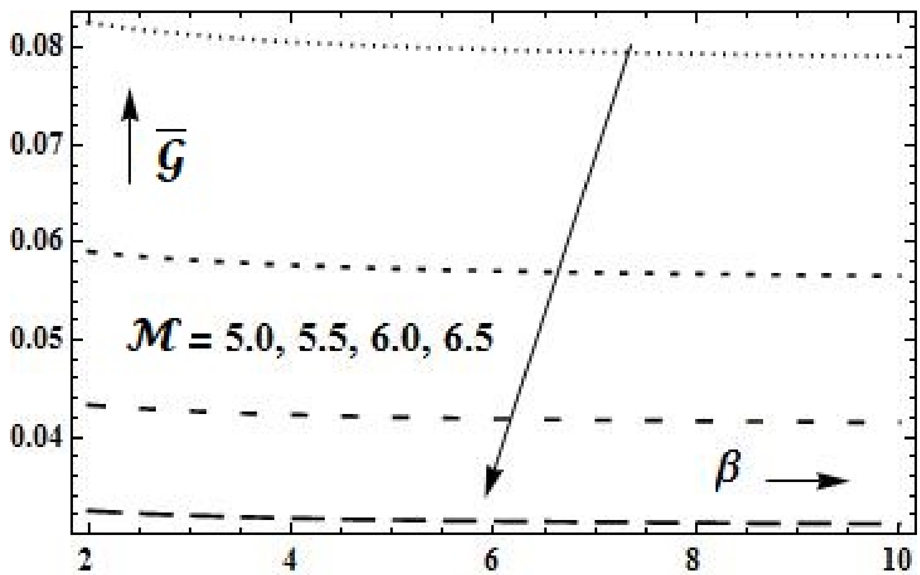

Figure 7.5: Illustration of $\bar{\mathcal{G}}$ for $\mathcal{M}$ when $\varepsilon = 0.2$, $\alpha = 1.0$, $\gamma = 6.0$, $\mathcal{E}_1 = 0.1$, $\mathcal{E}_2 = 0.0$, $\mathcal{E}_3 = 0.06$

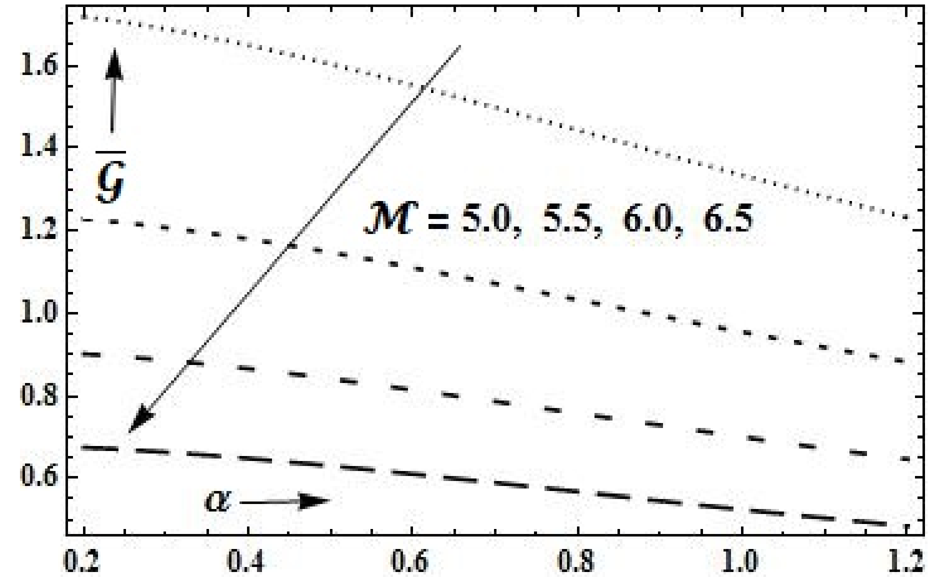

Figure 7.6: Illustration of $\bar{\mathcal{G}}$ for $\mathcal{M}$ when $\varepsilon = 0.2$, $\beta = 5.0$, $\gamma = 6.0$, $\mathcal{E}_1 = 0.1$, $\mathcal{E}_2 = 4.0$, $\mathcal{E}_3 = 0.06$

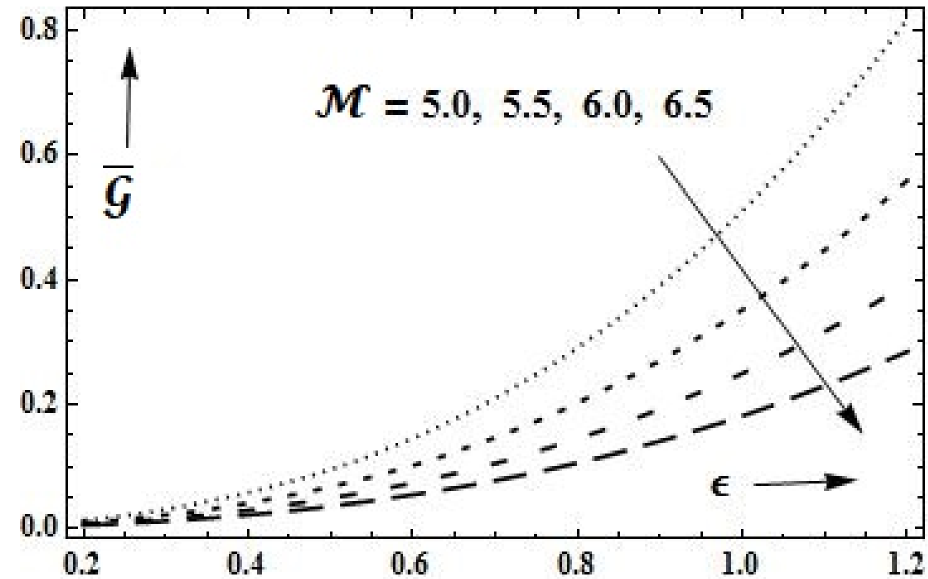

Figure 7.7: Illustration of $\bar{\mathcal{G}}$ for $\mathcal{M}$ when $\alpha = 1.0$, $\beta = 5.0$, $\gamma = 6.0$, $\mathcal{E}_1 = 0.1$, $\mathcal{E}_2 = 4.0$, $\mathcal{E}_3 = 0.00$

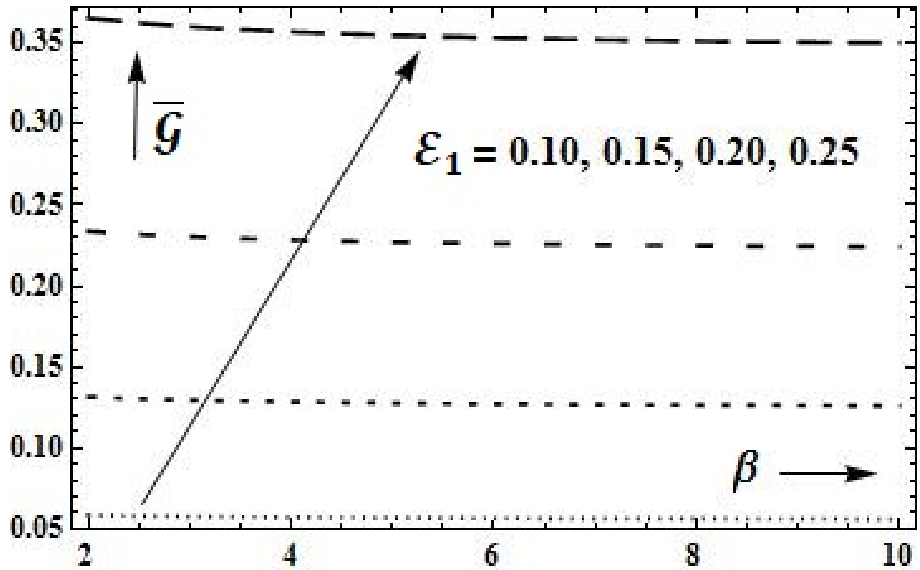

Figure 7.8: Illustration of $\bar{\mathcal{G}}$ for $\mathcal{E}_1$ when $\varepsilon = 0.2$, $\alpha = 1.0$, $\mathcal{M} = 5.5$, $\gamma = 6.0$, $\mathcal{E}_2 = 0.0$, $\mathcal{E}_3 = 0.0$

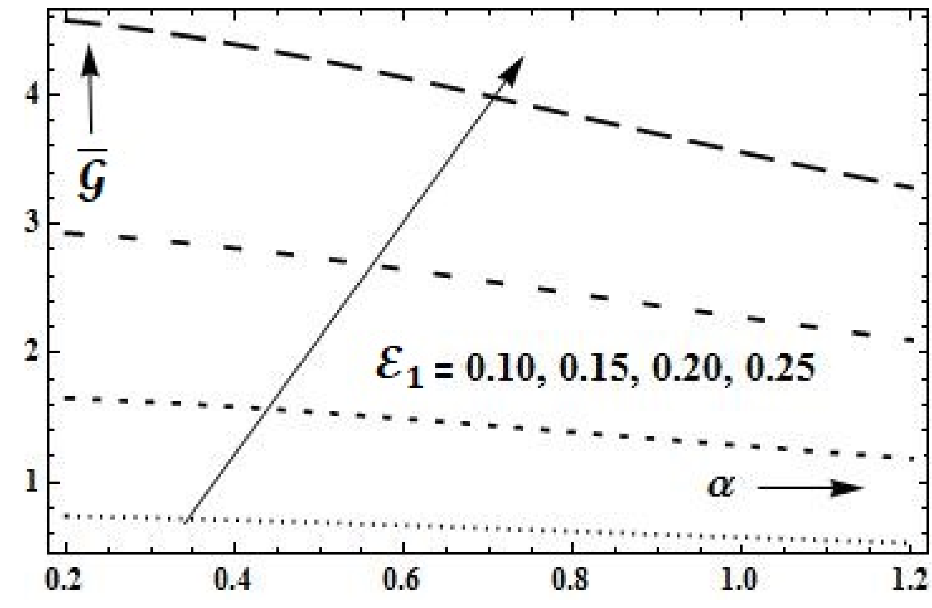

Figure 7.9: Illustration of $\bar{\mathcal{G}}$ for $\mathcal{E}_1$ with $\varepsilon = 0.2$, $\beta = 5.0$, $\mathcal{M} = 5.5$, $\gamma = 6.0$, $\mathcal{E}_2 = 0.0$, $\mathcal{E}_3 = 0.06$

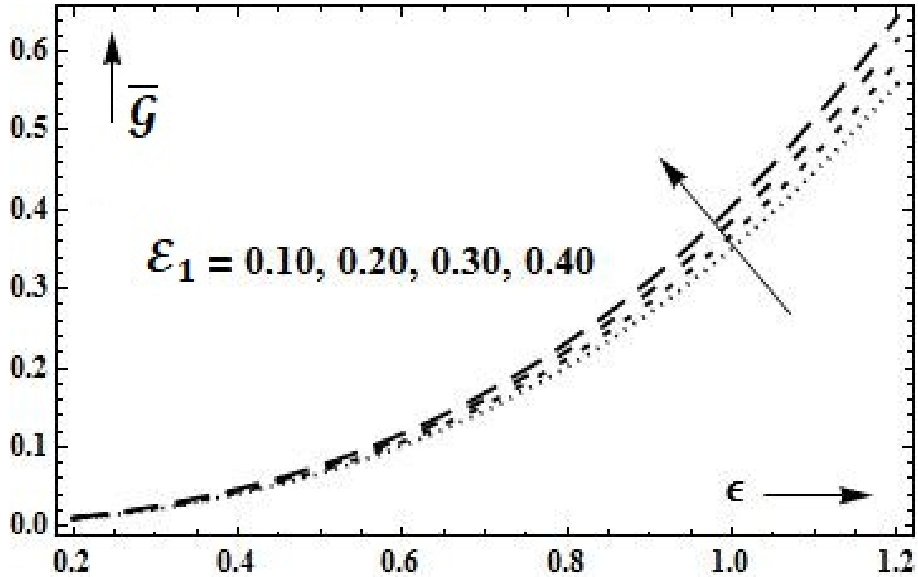

Figure 7.10: Illustration of $\bar{\mathcal{G}}$ for $\mathcal{E}_1$ when $\alpha = 1.0$, $\beta = 5.0$, $\mathcal{M} = 5.5$, $\gamma = 6.0$, $\mathcal{E}_2 = 4.0$, $\mathcal{E}_3 = 0.00$

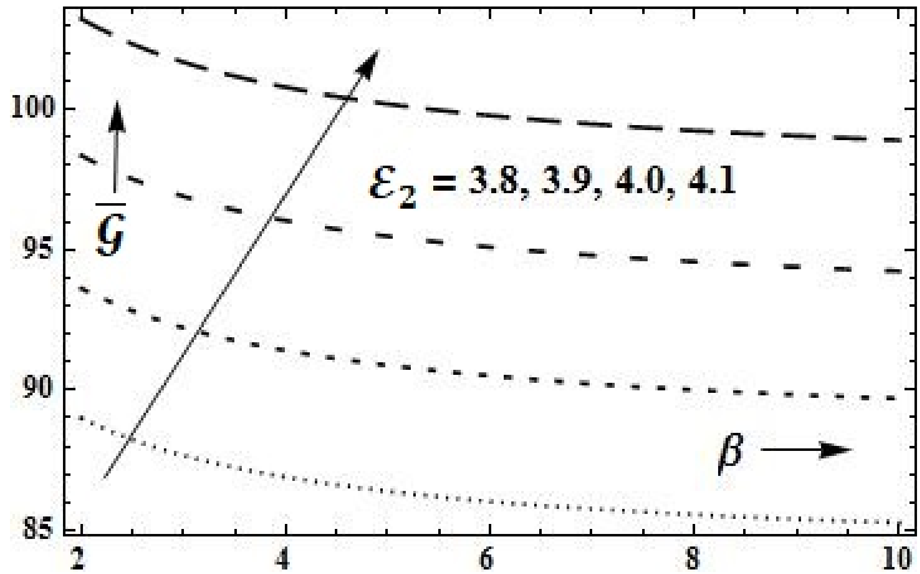

Figure 7.11: Illustration of $\bar{\mathcal{G}}$ for $\mathcal{E}_2$ when $\varepsilon = 0.2$, $\alpha = 1.0$, $M = 5.5$, $\gamma = 6.0$, $\mathcal{E}_1 = 0.1$, $\mathcal{E}_3 = 0.00$

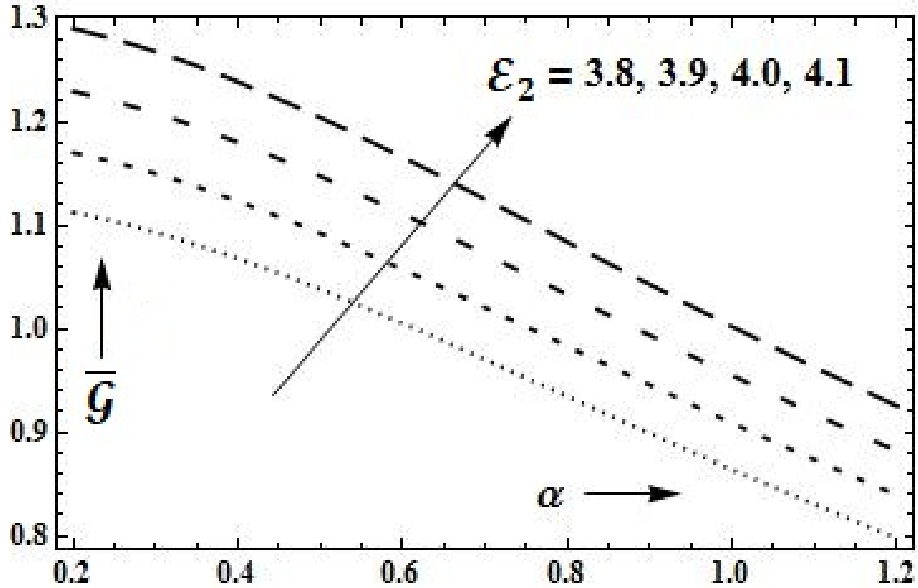

Figure 7.12: Illustration of $\bar{\mathcal{G}}$ for $\mathcal{E}_2$ when $\varepsilon = 0.2$, $\beta = 5.0$, $\mathcal{M} = 5.5$, $\gamma = 6.0$, $\mathcal{E}_1 = 0.1$, $\mathcal{E}_3 = 0.06$

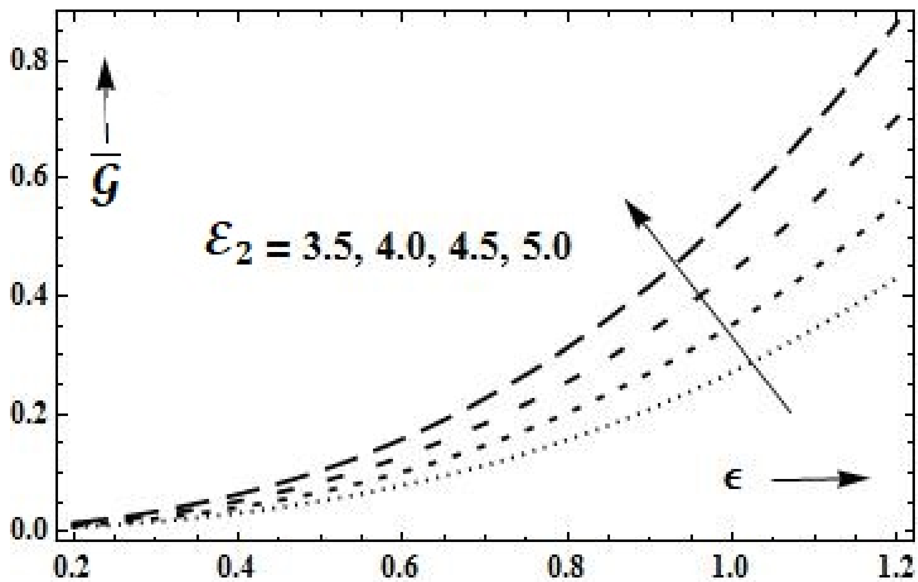

Figure 7.13: Illustration of $\bar{\mathcal{G}}$ for $\mathcal{E}_2$ when $\alpha = 1.0$, $\beta = 5.0$, $\mathcal{M} = 5.5$, $\gamma = 6.0$, $\mathcal{E}_1 = 0.1$, $\mathcal{E}_3 = 0.06$

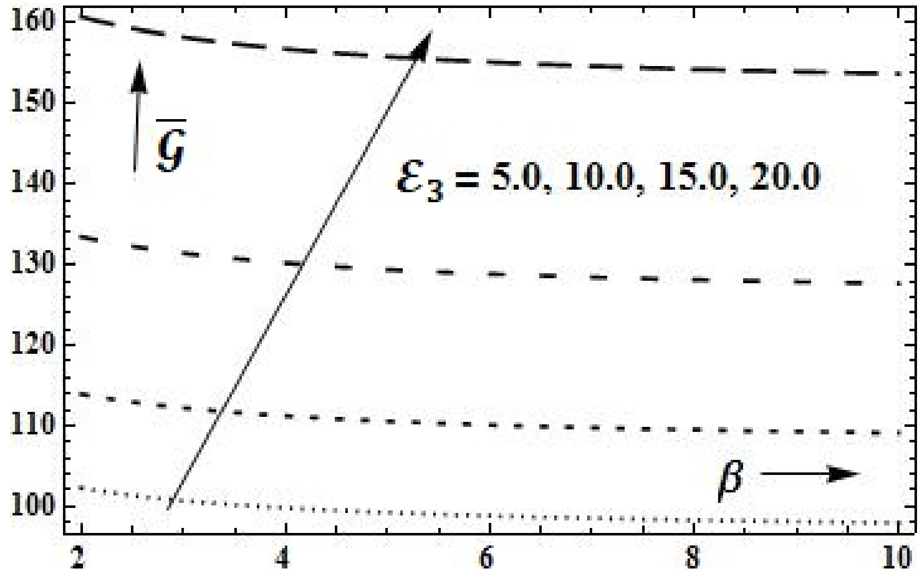

Figure 7.14: Illustration of $\bar{\mathcal{G}}$ for $\mathcal{E}_3$ when $\varepsilon = 0.2$, $\alpha = 1.0$, $\mathcal{M} = 5.5$, $\gamma = 6.0$, $\mathcal{E}_1 = 0.1$, $\mathcal{E}_2 = 4.0$

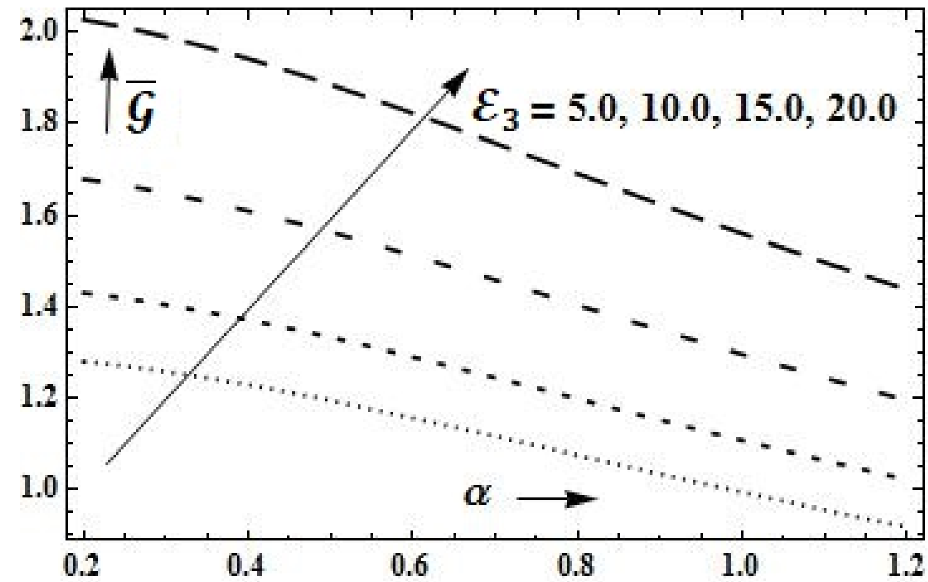

Figure 7.15: Illustration of $\bar{\mathcal{G}}$ for $\mathcal{E}_3$ when $\varepsilon = 0.2$, $\beta = 5.0$, $\mathcal{M} = 5.5$, $\gamma = 6.0$, $\mathcal{E}_1 = 0.1$, $\mathcal{E}_2 = 4.0$

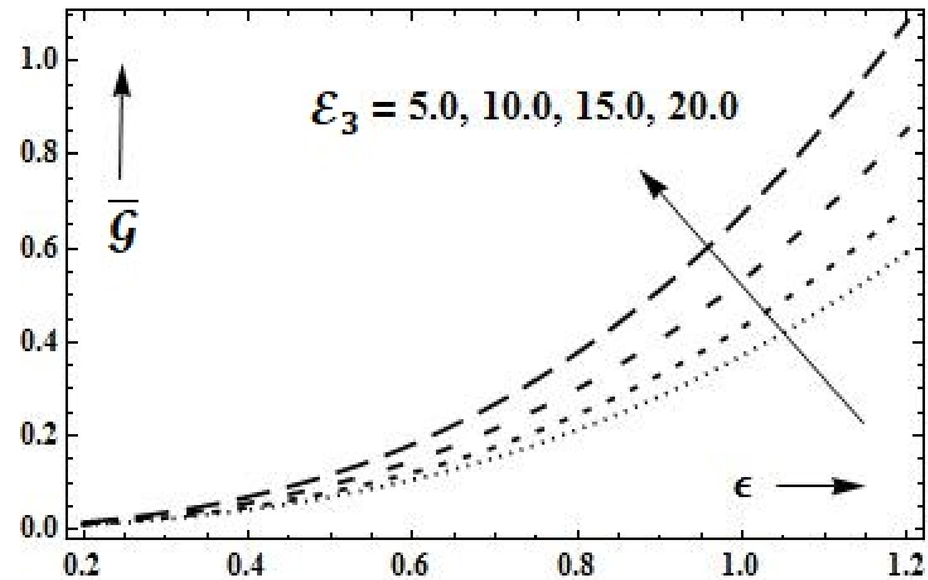

Figure 7.16: Illustration of $\bar{\mathcal{G}}$ for $\mathcal{E}_3$ when $\alpha = 1.0$, $\beta = 5.0$, $\mathcal{M} = 5.5$, $\gamma = 6.0$, $\mathcal{E}_1 = 0.1$, $\mathcal{E}_2 = 4.0$

Chapter 8

Conclusions and Scope for Future Work

8.1 Conclusions

Peristalsis and dispersion are very important aspects in physiological systems. Hence, in this thesis we studied the effects of combined homogeneous and heterogeneous chemical reactions on dispersion of a solute in the peristaltic transport of Newtonian and non-Newtonian fluids with wall properties by considering different characteristics such as magnetic field, porous medium in the uniform cross section. The incompressible viscous and couple stress fluid models have been used since these are known to be better models for physiological fluids like blood, bile, chyme and etc. The equations of motion have been linearized using long wave length approximation and analytical solutions have been obtained for the average effective dispersion coefficient under Taylor's limiting condition and dynamic boundary conditions at the flexible walls. The effects of various relevant constraints such as amplitude ratio, homogeneous chemical response rate, heterogeneous chemical response rate, magnetic field, permeability, and couple stress constraints on dispersion have been studied.

Following are some of the important observations:

Newtonian Fluid:

In the case of scattering of a solute material in peristaltic transport of an incompressible viscous fluid under different circumstances, it is noticed that peristalsis enhances scattering. It is also observed that scattering increases with wall constraints such as rigidity, stiffness and dissipative nature of the walls. Further, magnetic field constraint, homogeneous and heterogeneous chemical response rates tend to decrease scattering, but the permeability constraint increase scattering.

Couple Stress Fluid:

In the case of scattering of a solute matter in the peristaltic flow of a couple stress fluid with wall features, it is revealed that scattering is more in the existence of peristalsis. It is also observed that scattering decreases with magnetic field and couple stress constraints, homogeneous and heterogeneous response rates, but increases with wall constraints, permeability constraint.

8.2 Future Work

The investigations carried out in this thesis deal with dispersion of a solute in the peristaltic transport of Newtonian and non-Newtonian fluid models with wall features under various limitations. The flow equations have been linearized by assuming that the wavelength of the peristaltic wave is very large in comparison to the mean half width of the channel. The same issues can be studied with arbitrary wavelength.

In this thesis, we have used Cartesian coordinate system in the analysis of the issues considered. These issues can be studied using polar coordinate system.

Further, the above issues can be extended by considering the inclination and curvature of the duct.

Similarly, we have used an incompressible viscous and Couple stress fluid models. These problems can be done using other non-Newtonian fluid models such as Herschel Bulkley fluid and Casson fluid, etc.

We have used analytical method to obtain the closed form solution under certain conditions. These problems can be studied by applying numerical techniques.

Bibliography

[1] A. M. Abd-Alla and S. M. Abo-Dahab. Effect of rotation on peristaltic flow of fluid in a symmetric channel through a porous medium with magnetic field. *Journal of Computational and Theoretical Nanoscience*, 12(6):934–943, 2015.

[2] A. M. Abd-Alla, S. M. Abo-Dahab, and M. M. Albalawi. Magnetic field and gravity effects on peristaltic transport of a Jeffrey fluid in an asymmetric channel. *Abstract and Applied Analysis*, 896121:1–11, 2014.

[3] A. E. H. Abd El Naby and A. E. M. EL. Miseiry. Effects of an endoscope and generalized Newtonian fluid on peristaltic motion. *Journal of Applied mathematics and computer Science*, 128:19–35, 2002.

[4] A. Afsar Khan, R. Ellahi, and K. Vafai. Peristaltic transport of a Jeffrey fluid with variable viscosity through a porous medium in an asymmetric channel. *Advances in Mathematical Physics*, 169642:1–12, 2012.

[5] R. P. Agarwal and P. Chandra. Dispersion in simple microwfluid flows. *International Journal of Engineering Science*, 21:431–442, 1983.

[6] S. Ahmed and A. J. Chamkha. Effects of chemical reaction, heat and mass transfer and radiation on MHD flow along a vertical porous wall in the presence of induced magnetic field. *International Journal of Industrial Mathematics*, 2:245–261, 2010.

[7] N. S. Akbar and S. Nadeem. Mixed convective magnetohydrodynamic peristaltic flow of a Jeffrey nanofluid with Newtonian heating. *Z. Naturforsch*, 68(A):433–441, 2013.

[8] S. Akram. Effects of slip and heat transfer on a peristaltic flow of a Carreau fluid in a verticle asymmetric channel. *Computational Mathematics and Mathematical Physics*, 54(12):1886–1902, 2014.

[9] H. Alemayehu and G. Radhakrishnamacharya. The effect of peristalsis on dispersion of micropolar fluid in the presence of magnetic field. *International Journal of Engineering and Natural Sciences*, 4(4):220–226, 2010.

[10] H. Alemayehu and G. Radhakrishnamacharya. Dispersion of solute in peristaltic motion of a couple stress fluid through a porous medium. *Tamkang Journal of Mathematics*, 43(4):541–555, 2012.

[11] R. Aris. On the dispersion of a solute in a fluid flowing through a tube. *Proceedings of Royal Society London*, 35(A):67–77, 1956.

[12] S. Ashgar, C. Khalique, and R. Ellahi. Influence of a partial slip on flows of a second grade fluid in porous medium. *Journal of Porous Media*, 10:797–805, 2007.

[13] S. Bandyopadhyay and B. S. Mazumder. On contaminant dispersion in unsteady generalized couette flow. *International Journal of Engineering Science*, 37:1407–1423, 1999.

[14] H. Bergman. *The Ureter*. Springer-Verlag, 1981.

[15] B. S. Bhatt and N. C. Sacheti. On the analogy in slip flows. *Indian Journal of Pure and Applied Mathematics*, 10:303–306, 1979.

[16] G. Bohme and R. Friedrich. Peristaltic flow of visco-elastic liquids. *Journal of Fluid Mechanics*, 128:109–122, 1983.

[17] N. M. Bujurke and G Jayaraman. The influence of couple-stresses in squeeze films. *International Journal of Mechanical Sciences.*, 24:369–376, 1982.

[18] J. C. Burns and J. Parkes. Peristaltic motion. *Journal of Fluid Mechanics*, 29(4):731–743, 1967.

[19] P. Chandra and D. Philip. Effect of heterogeneous and homogeneous reactions on the dispersion of a solute in simple microwfluid. *Indian Journal of Pure and Applied Mathematics*, 24:551–561, 1993.

[20] M. K. Chaube, S. K. Pandey, and Tripathi. D. Slip effect on peristaltic transport of micropolar fluids. *Applied Mathematical Sciences*, 4(43):2105–2117, 2010.

[21] C. V. Criskysikopoulos, P. K. Kitanidis, and P. V. Roberts. Analysis of one dimensional solute transport through porous media with spatially variable retardation factor. *Water Resources Research*, 26:437–446, 1990.

[22] M. Dentz, T. L. Borgne, A. Englert, and B. Bijeljic. Mixing, spreading and reaction in heterogeneous media: A brief review. *Journal of Contaminant Hydrology*, 120:1–7, 2011.

[23] B. K. N. Dutta, N. C. Roy, and A. S. Gupta. Dispersion of a solute in a non-Newtonian fluid with simultaneous chemical reaction. *Mathematica Mechanica fasc.*, 2:78–82, 1974.

[24] A. Ebaid. Effect of magnetic field and wall slip condition on the peristaltic transport of a Newtonian fluid in an asymmetric channel. *Physics Letter A*, 372:11265–1276, 2008.

[25] R. Ellahi, M. M. Bhatti, C. Fetecau, and K. Vafai. Peristaltic flow of couple stress fluid in a non uniform rectangular duct having compliant walls. *Communications in Theoretical Physics*, 65(1):66–72, 2016.

[26] Y. A. Elmaboud. Influence of induced magnetic field on peristaltic flow in an annulus. *Communications in Nonlinear Science and Numerical Simulation*, 17:685–698, 2012.

[27] O. Eytan and D. Elad. Analysis of intra-uterine motion induced by uterine contractions. *Bulletin of Mathematical Biology*, 61:221–238, 1999.

[28] Y. C. Fung and C. S. Yih. Peristaltic transport. *Journal of Applied Mechanics: ASME Transactions*, 35(4):669–675, 1968.

[29] Y. C. Fung and F. Yin. Peristaltic waves in circular cylindrical tubes. *Journal of Applied Mechanics*, 36(3):579–587, 1969.

[30] J. Golder, M. Joelson, and M. C. Nel. Mass transport with asorption in porous media. *Mathematics and Computers in Simultation*, 81:2181–2189, 2011.

[31] B. B. Gupta and V. Seshadri. Peristalticpumping in non-uniform tubes. *Journal of Biomechanics*, 9:105–109, 1976.

[32] P. S. Gupta and A. S. Gupta. Effect of homogeneous and heterogeneous reactions on the dispersion of a solute in the laminar flow between two plates. *Proceedings of Royal Society London*, 330(A):59–63, 1972.

[33] A. Gurju, G. Radhakrishnamacharya, and B. Shireesha. Effect of slip condition on couple stress fluid in a channel with mild stenosis in the presence of uniform magnetic field. *Applications and Applied Mathematics*, 9(1):54–67, 2014.

[34] A. El. Hakeem, A.El. Naby, and I. E. El. Shamy. Slip effects on peristaltic transport of power law fluid through an inclined tube. *Applied Mathematical Sciences*, 1(60):2967–2980, 2007.

[35] M. H. Haroun. Effect of wall compliance on peristaltic transport of a Newtonian fluid in an asymmetric channel. *Mathematical problems in Engineering*, Article ID 61475:1–19, 2006.

[36] M. H. Haroun. Non- linear peristaltic flow of a fourth grade fluid in an inclined asymmetric channel. *Computational Materials sciences*, 39:324–333, 2007.

[37] Z. Hasan and V. Gupta, B. B.and Seshadri. Peristaltic pumping in non-uniform distensible tubes with different wave forms. *Journal of Biophysics and Numerical Methods*, 8(1):9–14, 1984.

[38] T. Hayat and Nasir A. Effect of variable viscosity on the peristaltic transport of a Newtonian fluid in an asymmetric channel. *Applied Mathematical Modelling*, 32:761–774, 2008.

[39] T. Hayat, N. S. Akbar, M. S. Alhothuali, S. Ashghar, and A. Alhomaidan. Peristaltic flow under the effects of an induced magnetic field with heat and mass transfer. *International Journal of Heat and Mass Transfer*, 55:433–452, 2012.

[40] T. Hayat, M. Khan, S. Ashghar, and A. M. Siddiqui. A mathematical model of peristalsis in tubes through a porous medium. *Journal of porous media*, 9:55–67, 2006.

[41] T. Hayat, A. Tanveer, F. Alsaadi, and N. D. Alotaibi. Homogeneous-heterogeneous reaction effects in peristalsis through curved geometry. *AIP Advances*, 5(6):http://dx.doi.org/10.1063/1.4923396, 2015.

[42] T. Hayat, A. Tanveer, and A. Alsaedi. Simultaneous effects of radial magnetic field and wall properties on peristaltic flow of carreau-yasuda fluid in curved flow configuration. *AIP Advances*, 5(12):http://dx.doi.org/10.1063/1.4939541, 2015.

[43] T. Hayat, A. Tanveer, and A. Alsaedi. Mixed convective peristaltic flow of carreau-yasuda fluid with thermal deposition and chemical reaction. *International journal of Heat and Mass Transfer*, 96:474–481, 2016.

[44] T. Hayat, A. Tanveer, R. Sajjad, A. Alsaedi, T. Muhammad, and R. Ellahi. On squeezing flow of couple stress nanofluid between two parallel plates. *Results in Physics*, 7:553–561, 2017.

[45] T. Hayat, A. Tanveer, H. Yasmin, and A. Alsaedi. Homogeneous-heterogeneous reactions in peristaltic flow with convective conditions. *PLOS one*, 9(12):http://dx.doi.org/10.1371/journal.pone.0113851, 2014.

[46] S. B. hazra, A. S. Gupta, and P. Niyogi. On the disperson of a solute in oscillating flow of a non - Newtonian fluid in a channel. *Heat and Mass Transfer*, 32:481–487, 1997.

[47] S. Hina, M. Mustafa, and Hayat T. On the exact solution for peristaltic flow of couple stress fluid with wall properties. *Bulgarian chemical communications*, 47(1):30–37, 2015.

[48] N. A. jaafar, Y. M. Yatim, and D. S. Sankar. Mathematical modelling of shear augmented dispersion of solute in blood flow. *AIP Conference Proceedings*, 1605, 2014.

[49] M. Y. Jaffrin and A. H. Shapiro. Peristaltic pumping. *Annual Review of Fluid Mechanics*, 3:13–36, 1971.

[50] M. Y. Jaffrin, A. H. Shapiro, and S. L. Weinberg. Peristaltic pumping with long wavelengths at low reynolds number. *Journal Fluid Mechanics*, 37:799–825, 1969.

[51] J. Jiang and J. Wu. A transition rate transformation method for solving advection-dispersion equation. *Journal of Computational Physics*, 230:5556–5563, 2011.

[52] M. R. Kaimal. Peristaltic pumping of a Newtonian fluid with particles suspended in it at low reynolds number under long wave length approximation. *ASME: Journal of Applied Mechanics*, 45:32–35, 1978.

[53] M. Khan and R. Ellahi. Exact solution for oscillatory flows of generalized oldroyd-B fluid through porous medium in a rotating frame. *Journal of Porous Media*, 12:777–788, 2009.

[54] F. Kill. *The function of the urethra and the renal pelvis*. Saunders, Philadelphia, 1957.

[55] M. C. kim and C. K. Choi. Effect of first order chemical reactions on gravitational instability in a porous medium. *Physics Review E*, 90:053016: 1–15, 2014.

[56] Y. J. Kim. Heat and mass transfer in MHD micropolar flow over a verticle moving porous plate in a porous medium. *Transport in Porous Media*, 56:17–37, 2004.

[57] S. Koo and K. H. Song. Taylor dispersion coefficients for longitudinal laminar flow in shell and tube exchangers. *Korean Journal of Chemical Engineering*, 22(2):184–189, 2005.

[58] M. Kothandapani, J. Prakash, and V. pusharaj. Analysis of heat and mass transfer on MHD peristaltic flow through a tapered asymmetric channel. *Journal of Fluid Mechanics*, 56123:1–9, 2015.

[59] M. Kothandapani and S. Srinivas. Non-linear peristaltic transport of a Newtonian fluid in an inclined asymmetric channel through a porous medium. *Physics Letter A*, 372:1265–1276, 2008.

[60] M. Kothandapani and S. Srinivas. On the influence of wall properties in the MHD peristaltic transport with heat transfer and porous medium. *Physics Letter A*, 372(25):4586–4591, 2008.

[61] R. Krstic. *Human Macroscopic Anatomy*. Springer-Verlag, 1991.

[62] A. Kumar, D. K. Jaiswal, and N. Kumar. Analytical solutions to one dimensional advection-diffusion equation with variable coefficients in semi-infinite media. *Journal of Hydrology*, 380:330–337, 2010.

[63] J. P. Kumar, J. C. Umavathi, and A. J. Chamkha. Steady solute dispersion in composite porous medium between two parallel plates. *Journal of Porous Media*, 16:1087–1105, 2013.

[64] S. Kumar and G. Jayaraman. Method of moments for laminar dispersion in an oscillatory flow through curved channels with absorbing walls. *Heat and Mass Transfer*, 44(2):1324–1336, 2008.

[65] H. Kwang, W. Chua, and J. Fang. Peristaltic transport in a slip flow. *European Physical journal B*, 16:543–547, 2000.

[66] T. W. Latham. *Fluid motions in a peristaltic pump, Master's thesis*. Massachusetts Institute of Technology, Cambridge, 1966.

[67] J. S. Lee and Y. C. Fung. Flow in non-uniform small blood vessels. *Microvascular Research*, 3:272–279, 1971.

[68] E.N. Lightfoot. *Transport phenomena in living systems*. John Wiley and Sons, New York, 1974.

[69] T. MacKenzie and A. J. Roberts. Holistic discretisation of shear dispersion in a two dimensional channel. *ANZIAM Journal*, 44:512–530, 2003.

[70] S. Maiti and J. C. Misra. Peristaltic transport of a couple stress fliud: Some applications to hemodynamics. *Journal of Mechanics in Medicine and Biology*, 12(3):1250048–1–12, 2012.

[71] M. J. Manton. Long wavelength peristaltic pumping at low Reynolds number. *Journal of Fluid Mechanics*, 68:467–476, 1975.

[72] A. Medhavi. Peristaltic pumping of a particulate suspension in a catheterized tube. *e - Journal of Science and Technology*, 1:77–93, 2010.

[73] K. N. Mehta and M. C. Tiwari. Dispersion in presence of slip and chemical reactions in porous wall tube flow. *Defence Science Journal*, 38:1–11, 1988.

[74] Kh. S. Mekheimer. Peristaltic transport of a couple stress fluid in a non-uniform channels. *Journal of Biorheology*, 39(6):755–765, 2002.

[75] Kh. S. Mekheimer. Peristaltic flow of blood under effect of a magnetic field in a non-uniform channels. *Applied Mathematics and Computation*, 153(3):763–777, 2004.

[76] Kh. S. Mekheimer. Effect of the induced magnetic field on the peristaltic flow of a couple stress fluid. *Physics Letters A*, 372(23):4271–4278, 2008.

[77] Kh. S. Mekheimer. Peristaltic flow of a Magneto-Micropolar fluid: Effect of induced magnetic field. *Journal of Applied Mathematics*, 57:1–23, 2008.

[78] Kh. S. Mekheimer and A. ABD Elmabounf. The influence of heat transfer and magnetic field on peristaltic transport of a Newtonian fluid in a vertical annulus: Application of an endoscope. *Physics Letters A*, 372:1657–1665, 2008.

[79] A. M. EL. Misery, E. F. EL. Shehawey, and A. Hakeem. Peristaltic motion of an incompressible generalized Newtonian fluid in a planar channel. *Journal of Physical Society of Japan*, 85(1):3524–3529, 1996.

[80] M. Mishra and A. R. Rao. Peristaltic transport of a non-Newtonian fluid in an asymmetric channel peripheral layer. *ZAMP*, 54:532–550, 2003.

[81] J. C. Misra and S. K. Ghosh. A mathematical model for the study of blood flow through a channel with permeable walls. *Acta Mechanica*, 122:137–153, 1997.

[82] J. C. Misra, S. Maiti, and G. C. Shit. Peristaltic transport of a physiological fluid in an asymmetric porous channel in presence of an external magnetic field. *Journal of Mechanics in Medicine and Biology*, 8:507–525, 2008.

[83] J. C. Misra and S. K. Pandey. Peristaltic transport of a particle fluid suspension in a cylindrical tube. *Computers and Mathematics with Applications*, 28:131–145, 1994.

[84] J. C. Misra and S. K. Pandey. Peristaltic transport of a non-Newtonian fluid with a peripheral layer. *International Journal of Engineering Science*, 37(14):1841–1858, 1999.

[85] J. C. Misra and S. K. Pandey. Peristaltic flow of a multilayered power law fluid through a cylindrical tube. *International Journal of Engineering Science*, 39:387–402, 2001.

[86] T. K. Mittra and N. S. Prasad. On the influence of wall properties and poiseuille flow in peristalsis. *Journal of Biomechanics*, 6:681–693, 1973.

[87] P. Muttu, B. V. Ratishkumar, and P. Chandra. On the influence of wall properties in the peristaltic motion of micropolar fluid. *ANZIAM Journal*, 45:246–260, 2003.

[88] S. Nadeem, N. S. Akbar, B. Naheeda, and A. Sadaf. Influence of heat and mass transfer on peristaltic flow of a third order fluid in diverging tube. *Communications in Nonlinear Science and Numerical Simultation*, 15:2916–2931, 2010.

[89] S. Nadeem, A. Riaz, R. Ellahi, and N. S. Akbar. Mathematical model for the peristaltic flow of nanofluid through eccentric tubes comprising porous medium. *Applied Nanoscience*, 4(6):733–743, 2014.

[90] P. Nagarani, G. Sarojamma, and G. Jayaraman. The effect of boundary absorption in dispersion in Casson fluid flow in a tube. *Annals of Biomedical Engineering*, 32(5):706–719, 2004.

[91] C. O. Ng. Dispersion in steady and oscillatory flows through a tube with reversible and irreversible wall reactions. *Proceedings of Royal Society Londan*, 462(A):481–515, 2006.

[92] S. Noreen, A. Alsaedi, and T. Hayat. Peristaltic flow of pseudoplastic fluid in an asymmetric channel. *ASME: Journal of Applied Mechanics*, 79:054501:1–6, 2012.

[93] D. Padma and V. V. Ramana Rao. Homogeneous and heterogeneous reaction on the dispersion of a solute in MHD Couette flow - *I*. *Current Science*, 44:803–804, 1975.

[94] D. Padma and V. V. Ramana Rao. Effect of homogeneous and heterogeneous reactions on the dispersion of a solute in laminar flow between two parallel porous plates. *Indian Journal of Technology*, 14:410–412, 1976.

[95] D. Padma and V. V. Ramana Rao. Homogeneous and heterogeneous reaction on the dispersion of a solute in MHD Couette flow - *II*. *Current Science*, 46:42–43, 1977.

[96] D. Pal. Effect of chemical reaction on the dispersion of a solute in a porous medium. *Applied Mathematical Modeling*, 23(7):557–566, 1999.

[97] S. K. Pandey and M. K. Chaube. Peristaltic flow of a microploar fluid through a porous medium in the presence of an external mangetic field. *Communications in Nonlinear Science and Numerical Simultation*, 16:3591–3601, 2011.

[98] S. K. Pandey and M. K. Chaube. Study of wall properties on peristaltic transport of a couple stress fluid. *Meccanica*, 46:1319–1330, 2011.

[99] P. D. Patel, B. F. Picologou, and P. S. Lykoudis. Biorheological aspects of colonic activity. *II*. Experimental investigation of the rheological behaviour of human faeces. *Biorheology*, 10:441–445, 1973.

[100] A. B. Patil. *Study of peristaltic motion of non-Newtonian fluids through porous medium, Ph.D's thesis*. Visvesvaraya Technological University, Belagavi, 2017.

[101] S. Paul. Dispersion in unsteady Couette-Poiseuille flows. *International Journal of Engineering and Science*, 46:1203–1217, 2008.

[102] S. Paul. Axial dispersion in pressure perturbed flow through an annular pipe oscillating around its axis. *Z. Angew Mathematics and Physics*, 60:899–920, 2009.

[103] B. F. Picologou, P. D. Patel, and P. S. Lykoudis. Biorheological aspects of colonic activity. *I*. Theoretical considerations. *Biorheology*, 10:431–440, 1973.

[104] G. M. Porta, M. Riva, and A. Guadagnini. Upscalling solute transport in porous media in the presence of an irreversible bimolecular reaction. *Advances in Water Resources*, 35:151–162, 2012.

[105] C. Pozrikidis. A study of peristaltic flow. *Journal of Fluid Mechanics*, 180:515–527, 1987.

[106] D. R. V. Prasad Rao, D. V. Krishna, and D. Lokenath. Free convection in hydromagnetic flows in a vericle wavy channel. *International Journal of Engineering Science*, 21(9):1025–1039, 1983.

[107] A. M. Provost and W. H. Schwarz. A thoeretical study of viscous effects in peristaltic pumping. *Journal of Fluid Mechanics*, 279:177–195, 1994.

[108] M. Quintard, F. Cherblan, and S. Whitaker. Dispersion in heterogeneous porous media: One equation non-equilibrium model. *Transport in Porous Media*, 44:181–203, 2001.

[109] G. Radhakrishnamacharya. Long wavelength approximation to peristaltic motion of a power law fluid. *Rheologica Acta*, 21:30–35, 1982.

[110] G. Radhakrishnamacharya and V. Radhakrishna Murthy. Heat transfer to peristaltic transport in a non - uniform channel. *Defence Science Journal*, 43:275–280, 1993.

[111] G. Radhakrishnamacharya and V. Radhakrishna Murthy. Heat transfer to peristaltic transport in a uniform channel in the presence of magnetic field. *Banyan Mathematics Journal*, 2:57–68, 1995.

[112] G. Radhakrishnamacharya and R. Sharma. Motion of a self propelling microorganism in a channel under peristalsis: Effects of viscosity variation. *Non-linear Analysis: Modelling and Control*, 12(3):409–418, 2007.

[113] G. Radhakrishnamacharya and Ch. Srinivasalu. Influence of wall properties on peristaltic transport with heat transfer. *C. R. Mechanics*, 335:369–373, 2007.

[114] T. Raghunath Rao. Peristaltic transport of a Newtonian fluid with wall properties in an asymmetric channel. *International Journal of Advances and Applied Mathematics and Mechanics*, 3(1):102–109, 2015.

[115] A. V. Ramanakumari and G. Radhakrishnamacharya. Effect of slip and magnetic field on peristaltic flow in an inclined channel with wall effects. *International Journal of Biomathematics*, 5(6):http://dx.doi.org/10.1142/S1793524511001568, 2012.

[116] A. R. Rao and M. Mishra. Peristaltic transport of a power- law fluid in a porous tube. *Journal of non-Newtonian Fluid Mechanics*, 121:163–174, 2004.

[117] H. J. Rath and G. W. Reese. Peristaltic flow of non-Newtonian fluids containing small spherical particles. *Archives of Mechanics*, 36(2):263–277, 1984.

[118] V. P. Rathod and P. Kulkarni. The influence of wall properties on peristaltic transport of dusty fluid through a porous medium. *International Journal of Mathematical Archive*, 2(12):2777–2789, 2011.

[119] B. V. Ratish Kumar and K. B. Naidu. A numerical study of magnetic effects on peristaltic flows. *Journal of Applied Mechanical Engineering*, 1(4):485–506, 1996.

[120] G. Ravikiran. *Effect of peristalsis on dispersion in non-Newtonain fluid flows with wall properties, Ph.D's thesis*. National Institute of Technology, Warangal, 2015.

[121] G. Ravikiran and G. Radhakrishnamacharya. Effect of homogeneous and heterogeneous chemical reactions on peristaltic transport of a Jeffrey fluid through a porous medium with slip condition. *Journal of Applied Fluid Mechanics*, 8(3):521–258, 2015.

[122] G. RaviKiran and G Radhakrishnamacharya. Effects homogeneous and heterogeneous chemical reactions of peristaltic flow of a micropolar fluid through a porous medium with wall effects in the presence of slip. *International Journal of Humanities and Management Sciences*, 3(2):54–61, 2015.

[123] G. RaviKiran and G. Radhakrishnamacharya. Effects of homogeneous and heterogeneous chemical reactions on peristaltic transport of a MHD micropolar fluid with wall effects. *Mathematical Methods in the Applied Sciences*, 39(6):1349–1360, 2016.

[124] G. Ravikiran and G. Radhakrishnamacharya. Peristaltic flow and hydrodynamic dispersion of a reactive micropolar fluid simulation of chemical effects in the digestive process. *Journal of Mechanics in Medicine and Biology*, 17(1):1750013–1750030, http://dx.doi.org/10.1142/S0219519417500130., 2017.

[125] P. G. Saffman. On the boundary conditions at the surface of a porous medium. *Studies in Applied Mathematics*, 50(2):93–101, 1971.

[126] R. V. Sagayamary and R. Devanathan. Steady flow of couple stress fluid through tubes of slowly varying cross-sections - Application to blood flows. *Biorheology*, 26(4):753–769, 1989.

[127] A. Saini, V. K. Katiyar, and Pratibha. Effects of first order chemical reactions on the dispersion coefficient associated with laminar flow through the lungs. *International Journal of Biomathematics*, 7(2):1450021:1–12, 2014.

[128] G. C. Sankad and G. Radhakrishnamacharya. Effect of magnetic field on peristaltic motion of micropolar fluid with wall effects. *Journal of Applied Mathematics and Fluid Mechanics*, 1:37–50, 2009.

[129] G. C. Sankad and G. Radhakrishnamacharya. Effect of magnetic field on the peristaltic transport of couple stress fluid in a channel with wall effects. *International Journal of Biomathematics*, 4(3):365–378, 2011.

[130] G. C. Sankad, G. Radhakrishnamacharya, and J. V. Ramanamurthy. Long wave length approximation to peristaltic motion of micropolar fluid with wall effects. *Advances in Applied Mathematics and Mechanics*, 2:222–237, 2010.

[131] A. Sarkar and G. Jayaraman. The effect of wall absorption on dispersion annular flows. *Acta Mechanica*, 158:105–119, 2002.

[132] A. Sarkar and G. Jayaraman. The effect of wall absorption on dispersion in oscillatory flow in an annulus: Application to a catheterized artery flows. *Acta Mechanica*, 172:151–167, 2004.

[133] A. H. Shapiro. Pumping and retrograde diffusion in peristaltic waves, proceedings of workshop ureteral on reflux in children. *National Academic os Science*, 1967.

[134] E. F. El. Shehawey and Kh. S. Mekheimer. Couple stresses in peristaltic transport of fluids. *Journal of Biomathematics*, 9(1):1–14, 1994.

[135] E. F. EL. Shehawey, Kh. S. Mekheimer, S. F. Kalidas, and N. A. S. Afifi. Peristaltic transport through a porous medium. *Journal of Biomathematics*, 14:217–230, 1999.

[136] E. F. EL. Shehawey and W. El. Sebaei. Peristaltic transport in a cylindrical tube through a porous medium. *International Journal of Mathematics and Mathematical Sciences*, 24(4):217–230, 2000.

[137] G. C. Shit and M. Roy. Hydromagnetic effect on inclined peristaltic flow of a couple stress fluid. *Alexandria Engineering Journal*, 53(4):949–958, 2014.

[138] J. B. Shukla, P. Chandra, R. Sharma, and G. Radhakrishnamacharya. Effects of peristaltic and longitudinal wave motion of the channel wall on movement of microorganisms: Application to spermatozoa transport. *Journal of Biomechanics*, 21:947–954, 1988.

[139] J. B. Shukla, R. S. Parihar, and B. R. P. Rao. Dispersion in non-Newtonian fluids: Effects of chemical reactions. *Rheological Acta*, 18:740–748, 1979.

[140] A. M. Sobh. Interaction of couple stresses and slip flow on peristaltic transport in uniform and non-uniform channels. *Turkish Journal of Engineering and Enviornmental Sciences*, 32:117–123, 2008.

[141] A. M. Sobh. Heat transfer in a slip flow of peristaltic transport of a magneto-Newtonian fluid through a porous medium. *International Journal of Biomathematics*, 2:299–309, 2009.

[142] A. M. Sobh. Effect of homogeneous and heterogeneous reactions on the dispersion of a solute in MHD Newtonian fluid in an asymmetric channel with peristalsis. *British Journal of Mathematics and Computer Science*, 3(4):664–679, 2013.

[143] A. M. Sobh and H. H. Mady. Peristaltic flow through a porous medium in a non-uniform channel. *Journal of Applied Sciences*, 8:1085–1090, 2008.

[144] S. Srinivas, R. Gayathri, and M. kothandapani. The influence of slip conditions, wall properties and heat transfer on MHD peristaltic transport. *Computers Physics Communications*, 180(1):2115–2122, 2009.

[145] D. Srinivasacharya, G. Radhakrishnamacharya, and Ch. Srinivasulu. The effects of wall properties on peristaltic transport of of dusty fluid. *Turkish Journal of Engineering and Environmental Sciences*, 32:357–365, 2008.

[146] Ch. Srinivasalu and G. Radhakrishnamacharya. Peristaltic transport in a non-uniform channel with elastic effects. *Proceedings of the National Academy of science, India*, 72(A):279–288, 2002.

[147] L. M. Srivastava. Peristaltic transport of a couple stress fluid. *Rheologica Acta*, 25:638–641, 1986.

[148] L. M. Srivastava and R. P. Agrawal. Oscillating flow of a conducting fluid with a suspension of spherical particles. *Journal of Applied Mechanics*, 47:196–199, 1980.

[149] L. M. Srivastava and V. P. Srivastava. Peristaltic transport of blood: Casson model II. *Journal of Biomechanics*, 17:821–823, 1984.

[150] L. M. Srivastava, V. P. Srivastava, and S. N. Sinha. Peristaltic transport of a physiological fluid. part - I. flow in non - uniform geometry. *Biorheology*, 20(2):153–166, 1983.

[151] V. K. Stokes. Couple stress fluids. *Physics of Fluids*, 9:1709–1715, 1966.

[152] V. K. Sud, G. S. Sakhon, and R. K. Mishra. Pumping action on blood by a magnetic field. *Bulletin of Mathematical Biology*, 39:385–390, 1977.

[153] S. Takabatake and K. Ayukawa. Numerical study of two dimensional peristaltic flows. *Journal of Fluid Mechanics*, 122:439–465, 1978.

[154] D. Takagi and N. J. Balmforth. Peristaltic pumping of viscous fluid in an elastic tube. *Journal of Fluid Mechanics*, 672:196–218, 2011.

[155] P. N. Tandon, J. K. Misra, and K. K. Srivastava. Microstructural and peripheral- layer viscosity effects on peristaltic transport of seminal fluid. *Biorheology*, 19:707–715, 1982.

[156] G. I. Taylor. Dispersion of soluble matter in solvent flowing slowly through a tube. *Proceedings of Royal Society London*, 219(A):186–203, 1953.

[157] G. I. Taylor. Conditions under which dispersion of a solute in a stream of solvent can be used to measure molecular diffusion. *Proceedings of Royal Society London*, 225(A):473–477, 1954.

[158] G. I. Taylor. The dispersion of matter in turbulent flow through a pipe. *Proceedings of Royal Society London*, 223(A):446–468, 1954.

[159] R. M. Terrill. A note on laminar flow in a porous tube. *IMA Journal of Applied Mathematics*, 33:543–547, 1984.

[160] M. M. Teymoori and E. Abbaspour-Sani. Design and simulation of a novel electrostatic peristaltic micromachined pump for drug delivery applications. *Sensors and Actuators A: Physical Journal*, 117(2):222–229, 2005.

[161] E. Toklu. A new mathematical model of peristaltic flow on esophageal bolus transport. *Journal of Fluid Mechanics*, 6(31):6584–6593, 2011.

[162] D. Tripathi and O. Anwar Beg. Peristaltic propulsion of generalized burgers fluids through a nano-uniform porous medium: A study of chyme dynamics tnrough the diseased intestine. *Mathematical Biosciences*, 248:67–77, 2014.

[163] D. Tripathi and O. A. Beg. Magnetohydrodynamic peristaltic flow of a couple stress fluid through coaxial channels containing a porous medium. *Journal of Mechanics in Medicine and Biology*, 12(5):125008–1–20, 2012.

[164] D. Tripathi and O. A. Beg. A study on peristaltic flow of nanofluids: Application in drug delivery systems. *International Journal of Heat and Mass Transfer*, 70:61–70, 2014.

[165] D. Tripathi, M. K. Chaube, and P. K. Gupta. Stokes flow of micropolar fluids by peristaltic pumping through tube with slip boundary condition. *Applied Mathematics and Mechanics*, 32:1587–1598, 2011.

[166] K. Vajravelu, S. Sreenadh, and B. V. Ramesh. Peristaltic pumping of a herschel - Bulkley fluid in a channel. *Applied Mathematics and Computation*, 169:726–735, 2005.

[167] K. C. Valanis and C. T. Sun. Poiseuille flow of a fluid with couple-stress with applications to blood flow. *Biorheology*, 6:85–97, 1969.

[168] X. L. Wang, K. Q. Zhu, and S. Z. Wen. Thermohydrodynamic analysis of journal bearings lubricated with couple stress fluids. *Tribol. Int.*, 34:335–343, 2001.

[169] S. L. Weinberg, E. C. Eckistein, and A. H. Shapiro. An experimental study of peristaltic pumping. *Journal of Fluid Mechanics*, 49:461–497, 1971.

[170] Y. Yang, C. T. Crowe, J. N. Chung, and T. R. Troutt. Experiments on particle dispersion in a plane wake. *International Journal of Multiphase Flow*, 26:1583–1607, 2000.

[171] L. U. Zhangji, S. Dong, Y. Shen, and G. Zheng. Dispersion of soluble matters in Newton-dipolar stratified fluid and effects of peripheral layer. *Communications in Nonlinear Science and Numerical Simultation*, 3:236–241, 1998.

[172] T. F. Zien and S. A. Ostrach. A long wavelength approximation to peristaltic motion. *Journal of Biomechanics*, 3:63–75, 1970.

List of Papers: Published/Communicated

List of Publications

1. Sankad G. C., Nagathan P. S., Asha Patil and **Dhange M. Y.**, **Peristaltic transport of a Herschel-Bulkley fluid in a non-uniform channel with wall effects**, *International Journal of Engineering Science and Innovative Technology*, **3(3)** (2014), 669-678.

2. Sankad Gurunath and **Dhange Mallinath**, **Peristaltic pumping of an incompressible viscous fluid in a porous medium with wall effects and chemical reactions**, *Alexandria Engineering Journal*, **55** (2016), 2015-2021.

3. Sankad G. C. and **Dhange M. Y.**, **Effect of compliant walls on magneto-hydrodynamic peristaltic pumping of an incompressible viscous fluid with chemical reactions**, *ARPN Journal of Engineering and Applied Sciences*, **12(3)** (2017), 654-660.

4. **Dhange Mallinath** and Sankad Gurunath, **On magnetohydrodynamic peristaltic pumping of an incompressible viscous fluid in an inclined channel with chemical reactions and wall properties**, *International Journal of Pure and Applied Mathematics*, **113(7)** (2017), 32-41.

5. Sankad G. and **Dhange M.**, **Effect of chemical reactions on dispersion of a solute in peristaltic motion of Newtonian fluid with wall properties**, *Malaysian Journal of Mathematical Sciences*, **11(3)** (2017), 347-363.

6. **Dhange M. Y.** and Sankad G. C., **Peristaltic pumping and dispersion of a MHD couple stress fluid with chemical reaction and wall effects**, *Journal of advances in Mathematics and Computer Science*, **24(3)** (2017), 1-12.

7. Sankad Gurunath and **Dhange Mallinath**, **Slip and chemical reaction effects on peristaltic transport of a couple stress fluid through a permeable medium with compliant wall**, Accepted for publication in *Applications and Applied Mathematics: An International Journal*.

8. **Dhange M. Y.** and Sankad G. C., **Dispersion of a solute in peristaltic motion: An overview**, Presented in 2^{nd} *International Conference on Applications of Fluid Dynamics (ICFD-2014)*, 21 - 23 July, 2014 held at Department of Mathematics, Sri Venkateswara University, Tirupati, Andra Pradesh (INDIA) in association with University of Botswana, Gaborone.

9. **Dhange Mallinath** and Sankad Gurunath, **Outcome of wall features on the creeping sinusoidal flow of MHD couple stress fluid in an inclined channel with chemical reaction**, Presented in 2^{nd} *International Conference on Modern Mathematical Methods and High performance Computing in Science and Technology (M3HPCST-2018)*, 04 - 06 January, 2018 held at Inderprastha Engineering College,Ghaziabad, Uttar Pradesh (INDA). Accepted for publication in Springer series book - Advances in Mechanics and Mathematics.

List of the Papers Communicated for Publication

1. Sankad Gurunath and **Dhange Mallinath**, **Peristaltic Pumping of Newtonian fluid in a porous medium with compliant wall and slip condition: Analytic Solution in the case of chemical reactions**, communicated to *Jordan Journal of Mechanical and Industrial Engineering.*

2. G. C. Sankad and **M. Y. Dhange**, **Creeping sinusoidal flow and dispersion of a couple stress fluid through a porous medium with compliant walls and chemical effects**, communicated to *Thai Journal of Mathematics.*

3. **M. Y. Dhange** and G. C. Sankad, **Creeping sinusoidal flow and dispersion of a couple stress fluid with chemical reaction and wall effects**, communicated to *ASRO Journal of Applied Mechanics.*